
On the correlation lengths and Drude weight of the
anisotropic Heisenberg chain

Inaugural-Dissertation
zur
Erlangung des Doktorgrades
der Mathematisch-Naturwissenschaftlichen Fakultät
der Universität zu Köln

vorgelegt von
Christian Scheeren
aus Dortmund

KÖLN 2000

Berichterstatter: Prof. Dr. A. Klümper
Prof. Dr. J. Zittartz

Tag der mündlichen Prüfung:

Contents

1. Motivation	6
1.1. Outline of this work	7
2. Introduction to exactly solvable models	8
2.1. Two dimensional classical vertex models	9
2.2. Correlation lengths in the transfer matrix approach	14
2.3. The six-vertex model	16
2.3.1. Origin of the six-vertex model	16
2.4. Classification of phases	18
2.5. The relation between quantum chains and two-dimensional classical models	21
2.5.1. The quantum transfer matrix of the six- and eight-vertex model . .	23
2.6. The algebraic Bethe ansatz	26
2.6.1. Bethe ansatz equation for the quantum transfer matrix	29
3. The XXZ-Heisenberg model	30
3.1. Spin models	31
3.1.1. Néel or RVB-state	31
3.1.2. Spinons	32
3.2. The XXZ -Heisenberg model	33
3.2.1. Identification of excitations in BAE-patterns	33
3.3. The non-linear integral equations (NLIE) for the XXZ -model at arbitrary temperature	37
3.3.1. The non-linear integral equations	37
3.3.2. Description of the string motion	40
3.3.3. Analytic continuation	40
3.3.4. Crossover scenario	40
3.4. Crossover in the correlation length	43
4. The Drude weight at finite temperature	46
4.1. Linear Response and Drude weight at $T = 0$	47
4.1.1. Twisted boundary conditions and external fields	50
4.1.2. Curvature of energy levels and Drude weight	50
4.1.3. Drude weight at arbitrary temperature	51
4.2. The Drude weight with magnons	52
4.3. The connection between standard TBA and the quantum transfer matrix approach	55
4.4. Alternative derivation of the Drude weight	57
4.4.1. The Drude weight for $T = 0$	64

4.5. Results	65
5. Summary and outlook	68
A. Jacobian elliptic functions and related quantities	70
B. Parameterization of the eight- and six-vertex model	72
C. The connection between spinon and magnon approach	75
D. Derivation of the non-linear integral equations for the XXZ-Heisenberg model	76
D.1. Integral equations for the leading eigenvalue Λ_0	77
D.2. Excitations I: pure two hole case	79
D.3. Excitations II: 1-string case	80
D.4. Derivation of the integral expressions for the second strip	83
E. Perturbation theory for the ring Hamiltonian	84
	86
Kurzzusammenfassung	90
Zusammenfassung	91
Erklärung	93
Danksagung	94
Lebenslauf	95

Abstract

In the first part of the present work the asymptotic behaviour of spin-spin-correlation functions for the integrable Heisenberg chain is investigated. To this end the quantum transfer matrix (QTM) technique developed in [7] is used which results in a set of non-linear integral equations (NLIE). In the case of the largest eigenvalue the solution to these equations yields the free energy and by modifications of the paths of integration the next-leading eigenvalues and hence the correlation lengths are obtained. At finite field $h > 0$ and sufficiently high temperature T the next-leading eigenvalue is unique and given by a 1-string solution to the QTM taking real and negative values thus resulting into exponentially decaying correlations with anti-ferromagnetic oscillations. At sufficiently low temperatures a different behaviour sets in where the next-leading eigenvalues to the QTM are given by a complex conjugate pair of eigenvalues resulting into incommensurate oscillations.

The above scenario is the result of analytical and numerical investigations of the QTM establishing a well defined crossover temperature T_c at which the 1-string eigenvalue to the QTM gets degenerate with the 2-string solution.

In the second part the Drude weight of the anisotropic Heisenberg chain is analytically calculated. An interesting connection [40] between the QTM-technique and the standard thermodynamic Bethe Ansatz (TBA) is used. We get *exact* results for *finite* temperatures. At the isotropic point logarithmic corrections for the Drude weight at low temperatures are found.

1. Motivation

The present work is dedicated to the study of temperature-dependent properties of the one-dimensional anisotropic Heisenberg model. The calculation of such quantities traditionally belongs to the field of statistical mechanics where one usually is interested in the investigation of interacting systems of macroscopic size. However, the exact calculation of physically relevant quantities for any large realistic system turns out to be exceedingly difficult. One is therefore forced to either make some sort of approximation in the course of the calculation or to replace the system by some simple idealization that makes the calculation of the quantities of interest possible.

Up to now exact solutions are, as far as quantum mechanical systems are concerned, known only for one-dimensional models, so-called quantum chains. The fundamental conception for the solution of such models is the famous *Bethe ansatz* [1] introduced 1931 giving the solution of the linear atomic chain (*XXX*-model [2]). The invention of this ansatz initiated an extensive search for exact solutions in statistical mechanics. Unfortunately, the structure of the Bethe ansatz wave function is highly complex, especially when systems with additional internal degrees of freedom are considered. In most cases even the calculation of groundstate properties of a Bethe ansatz solvable model turns out to be difficult [18, 17, 56]. It is evident that the calculation of thermodynamic quantities has to take into account *all* excited states. The pioneering works were performed by Takahashi [9] in the early seventies. However, unsupported conjectures about the structure of the excitations (string hypothesis) had to be made in order to achieve a solution. Within this framework the free energy of the isotropic Heisenberg chain could be calculated, but correlation functions at finite temperature remained out of reach.

It was the well known connection between one-dimensional quantum mechanical and two-dimensional classical models [57, 11] that allowed for an alternative approach of calculating thermodynamic quantities of quantum chains. In this method the partition function of the one-dimensional model can be mapped onto that of a two-dimensional classical one. It is crucial that the thermodynamic quantities can be expressed in terms of only the largest eigenvalue of the corresponding transfer matrix. Here, the rich knowledge of two-dimensional classical models [8, 4] could be used. Even the calculation of correlation lengths is possible in this approach and the string hypothesis is obsolete.

The purpose of this work is twofold:

On the one hand, the longitudinal correlation length and the Drude weight of the anisotropic Heisenberg chain are calculated by means of the quantum transfer matrix and a mapping onto a *finite* set of non-linear integral equations. On the other hand, this calculation of the Drude weight gives an interesting insight into the relation between the formulation of the thermodynamics by Takahashi [9] and the equations gained by the quantum transfer matrix approach [7].

1.1. Outline of this work

In chapter 2 the basic methods for the treatment of exactly solvable models by means of the transfer matrix are given. Especially, the quantum transfer matrix for the anisotropic Heisenberg chain is introduced.

The next chapter is dedicated to the analysis of the solutions of the Bethe ansatz equations and the way to derive non-linear integral equations for the calculation of the thermodynamics of the model. In order to calculate the longitudinal correlation length modifications of the integral equations have to be done. In the end we get exact results for the temperature dependence of the longitudinal correlation length.

In the second part of this work the calculation of the Drude weight at arbitrary temperature is done. This derivation is also based on the integral equations for the thermodynamics of the model, but we need to benefit from techniques of the standard thermodynamic Bethe ansatz (TBA) in order to obtain a straightforward result. This will be illuminating the relation of the two different approaches to the thermodynamics and will be again leading to *exact* values of the Drude weight at *finite* temperatures.

It should be mentioned that the calculation of the temperature dependence of the correlation length and the Drude weight are the main results of this work. These results were obtained by a numerical treatment of the integral equations. For the sake of brevity the presentation of this extensive numerical work is not done here.

2. Introduction to exactly solvable models

2.1. Two dimensional classical vertex models

As the integrability of a one dimensional quantum chain is based on the exact solvability of a two dimensional classical vertex model [24, 25, 13, 14] some of the basic features of such models shall be described here, following [23].

Regard variables on every bond between the sites of a rectangular $M \times N$ lattice that have the possible values $1, 2, \dots, q$. Each configuration of values on the vertex is connected

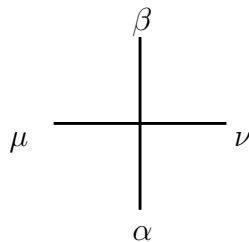


Figure 2.1.: Variables at a vertex with Boltzmann weight $R_{\alpha}^{\beta}(\mu, \nu)$.

to a certain energy ϵ_i and the corresponding Boltzmann weight $\exp\{-\epsilon_i/T\}$ is denoted by $R_{\alpha}^{\beta}(\mu, \nu)$. These are in general q^4 different complex numbers¹. In this work we focus on $q = 2$ that leads to 16 different vertex combinations. Possible values on the bond are now $\sigma = \pm 1$ in analogy to classical spins on the lattice sites.² The total energy of a given configuration of arrows on the lattice is

$$E = \sum_{j=1}^{16} N_j \epsilon_j \quad (2.1)$$

where N_j is the number of vertices with a j -type combination of arrows. The partition function of the model is

$$\mathcal{Z} = \sum_{\text{all configurations}} e^{-\beta E} \quad (\beta = \frac{1}{T}). \quad (2.2)$$

The formalism developed in the following provides a skillfull way to calculate that partition function. The multi-indices $\alpha = \{\alpha_1, \dots, \alpha_N\}$ help to define the so-called *transfer matrix* T with elements

$$T_{\alpha\alpha'} = \sum_{\gamma_1} \dots \sum_{\gamma_N} R_{\alpha_1}^{\alpha'_1}(\gamma_1, \gamma_2) R_{\alpha_2}^{\alpha'_2}(\gamma_2, \gamma_3) \dots R_{\alpha_N}^{\alpha'_N}(\gamma_N, \gamma_1). \quad (2.3)$$

In that way a row of the lattice occupied with arrows featuring periodic boundary conditions is constructed (see fig. 2.2). The inner degrees of freedom in the row are summed out and T is a $2^N \times 2^N$ -matrix. Now one can express (2.2) as

$$\mathcal{Z} = \text{trace } T^M = \sum_i \Lambda_i^M. \quad (2.4)$$

To prove this, arrange the summation in (2.2) first along the horizontal directions and then along the vertical ones. Thus, we reduce the problem of evaluating the partition function

¹The weights can be complex if we allow for unphysical complex energies in the general case.

²Convention: +1 for arrows pointing up or to the right, -1 for those pointing down or to the left.

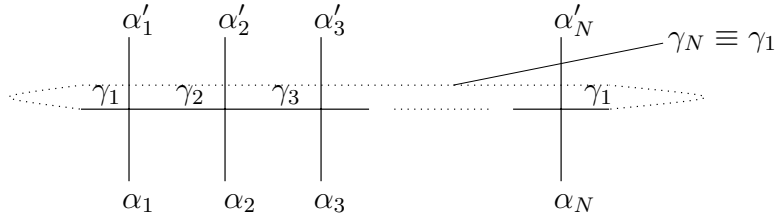


Figure 2.2.: Row-to-row transfer matrix

to the problem of diagonalizing the corresponding transfer matrix. The idea is to embed the transfer matrix into a family of commuting transfer matrices and to try to diagonalize the whole family simultaneously. Suppose we have two sets $\{v_j\}$ and $\{v'_j\}$ of Boltzmann weights and corresponding transfer matrices T and T' . We search for a criterion in terms of the Boltzmann weights only, so that

$$[T, T'] = 0 \quad (2.5)$$

holds. Now let us consider another object \mathcal{T} for which we demand

$$T = \text{trace } \mathcal{T}. \quad (2.6)$$

By the look at fig. (2.2) we conclude the graphical representation of \mathcal{T} . The 2×2 -matrix

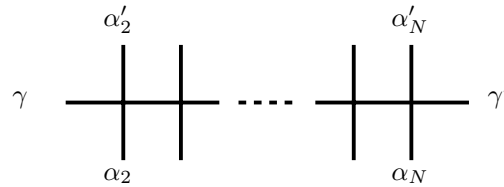


Figure 2.3.: Monodromy matrix

\mathcal{T} is called *monodromy* matrix and its elements are operators that act on \mathbb{C}^{2^N} . In order to derive the explicit form of \mathcal{T} it is convenient to regard the space on which \mathcal{T} acts

$$\mathcal{H}_N = \prod_{n=1}^N \mathfrak{h}_n, \quad \mathfrak{h}_n \approx \mathbb{C}^2. \quad (2.7)$$

With the Pauli matrices³ taken as a basis, the Boltzmann weight can be written as

$$R_{\alpha}^{\alpha'}(\gamma, \gamma') = \sum_{i,j=1}^4 w_{ij} \sigma_{\gamma'\gamma}^i \sigma_{\alpha\alpha'}^j. \quad (2.8)$$

Define the *local L-operator*

$$L_n = \sum_{i,j=1}^4 w_{ij} \sigma_n^i \sigma_n^j \quad (2.9)$$

³ σ^4 denotes the identity matrix.

with σ_n^j being matrices in \mathcal{H}_N

$$\sigma_n^j = 1 \otimes 1 \otimes \cdots \otimes 1 \underbrace{\otimes \sigma_n^j}_{\text{site } n} \otimes 1 \otimes \cdots \otimes 1 \quad (2.10)$$

that only act non-trivially on site n . Thus, the L -operator has the form of a 2×2 -matrix with operators in \mathcal{H}_N as elements

$$L_n = \begin{pmatrix} \hat{\alpha}_n & \hat{\beta}_n \\ \hat{\gamma}_n & \hat{\delta}_n \end{pmatrix}. \quad (2.11)$$

For the monodromy matrix \mathcal{T} this results into

$$\mathcal{T} = L_1 \cdots L_N. \quad (2.12)$$

It follows

$$\mathcal{T} = \begin{pmatrix} A & B \\ C & D \end{pmatrix}, \quad T = A + B. \quad (2.13)$$

A, B, \dots are of the same operator-type as $\hat{\alpha}_n, \hat{\beta}_n, \dots$. We want to derive the commutation of any two transfer matrices from a *local* condition known as the *Yang-Baxter equations* (YBE, 2.14). Assume it exists a non-singular matrix⁴ R . We require

$$R [L_n \otimes L'_n] = [L'_n \otimes L_n] R \quad (2.14)$$

and need the expression for the tensor product of two monodromy matrices \mathcal{T} and \mathcal{T}'

$$\mathcal{T} \otimes \mathcal{T}' = \begin{pmatrix} AT' & BT' \\ CT' & DT' \end{pmatrix}. \quad (2.15)$$

The elements of \mathcal{T}' are accordingly A', B', \dots . So $\mathcal{T} \otimes \mathcal{T}'$ has 2×2 -matrices as elements. We have

$$\begin{aligned} & R (\mathcal{T} \otimes \mathcal{T}') R^{-1} \\ &= R \{ (L_1 \otimes L'_1) \cdots (L_N \otimes L'_N) \} R^{-1} \\ &= R (L_1 \otimes L'_1) R^{-1} R (L_2 \otimes L'_2) R^{-1} \cdots R (L_N \otimes L'_N) R^{-1} \\ &\stackrel{2.14}{=} \underbrace{(L'_1 \otimes L_1)} \cdots (L'_N \otimes L_N) = \mathcal{T}' \otimes \mathcal{T}. \end{aligned} \quad (2.16)$$

From (2.16) follows

$$\mathcal{T} \otimes \mathcal{T}' = R^{-1} \mathcal{T}' \otimes \mathcal{T} R \quad (2.17)$$

and with cyclic exchange under the trace

$$\text{trace } \mathcal{T} \otimes \mathcal{T}' = \text{trace } R^{-1} \mathcal{T}' \otimes \mathcal{T} R = \text{trace } \mathcal{T}' \otimes \mathcal{T}. \quad (2.18)$$

This is already the result because $\text{trace } \mathcal{T} \otimes \mathcal{T}' = AA' + AD' + DA' + DD' = (A + D)(A' + D') = \mathcal{T} \cdot \mathcal{T}'$. In this way the Yang-Baxter equations (2.14) are a *sufficient* condition for $[\mathcal{T}, \mathcal{T}'] = 0$.

If we allow for $q = 2$ at the vertex we get 16 different configurations. This so-called

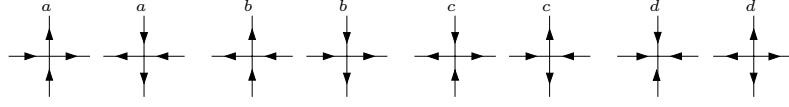


Figure 2.4.: Eight-vertex model

sixteen-vertex model is not exactly solvable because it has no R -matrix. However, in case of the eight-vertex model without external magnetic field such a matrix exists. Because of the system being invariant under reversion of arrows each two combinations lead to one Boltzmann weight (see fig. 2.4). Now write down

$$L_n = \sum_{j=1}^4 w_j \sigma^i \sigma_n^j, \quad L'_n = \sum_{j=1}^4 w'_j \sigma^i \sigma_n^j, \quad (2.19)$$

where

$$w_1 = \frac{c+d}{2}, \quad w_2 = \frac{c-d}{2}, \quad w_3 = \frac{a-b}{2}, \quad w_4 = \frac{a+b}{2}. \quad (2.20)$$

The weights of the primed model are respectively a', b', c' and d' . We try to find the R -matrix in the form

$$R = \mathcal{P} \sum_{j=1}^4 w''_j \sigma^j \otimes \sigma^j. \quad (2.21)$$

\mathcal{P} is the permutation matrix in \mathbb{C}^4

$$\mathcal{P}(e \otimes f) = f \otimes e. \quad (2.22)$$

Inserting (2.21) and (2.22) in the Yang-Baxter equations (2.14) we get six independent equations. Considering the coefficients w''_j unknown we have the following solvability condition

$$\begin{aligned} \Delta &:= \frac{w_j^2 - w_k^2}{w_l^2 - w_n^2} \text{ invariant under the exchange } w \rightarrow w' \\ &(i, j, k, n \text{ are cyclic permutations of } \{1, 2, 3, 4\}), \text{ or} \\ \Delta &:= \frac{a^2 + b^2 - c^2 - d^2}{2(ab + cd)} \text{ invariant under the exchange } a \rightarrow a' \dots \\ \Gamma &:= \frac{ab - cd}{ab + cd}. \end{aligned} \quad (2.23)$$

A parameterization that fulfills such a condition is

$$\begin{aligned} a &= -i\rho\Theta(i\lambda)H \left[\frac{1}{2}i(\lambda - v) \right] \Theta \left[\frac{1}{2}i(\lambda + v) \right] \\ b &= -i\rho\Theta(i\lambda)\Theta \left[\frac{1}{2}i(\lambda - v) \right] H \left[\frac{1}{2}i(\lambda + v) \right] \\ c &= -i\rho H(i\lambda)\Theta \left[\frac{1}{2}i(\lambda - v) \right] \Theta \left[\frac{1}{2}i(\lambda + v) \right] \\ d &= i\rho H(i\lambda)H \left[\frac{1}{2}i(\lambda - v) \right] H \left[\frac{1}{2}i(\lambda + v) \right] \end{aligned} \quad (2.24)$$

⁴ R is the quantum- R -matrix.

where the definitions of the elliptic functions are given in appendix A.

The “anti-ferroelectric” regime of the eight-vertex model is given by the restrictions

$$0 < k < 1, \quad 0 < \frac{\gamma}{2} < K', \quad -\frac{\gamma}{2} < v < \frac{\gamma}{2}. \quad (2.25)$$

The explanation how to derive such a parameterization from (2.23) will be given in appendix B.

The model above is non-critical for $0 < k < 1$. It is obvious from the definition of d that for $k \rightarrow 0$ d is zero and in that way a six-vertex model is achieved. The limit $k \rightarrow 1$ also leads to only six vertices which is not obvious in this parameterization. It should only be remarked here that this limit is the relevant one for the critical XXZ -chain on which we are focussed in this work.⁵

⁵There are certain similarity transformations that will transform the parameterization above into a convenient one for the limit $k \rightarrow 1$ [8].

2.2. Correlation lengths in the transfer matrix approach

The one-dimensional Ising model [3] is one of the simplest models that can be treated by the transfer matrix approach. So it is suitable in order to explain how to calculate correlation lengths using this method. Regard a chain of length L filled with classical spins $\sigma_i = \pm 1$ on every site i . The partition function is given by

$$\mathcal{Z}_L = \sum_{\sigma_1, \sigma_2, \dots, \sigma_L} e^{K \sum_{\langle i, j \rangle} \sigma_i \sigma_j + h \sum_i \sigma_i} \quad (2.26)$$

with periodic boundary conditions $\sigma_{L+1} = \sigma_1$. $\langle i, j \rangle$ denotes the summation over nearest neighbours. $\mathcal{Z} = \text{trace } T^L$ holds with the 2×2 transfer matrix

$$T = \begin{pmatrix} e^{K+h} & e^{-K} \\ e^{-K} & e^{K-h} \end{pmatrix}. \quad (2.27)$$

Consider a local operator Θ_i on the lattice site i only depending on σ_i and its expectation value

$$\langle \Theta_1 \Theta_{r+1} \rangle = \frac{\sum_{\sigma_1, \sigma_2, \dots, \sigma_L} \Theta(\sigma_1) \Theta(\sigma_{r+1}) e^{K \sum_{\langle i, j \rangle} \sigma_i \sigma_j + h \sum_i \sigma_i}}{\sum_{\sigma_1, \sigma_2, \dots, \sigma_L} e^{K \sum_{\langle i, j \rangle} \sigma_i \sigma_j + h \sum_i \sigma_i}}. \quad (2.28)$$

That can be expressed in terms of the transfer matrix as

$$\begin{aligned} \langle \Theta_1 \Theta_{r+1} \rangle &= \frac{\sum_{\sigma_1, \sigma_2, \dots, \sigma_L} [\Theta(\sigma_1) T_{\sigma_1 \sigma_2} T_{\sigma_2 \sigma_3} \cdots T_{\sigma_r \sigma_{r+1}} \Theta(\sigma_{r+1}) T_{\sigma_{r+1} \sigma_{r+2}} \cdots]}{\text{trace } T^L} \\ &= \frac{\text{trace } (\boldsymbol{\sigma} T^r \boldsymbol{\sigma} T^{L-r})}{\text{trace } T^L}. \end{aligned} \quad (2.29)$$

$\boldsymbol{\sigma}$ is a diagonal matrix with the elements $\sigma_{\sigma\sigma'} = \Theta(\sigma) \cdot \delta(\sigma\sigma')$. Inserting two complete sets of eigenvectors $\mathbf{1} = \sum_i |\psi_i\rangle \langle \psi_i|$ of the transfer matrix leads to

$$\begin{aligned} \langle \Theta_1 \Theta_{r+1} \rangle &= \frac{\sum_{ij} \langle \psi_i | \boldsymbol{\sigma} T^r | \psi_j \rangle \langle \psi_j | \boldsymbol{\sigma} T^{L-r} | \psi_i \rangle}{\sum_i \langle \psi_i | T^L | \psi_i \rangle} \\ &= \frac{\sum_{ij} |\langle \psi_i | \boldsymbol{\sigma} | \psi_j \rangle|^2 \Lambda_j^r \Lambda_i^{L-r}}{\sum_i \Lambda_i^L} \\ &= \sum_j |\langle \psi_1 | \boldsymbol{\sigma} | \psi_j \rangle|^2 \cdot \left(\frac{\Lambda_j}{\Lambda_0} \right)^r \\ &= |\langle \psi_1 | \boldsymbol{\sigma} | \psi_1 \rangle|^2 + |\langle \psi_1 | \boldsymbol{\sigma} | \psi_2 \rangle|^2 \cdot \left(\frac{\Lambda_1}{\Lambda_0} \right)^r + \dots \end{aligned} \quad (2.30)$$

$\{\Lambda_i\}$ are the eigenvalues of the transfer matrix, Λ_0 the largest one. Taking for granted that exists a gap between the largest and second-largest eigenvalue the largest eigenvalue

dominates in the limit $L \rightarrow \infty$ of (2.30). Supposing typical Ornstein-Zernike behaviour

$$g(x) \sim x^{-\tau} e^{-x/\xi}, \quad x \rightarrow \infty \quad (2.31)$$

concerning the decay of correlations and comparing with (2.30) the leading correlation length is to be identified with

$$\xi^{-1} = -\ln(\Lambda_1/\Lambda_0). \quad (2.32)$$

2.3. The six-vertex model

In this section we want to have a closer look at the classical six-vertex model because it can be mapped onto the XXZ -Heisenberg chain at zero temperature. Within the framework of the quantum transfer matrix one needs a modified six-vertex model in order to derive the thermodynamics of the XXZ -chain.

2.3.1. Origin of the six-vertex model

At first consider models that describe ice. Oxygen atoms form a three-dimensional lattice with coordination number 4 and between each adjacent pair of atoms is a hydrogen atom. Each ion is located near one or the other end of the bond on which it lies. Slater (1941) proposed (on the basis of local electric neutrality) that the ions should satisfy the *ice rule*: *Of the four ions surrounding each atom, two are close to it, and two are removed from it, on their respective bonds.* As we can only achieve exact solvability in two dimensions we regard the following auxiliary model:

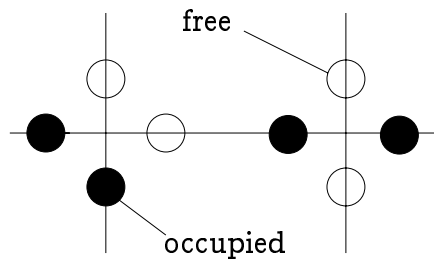


Figure 2.5.: Two-dimensional model for ice

Thus, local neutrality requires exactly two H -atoms per vertex what results in six possible vertex configurations. Now replace the combination free/occupied on a bond by \rightarrow and occupied/free by \leftarrow . Then the possible configurations can be represented as in fig. 2.6. Because there is no external electric field that breaks the arrow flip invariance two configurations at a time lead to one Boltzmann weight. The Yang-Baxter equations in terms of

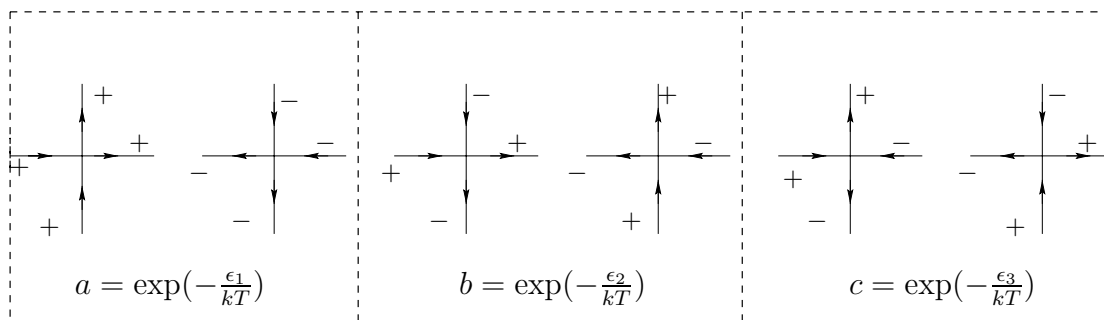


Figure 2.6.: Symmetric six-vertex model

urations at a time lead to one Boltzmann weight. The Yang-Baxter equations in terms of

those weights read

$$\sum_{\mu_1 \mu_2 \mu_3} R_{\sigma_3}^{\mu_3}(\sigma_2, \mu_2) R_{\mu_3}^{\sigma_4}(\sigma_1, \mu_1) R_{\mu_2}^{\sigma_5}(\mu_1, \sigma_6) = \sum_{\mu_1 \mu_2 \mu_3} R_{\sigma_2}^{\mu_2}(\sigma_1, \mu_1) R_{\sigma_3}^{\mu_3}(\mu_1, \sigma_6) R_{\mu_3}^{\sigma_4}(\mu_2, \sigma_5) \quad (2.33)$$

with the graphical representation in fig. 2.7. The rules of translating the graphs into the

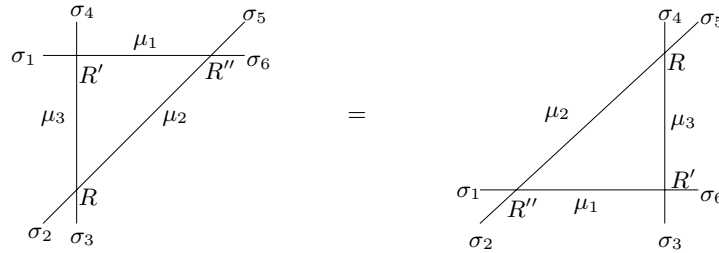


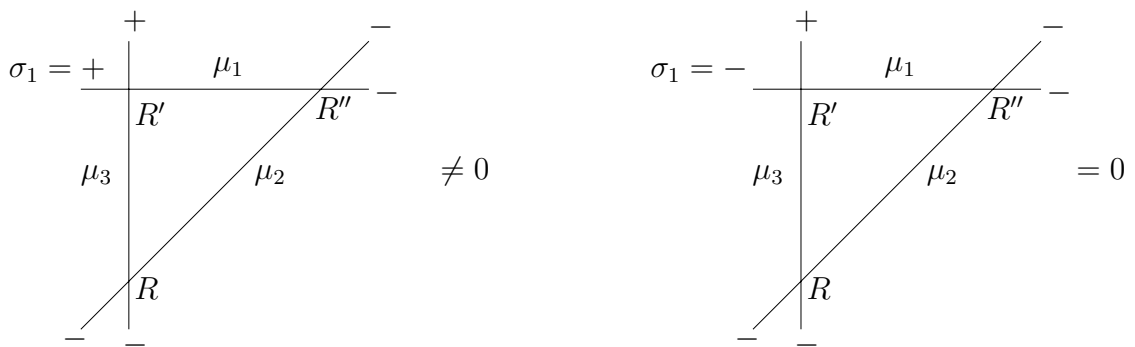
Figure 2.7.: Symmetric six vertex model

equations are

1. The boundary spins $\{\sigma_i\}$ are fixed.
2. Summation over internal degrees of freedom $\{\mu_i\}$ of products of local Boltzmann weights.

In order to solve these equations consider R and R' with the weights a, b, c, a', b', c' as given and search for R'', a'', b'' and c'' . It has to be remarked that only a set $\{\sigma_i\}$ with $\sigma_1 + \sigma_2 + \sigma_3 = \sigma_4 + \sigma_5 + \sigma_6$ leads to non-trivial equations.

Example: Note that every single Boltzmann weight in such a product must be non-zero.



1. First graph:

1. $\mu_3 = \mu_2 = + \Rightarrow \mu_1 = +$ and all weights are unequal to zero
2. $\mu_3 = \mu_2 = - \Rightarrow \mu_1 = -$ and all weights are unequal to zero.

2. Second graph:

1. $\mu_1 = \mu_2 = + \Rightarrow \mu_3 = - \Rightarrow R = 0$
2. $\mu_1 = \mu_2 = - \Rightarrow \mu_3 = + \Rightarrow R = 0$

The condition above reduces the number of non-trivial equations to 20. Arrow flip invariance halves this number. Exchanging $\sigma_1 \leftrightarrow \sigma_6$, $\sigma_2 \leftrightarrow \sigma_5$ and $\sigma_3 \leftrightarrow \sigma_4$ transforms the right-hand side of equation (2.33) into its left-hand side. Thus there are three pairs of equivalent equations left.

Graphically

$$ab'c'' = ba'c'' + cc'b'' \quad (2.34)$$

$$cb'a'' = ca'b'' + bc'c''. \quad (2.35)$$

These equations are linear in a'' , c'' and c'' , if and only if

$$\frac{a^2 + b^2 - c^2}{2ab} = \frac{a'^2 + b'^2 - c'^2}{2a'b'} =: \Delta \quad (2.36)$$

there exists a non-trivial solution.

It is suitable to find a parameterization of the weights a , b and c in terms of new parameters ϱ , λ and u in order to guarantee $\Delta = \Delta(\lambda)$. The derivation of such a parameterization will be given in appendix B. There are three different cases for the parameterization that have to be distinguished being explained in the next section.

2.4. Classification of phases

As a matter of fact the free energy of the six-vertex model takes a different form depending on whether $\Delta > 1$, $1 > \Delta > -1$, or $-1 > \Delta$. In terms of the Boltzmann weights a , b and c it follows from (2.36) that there are four cases to consider, the four regions that are shown in fig. 2.8 [8].

1. Ferroelectric phase: $a > b + c$ (region I)

In this case $\Delta > 1$ and $\epsilon_1 < \epsilon_3, \epsilon_5$. Thus, the lowest energy state is one in which all vertices are of type 1, or all of type 2. Either all arrows point up or to the right, or all point down or to the left. Hence, at very low temperature the system is ferroelectrically ordered (all parallel arrows point the same way), and the free energy f is equal to ϵ_1 . This means that excited states give a negligible contribution to the partition function and throughout the region I the system is frozen on one or other of the ground states. Or in other words, we have complete ferroelectric order.

2. Ferroelectric Phase: $b > a + c$ (region II)

This is the same as case I, except that now it is vertex types 3 and 4 that are dominant. There is complete ferroelectric order: Effectively all arrows either point up and to the left, or they all point down and to the right.

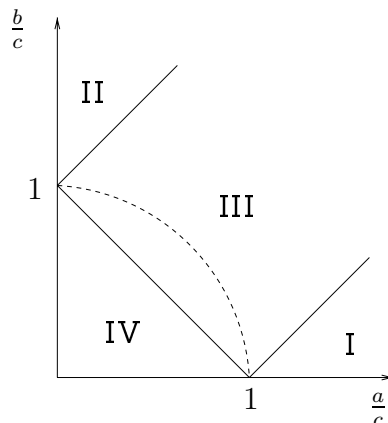


Figure 2.8.: The phase diagram of the zero field ice-type model in terms of the Boltzmann weights a, b, c . The dashed circular quadrant corresponds to the free-fermion case where $\Delta = 0$ and the model can be solved by Pfaffians [8].

3. Disordered phase: $a, b, c > \frac{1}{2}(a + b + c)$ (region III)

This is the case when $-1 < \Delta < 1$. It includes the infinite temperature case $a = b = c = 1$, so one might expect the system to be disordered. This is true in the sense that all correlations decay to zero with increasing distance r .

However, if $a^2 = b^2 = c^2$ (when the weight must lie in this region III) it follows that $\Delta = 0$. Then the model can be solved by Pfaffians [8]. The correlations decay as an inverse power law in r , rather than exponential. The correlation length is therefore infinite, so the system is not disordered in the usual sense.

The ice-type model is a special case of the eight-vertex model [8]. In this region III, the ice-type model corresponds to the eight-vertex model being at a critical temperature. There are infinitely many eigenvalues of the transfer matrix which are degenerate with the maximum one. There is no spontaneous order, but the correlation length is infinite. The ice-type model therefore has a very unusual property: It is critical for all a, b, c in the region III.

4. Anti-ferroelectric phase: $c > a + b$ (region IV)

In this case $\Delta < -1$ and $\epsilon_5 < \epsilon_1, \epsilon_3$. The lowest energy is the one where all neighbouring arrows on a straight line of the lattice point in opposite directions. This gives two possible lowest energy states. At sufficiently low temperature we therefore expect the system to be in an ordered state with this anti-ferroelectric order.

As the weights in region I and II can be parametrized in the same way we are led to three different parameterizations (derivation in appendix B)

1. Region I + II (ferroelectric, non-critical)

$$\begin{aligned} a, b, c &= \varrho \sinh(\lambda + u), \varrho \sinh(u), \varrho \sinh(\lambda) \\ u, \lambda &> 0 \text{ (for positive weights)} \\ \Delta &= \cosh(\lambda). \end{aligned}$$

2. Region IV (anti-ferroelectric, non-critical)

$$\begin{aligned}
 a, b, c &= \varrho \sinh(\lambda - u), \varrho \sinh(u), \varrho \sinh(\lambda) \\
 0 < u < \lambda & \text{ (for positive weights)} \\
 \Delta &= -\cosh(\lambda).
 \end{aligned}$$

3. Region III (anti-ferroelectric, critical)

$$\begin{aligned}
 a, b, c &= \varrho \sin(\lambda - u), \varrho \sin(u), \varrho \sin(\lambda) \\
 0 < u < \lambda \text{ and } 0 < \lambda < \pi & \text{ (for positive weights)} \\
 \Delta &= -\cos(\lambda).
 \end{aligned}$$

In all cases Δ does not depend on u . The weights R'' are generated by the parameters λ and $u'' = u' - u$ (simple difference type). λ is often referred to as *crossing parameter* and u is the *spectral parameter*.

2.5. The relation between quantum chains and two-dimensional classical models

Certain one-dimensional Hamiltonians can be embedded in a family of two-dimensional classical vertex models. Sometimes the partition function of the quantum mechanical model can be calculated in terms of the transfer matrix of the classical model. This section deals with the necessary conditions on the vertex model in this approach. In the ordinary definition of a statistical model one does not only consider a special set of Boltzmann weights, rather a whole family of weights depending on a spectral parameter $v \in \mathbb{C}$ is of interest. It follows that the Boltzmann weights R as well depend on v , $R = R(v)$. In addition, we may assume that a special value $v = \lambda$ of the spectral parameter v exists such that the vertices decouple. That means

$$R_{\alpha}^{\beta}(\mu, \nu) = \delta_{\alpha}^{\nu} \delta_{\beta}^{\mu}. \quad (2.37)$$

This expression is only well defined if quantum and auxiliary space are isomorphic

$$\mathfrak{h} \equiv V. \quad (2.38)$$

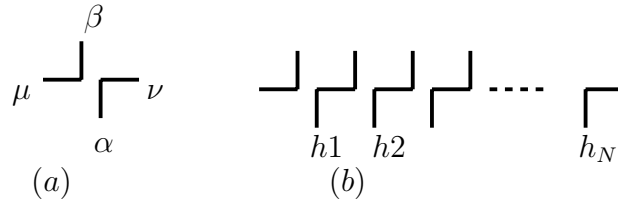


Figure 2.9.: Decoupling (a) at a single vertex, (b) of the transfer matrix

Figure 2.9 shows that decoupling means translation of one lattice site to the right which is the action of the translation operator

$$T(\lambda) = T_R, \quad (T_R)_{\alpha\beta} = \prod_i \delta_{\alpha_i \beta_{i+1}}. \quad (2.39)$$

Consider the derivative of $T(v)$ at the decoupling point $v = \lambda$ ⁶

$$\begin{aligned} & \left(\frac{d}{dv} T(v) \Big|_{v=\lambda} \right)_{\alpha\beta} = \\ & \left(\text{trace}_V \left\{ \sum_{i=1}^L \left(\prod_{j=1}^{i-1} R_j(\lambda) \cdot R'_i(\lambda) \cdot \prod_{j=i+1}^L R_j(\lambda) \right) \right\} \right)_{\alpha\beta} \\ & = \delta_{\mu\beta_1} \delta_{\alpha_1\beta_2} \cdots \delta_{\alpha_{i-2}\beta_{i-1}} \left(R_{\alpha_i}^{\beta_i}(\alpha_{i-1}, \beta_{i+1}) \right)'(\lambda) \delta_{\alpha_{i+1}\beta_{i+2}} \cdots \delta_{\alpha_L\mu}. \end{aligned}$$

Thus,

$$(T^{-1}(\lambda) \cdot T'(\lambda))_{\alpha\beta} = \sum_i \left\{ \prod_{j \neq i, i+1} \delta_{\alpha_j \beta_j} \right\} \left(R_{\alpha_i}^{\beta_{i+1}}(\beta_i, \alpha_{i+1}) \right)'(\lambda). \quad (2.40)$$

⁶Here the multiplication denotes $(R \cdot \bar{R})_{(\alpha\bar{\alpha})(\beta, \bar{\beta})}^{\mu\nu} = R_{\alpha}^{\beta}(\mu, \lambda) \bar{R}_{\bar{\alpha}}^{\bar{\beta}}(\lambda, \nu)$.

Note that the right-hand side consists of a sum of *local* operators $h_{i,i+1}$ that act non-trivially only on $\mathfrak{h}_i \otimes \mathfrak{h}_{i+1}$. The left-hand side can formally be written as the derivative of the logarithm of the transfer matrix

$$(\ln T)'(\lambda) = \sum_i h_{i,i+1} \equiv H. \quad (2.41)$$

Equation (2.41) shows the relation between the transfer matrix of the classical model and a quantum mechanical system with nearest neighbour interaction explicitly. If the transfer matrix is diagonalized with eigenvalues $\{\Lambda_k\}$, the spectrum of the Hamiltonian is known by $(\ln \Lambda_k)'(\lambda) = E_k$. Within the scope of this work however, we are interested in physical quantities at finite temperatures. So the question arises, under what conditions a quantum mechanical partition function can be calculated by means of the transfer matrix of the underlying vertex model. A Taylor expansion of the transfer matrix at the decoupling point $v = \lambda$ can be performed

$$T(\lambda - v) = T_R \cdot e^{vH + \mathcal{O}(v^2)}. \quad (2.42)$$

Another set of Boltzmann weights can be created by rotating the weights by 90° (see fig. 2.10). In this way a second family of transfer matrices is generated and let us assume that both families obey the Yang-Baxter equations (2.14) which are the sufficient conditions for the integrability of the vertex model. Given that the second family of transfer matrices $\bar{T}(v)$ decouples at the point $v = \bar{\lambda}$ and meets the same properties as above

$$\bar{T}(\bar{\lambda}) = T_R^{-1}, \quad (\ln \bar{T})' = H, \quad (2.43)$$

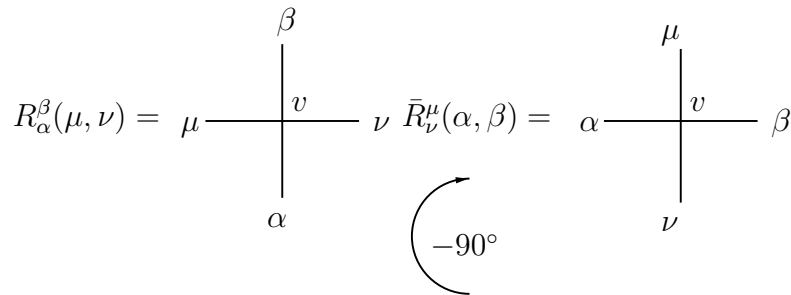


Figure 2.10.: Rotated vertex

\bar{T} can also be expanded

$$\bar{T}(\bar{\lambda} \mp v) = T_R^{-1} \cdot e^{-vH + \mathcal{O}(v^2)}. \quad (2.44)$$

At first sight this assumption may seem quite contrived, but the Boltzmann weights of most “good-natured” models possess certain symmetries which allow for example to chose $T \equiv \bar{T}$ and $\bar{\lambda} = -\lambda$. This is the case for the eight-vertex model.

Regard the first order expression

$$T(\lambda - v)\bar{T}(\bar{\lambda} \mp v) = e^{2vH + \mathcal{O}(v^2)} \quad (2.45)$$

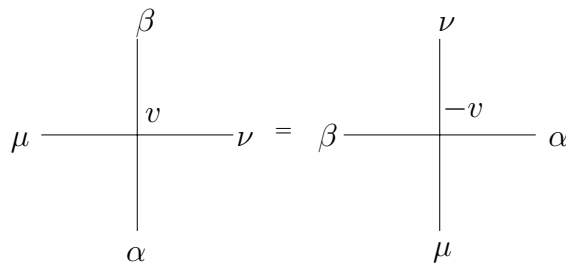


Figure 2.11.: Graphical representation of the “crossing” symmetry

and introduce the Trotter number M with $v = \frac{\beta}{M}$ such that raising (2.45) to the power of $\frac{M}{2}$ gives the quantum mechanical partition function

$$\begin{aligned} \left(T\left(\lambda - \frac{\beta}{M}\right) \bar{T}\left(\bar{\lambda} \mp \frac{\beta}{M}\right) \right)^{\frac{M}{2}} &= e^{-\beta H + \mathcal{O}(1/M)}, \\ Z &= \lim_{M \rightarrow \infty} \text{trace} \left(T\left(\lambda - \frac{\beta}{M}\right) \bar{T}\left(\bar{\lambda} \mp \frac{\beta}{M}\right) \right)^{\frac{M}{2}}. \end{aligned} \quad (2.46)$$

This is the Trotter-Suzuki mapping of a one-dimensional quantum mechanical system on a two-dimensional classical one [11]. Obviously, the classical model is inhomogeneous with alternating rows.

2.5.1. The quantum transfer matrix of the six- and eight-vertex model

The Boltzmann weights of the eight-vertex model (2.24) possess the “crossing” symmetry described above in the way that the weights are invariant under a combined rotation by 90° and the substitution of v by $-v$. We next consider the row-to-row transfer matrix $T(v)$ as a function of the spectral parameter v , holding k and λ fixed. $T(v)$ is a family of commuting matrices [8] with two decoupling points $v = \pm\lambda$. Hence (see above),

$$H_{XYZ} = \text{const} \pm (\ln T)'(\pm\lambda). \quad (2.47)$$

The related one-dimensional quantum chain is the XYZ -chain describing the exchange interaction of $\frac{1}{2}$ -spins

$$H_{XYZ} = -\frac{1}{2} \sum_{j=1}^L \left(J_x \sigma_j^x \sigma_{j+1}^x + J_y \sigma_j^y \sigma_{j+1}^y + J_z \sigma_j^z \sigma_{j+1}^z \right) \quad (2.48)$$

with cyclic boundary conditions $\sigma_{L+1} = \sigma_1$. The interaction coefficients are functions of k and λ

$$\begin{aligned} J_x &= \frac{1 + k \operatorname{snh}^2 \lambda}{2 \operatorname{snh} \lambda}, & J_y &= \frac{1 - k \operatorname{snh}^2 \lambda}{2 \operatorname{snh} \lambda} \\ J_z &= -\frac{\operatorname{cnh} \lambda \operatorname{dnh} \lambda}{2 \operatorname{snh} \lambda} \end{aligned} \quad (2.49)$$

which reads in the critical limit $k \rightarrow 1$

$$J_x = \frac{1}{\sin \gamma}, \quad J_y = \frac{\cos \gamma}{\sin \gamma}, \quad J_z = -\frac{1}{\sin \gamma} \quad (\gamma = 2\lambda). \quad (2.50)$$

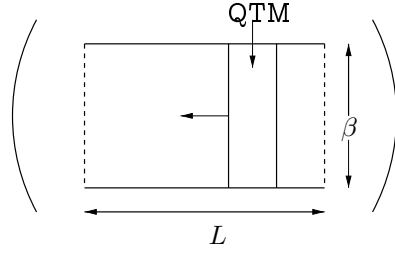


Figure 2.12.: Quantum transfer matrix

We get the quantum mechanical partition function by the explained reasoning

$$Z = \lim_{M \rightarrow \infty} \text{tr} \left[T \left(-\lambda + \frac{\beta}{M} \right) T \left(\lambda - \frac{\beta}{M} \right) \right]^{\frac{M}{2}}. \quad (2.51)$$

For the calculation of this partition function the column-to-column transfer matrix is best adapted. This “vertical” transfer matrix (or *quantum transfer matrix* QTM) is nothing but a row-to-row transfer matrix of an inhomogeneous eight-vertex model with alternating spectral parameters $\pm(\lambda - \frac{\beta}{M})$. This is easily understood from the crossing symmetry, cf. fig. 2.11. Thus we obtain the representation

$$Z = \lim_{M \rightarrow \infty} \text{tr} T^L \left(\lambda - \frac{\beta}{M}, -\lambda + \frac{\beta}{M} \right) \quad (2.52)$$

where $T(\dots, \dots)$ denotes the inhomogeneous transfer matrix with length M . The free energy per site is $f = \frac{F}{L} = -\frac{1}{\beta} \lim_{L \rightarrow \infty} \frac{\ln Z}{L}$ where first the limit $M \rightarrow \infty$ has to be taken and then $L \rightarrow \infty$. We are allowed to interchange these limits due to the theorems in [11, 12]. We come to the conclusion

$$f = -\frac{1}{\beta} \lim_{M \rightarrow \infty} \ln \Lambda_{max} \quad (2.53)$$

where Λ_{max} denotes the largest eigenvalue of the inhomogeneous transfer matrix $T(\dots, \dots)$. All other eigenvalues of $T(\dots, \dots)$ are separated by a gap which is finite for finite temperature even in the limit $M \rightarrow \infty$. This is an important difference to and an advantage over the transfer matrices on the lhs. of (2.51). The last comment in this section is dedicated to the study of the thermodynamics of the quantum chain in presence of an external magnetic field h coupled to the spin $S = \sum_{j=1}^L S_j$ where S_j denotes a certain component of the j th spin, for instance S_j^z . This changes (2.46) only trivially

$$\left[T \left(-\lambda + \frac{\beta}{M} \right) T \left(\lambda - \frac{\beta}{M} \right) \right]^{\frac{M}{2}} \cdot e^{\beta h S} = e^{-\beta(H-hS) + \mathcal{O}(\frac{1}{M})}. \quad (2.54)$$

On the lattice, the equivalent two-dimensional model is modified in a simple way by a horizontal seam. Each vertical bond of this seam carries an individual Boltzmann weight $e^{\pm \frac{\beta h}{2}}$, if $S_j = \pm \frac{1}{2}$, which indeed describes the action of the operator

$$e^{\beta h S} = \prod_{j=1}^L e^{\beta h S_j}. \quad (2.55)$$

Consequently, the vertical transfer matrix is modified by an h -dependent boundary condition. It turns out [7] that these modifications can still be treated exactly if the additional operators acting on the bonds belong to the symmetries of the model. Therefore, a magnetic field can not be studied unless limiting cases of the XYZ -chain are investigated such as the XXZ -chain.

2.6. The algebraic Bethe ansatz

The purpose of the algebraic Bethe ansatz is the diagonalization of the transfer matrix by means of explicit construction of its eigenstates. The procedure of diagonalization can be described as follows:

- At first search for a pseudo-vacuum state which is a simple eigenstate of the transfer matrix T which annihilates most of the operator-valued entries of the monodromy matrix \mathcal{T} . Thus, those operators are called annihilators.
- Now entries of the monodromy matrix that do not annihilate the pseudo-vacuum state are applied to that state. These operators will be referred to as generators.
- From the Yang-Baxter equations we get the commutators for the operator-valued entries of \mathcal{T} and under certain conditions, expressed by the so-called *Bethe ansatz equations* (BAE), we find the eigenstates of T .

Let us employ this procedure in order to get the BAE of the six-vertex model. Here the formalism developed in section 2.1 is used. The local L -operators L_i of the six-vertex model are defined as

$$L_i = \begin{pmatrix} \frac{a+b}{2} + \frac{a-b}{2}\sigma_i^z & c\sigma_i^+ \\ c\sigma_i^- & \frac{a+b}{2} - \frac{a-b}{2}\sigma_i^z \end{pmatrix} \quad (2.56)$$

with a, b, c given in 2.4 depending on the considered phase.⁷ The monodromy-matrix is (see section 2.1)

$$\mathcal{T} = L_1 \cdots L_N. \quad (2.57)$$

Now \mathcal{T} has to be applied to $|\Omega\rangle$, the pseudo-vacuum state. Here we consider a vacuum of up-pointing spins and the actions of the operators appearing in the following are basically connected to spin-flips. $|\Omega\rangle$ is annihilated by one of the off-diagonal elements and is also an eigenstate of the diagonal elements

$$|\Omega\rangle = \bigotimes_i^N |+\rangle_i. \quad (2.58)$$

If one applies \mathcal{T} on that state it becomes triangular

$$\mathcal{T}|\Omega\rangle = \begin{pmatrix} a^N |\Omega\rangle & 0 \\ B|\Omega\rangle & b^N |\Omega\rangle \end{pmatrix} \quad (2.59)$$

and we finally get for the transfer matrix T

$$T|\Omega\rangle = \text{trace}_V \mathcal{T}|\Omega\rangle = (a^N + b^N)|\Omega\rangle. \quad (2.60)$$

Therefore, $|\Omega\rangle$ is an eigenstate of T .

Now we use the operator B as creation operator for excitations and we claim that this

⁷As a reminder: $\sigma^+ = \sigma^x + i\sigma^y$ and $\sigma^- = \sigma^x - i\sigma^y$.

new state $|\Omega_1(v)\rangle := B(v)|\Omega\rangle$ (“one-particle state”) shall be again an eigenstate of $T(u) = A(u) + D(u)$ (see 2.13). What we need now is the knowledge of the operator algebra so that we can interchange $B(v)$ with $A(u)$ and $D(u)$ because we know everything about the action of $A(u)$ and $D(u)$ on $|\Omega\rangle$. This algebra can be drawn out of the YBE. But first of all we want to give a graphical representation of the YBE [21]

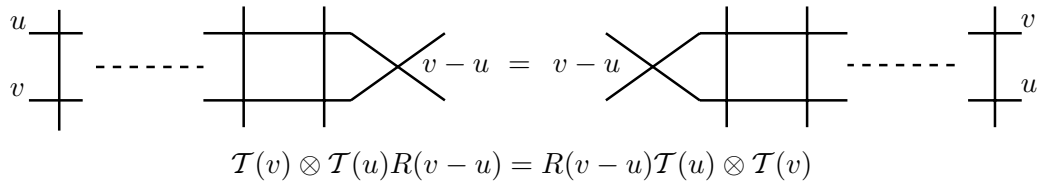


Figure 2.13.: Graphical YBE

By fixing the exterior spins we get all the commutators we need for interchanging the operators. We shall begin with the B -operator illustrated in fig. 2.14.

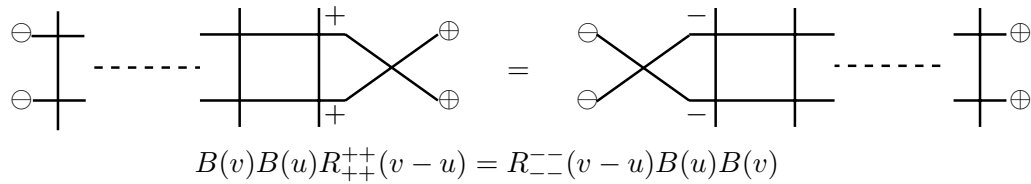


Figure 2.14.: B -operators

From 2.14 we get

$$[B(u), B(v)] = 0. \tag{2.61}$$

Now we look at A and B and use again the graphical representation shown in fig. 2.15. We gain

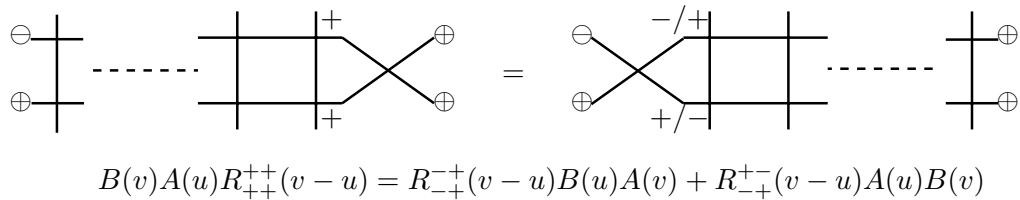


Figure 2.15.: A -operators

$$A(u)B(v) = \frac{a(v-u)}{b(v-u)}B(v)A(u) - \frac{c(v-u)}{b(v-u)}B(u)A(v). \tag{2.62}$$

And in the same way the last one shown in fig. 2.16 which reads in detail

$$D(u)B(v) = \frac{a(u-v)}{b(u-v)}B(v)D(u) - \frac{c(u-v)}{b(u-v)}B(u)D(v). \tag{2.63}$$

We have now derived all relations and need to apply $T(u)$ to $|\Omega_1\rangle$. It holds

$$B(v)D(u)R_{+-}^+(v-u) + D(v)B(u)R_{-+}^+(v-u) = R_{-+}^-(v-u)B(u)D(v)$$

Figure 2.16.: D -operators

$$T(u)|\Omega_1(v)\rangle = \left(\alpha(u) \frac{a(v-u)}{b(v-u)} + \delta(u) \frac{a(u-v)}{b(u-v)} \right) |\Omega_1(v)\rangle - \left(\alpha(v) \frac{c(v-u)}{b(v-u)} + \delta(v) \frac{c(u-v)}{b(u-v)} \right) B(u)|\Omega\rangle, \quad (2.64)$$

where we have used the abbreviations $a^N = \alpha$, $b^N = \delta$. For $|\Omega_1(v)\rangle$ being an eigenstate of the transfer matrix the second term in (2.64) has to vanish and the first one gives the eigenvalue

$$\frac{\alpha(v)}{\delta(v)} = -\frac{c(u-v)b(v-u)}{c(v-u)b(u-v)}, \quad (2.65)$$

$$\Lambda(u, v) = \alpha(u) \frac{a(v-u)}{b(v-u)} + \delta(u) \frac{a(u-v)}{b(u-v)}. \quad (2.66)$$

We generalize this to an n -particle state. The argument is quite the same as for just one excitation. We look at the following state

$$|\Omega(v_i)\rangle = \prod_{i=1}^n B(v_i)|\Omega\rangle \quad (2.67)$$

where the numbers v_i by pairs are distinct. If again we demand that this state be an eigenstate of $T(u)$ we get the following set of equations

$$\Lambda(u, v_i) = \alpha(u) \prod_{i=1}^n \frac{a(v_i-u)}{b(v_i-u)} + \delta(u) \prod_{i=1}^n \frac{a(u-v_i)}{b(u-v_i)} \quad (2.68)$$

$$\frac{\alpha(v_i)}{\delta(v_i)} = \prod_{i \neq j}^n -\frac{a(v_i-v_j)}{a(v_j-v_i)} \text{ for } i = 1, \dots, n. \quad (2.69)$$

This constraint gives nothing but the Bethe ansatz equations. We shall state here that one would have obtained the same set of equations by demanding that the eigenvalue be analytic in the whole complex plane

$$\text{Res } \Lambda(u = v_i) = 0 \quad \forall i. \quad (2.70)$$

The explicit expression for the six-vertex model in the anti-ferroelectric and critical regime (using the parameterization given in section 2.4) is

$$\left[\frac{\sinh(\tilde{v}_k + i\frac{\lambda}{2})}{\sinh(\tilde{v}_k - i\frac{\lambda}{2})} \right]^N = - \prod_{j=1}^N \left[\frac{\sinh(\tilde{v}_k - \tilde{v}_j + i\lambda)}{\sinh(\tilde{v}_k - \tilde{v}_j - i\lambda)} \right] \quad (2.71)$$

with the substitution $v_j = \frac{\lambda}{2} + i\tilde{v}_j$. These are the Bethe-ansatz equations (BAE) for the six-vertex model.

2.6.1. Bethe ansatz equation for the quantum transfer matrix

The treatment of inhomogeneous transfer matrices is described in Baxter's book [8]. We content ourselves with quoting the relevant formulae because the treatment of such problems is described precisely in this reference.

The limit $k \rightarrow 1$ in the eight-vertex model leads to the six-vertex model with BAE (2.71). As described above the columns of the quantum transfer matrix possess alternating spectral parameters. This classical model is connected to the critical anti-ferromagnetic XXZ -Heisenberg chain with an external magnetic field. The BAE for that model read

$$p(v_j) = -1 \quad \text{with} \quad p(x) = \frac{1}{\omega^2} \frac{\Phi(x - i\lambda)q(x + 2i\lambda)}{\Phi(x + i\lambda)q(x - 2i\lambda)} \quad (2.72)$$

for every root v_j of this equation and $\omega = e^{\beta h/2}$.

Because of

$$\begin{aligned} \Phi &:= \Phi_1 \cdot \Phi_2, & \Phi_{1/2} &:= \left(\sinh \frac{1}{2}(x \pm x_M) \right)^{\frac{M}{2}}, \\ x_M &= i\frac{\gamma}{2} - i\frac{\beta}{M}, \\ q(x) &:= \prod_{j=1}^{\frac{M}{2}} \sinh(x - v_j) \end{aligned} \quad (2.73)$$

the alternating structure of the quantum transfer matrix is visible in the BAE. With these definitions the eigenvalue $\Lambda(x)$ to the transfer matrix satisfies the equation

$$\Lambda(x)q(x) = s \left[\frac{1}{\omega} \Phi(x - i\frac{\gamma}{2})q(x + i\gamma) + \omega \Phi(x + i\frac{\gamma}{2})q(x - i\gamma) \right]. \quad (2.74)$$

3. The XXZ -Heisenberg model

3.1. Spin models

In order to motivate the relevance of spin models in solid state physics we follow the comprehensive introduction to such models in [41]. The physical properties of solids are determined by the valence electrons of the atoms constituting the solids. If the solid has a crystalline structure the atomic orbitals form bands that are partly or completely filled by valence electrons. If the solid is an insulator normally there are only completely filled or empty bands occurring that do not permit charge excitations for small energies. Therefore, the excitation of an electron or a hole requires a certain minimum of energy expressing that there is a gap for charge excitations. For undoped metallic oxides [42] this is typically the case because the stoichiometric composition ensures an even number of electrons per unit cell which implies filled or half-filled bands. Half-filling arises by twofold spin degeneracy and an uneven number of electrons.

However, systems with half-filled bands often are insulators because of the interaction of the electrons among each other. If this interaction is sufficiently strong the half-filled band splits into a lower and an upper Hubbard band where the lower one is filled and the upper one is empty. This is a so-called Mott-Hubbard insulator. Such a system is described by a Hubbard model at half-filling

$$H = -t \sum_{\langle i,j \rangle, \sigma} c_{i,\sigma}^\dagger c_{j,\sigma} + U \sum_i (n_{i,\uparrow} - 1/2)(n_{i,\downarrow} - 1/2). \quad (3.1)$$

The electron creation (annihilation) operators at site i for spin $\sigma \in \{\uparrow, \downarrow\}$ are $c_{i,\sigma}^\dagger$ ($c_{i,\sigma}$) and the operator for the number of particles is $n_{i,\sigma} = c_{i,\sigma}^\dagger c_{i,\sigma}$. The matrix element of hopping t characterizes the transmission amplitude from one atomic orbital to the neighbouring one under the influence of their mutual potentials. The interaction U denotes a strongly screened repulsive Coulomb potential that renders the presence of two electrons at a single atom energetically disadvantageous. For a sufficiently large interaction U we have a Mott-Hubbard insulator [43] because there can always be only one electron per site and thus there is no charge transport possible. The remaining degrees of freedom which are still important for low lying energies in such an insulator are the magnetic and phononic ones. At half-filling and large interaction $t/U \ll 1$ an expansion in terms of t/U in the limit of vanishing hopping makes sense. Up to second order, one gets the spin-isotropic, anti-ferromagnetic Heisenberg model

$$H = J \sum_{\langle i,j \rangle} \vec{S}_i \cdot \vec{S}_j \quad (3.2)$$

with $J = 4t^2/U$ [44, 45] where \vec{S}_i denotes the vector operator for spin 1/2 at site i .

3.1.1. Néel or RVB-state

The properties of such homogeneous quantum anti-ferromagnets mainly depend on two parameters: The dimension d of the lattice and the value of the spin S .

A useful first impression of a physical system is often given by a mean field approximation. Neglecting quantum fluctuations the spin operators are regarded as classical. Then the anti-ferromagnetic ground state consists of spins pointing up and down on two different sublattices A and B as depicted in fig. 3.1. Generally, all states with non-vanishing

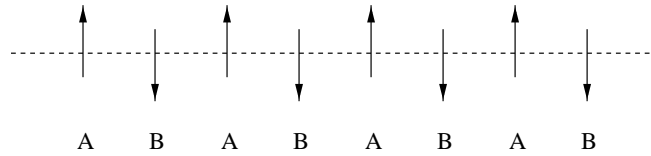


Figure 3.1.: Néel state of a one-dimensional anti-ferromagnet

sublattice magnetization $\langle S_A \rangle - \langle S_B \rangle$ are *Néel states*.

The counterdraft to Néel states are *Resonating Valence Bond* states (RVB) [15]. These are product states of all possible 2-spin-singlets. The real state is a superposition of singlet product states with appropriate weights [46]. Such RVB-states have no long range order and thus no spin direction is preferred. Models characterized by RVB-states are spin liquids. If the range of the singlets in the superposition is finite the excitations have a gap that stems from the finite energy that is necessary to break up a singlet. For an arbitrary range the Néel state can also be written as superposition of singlet product states [46]. It follows that long range RVB-states can show a vanishing energy gap. Then a distinction between Néel state and RVB-state is not possible any longer, mainly because RVB-states are ambiguous.

The spin- $\frac{1}{2}$ anti-ferromagnetic Heisenberg chain considered here is a gapless, critical system with quasi-long-range, algebraically decaying correlations for $|i - j| \rightarrow \infty$

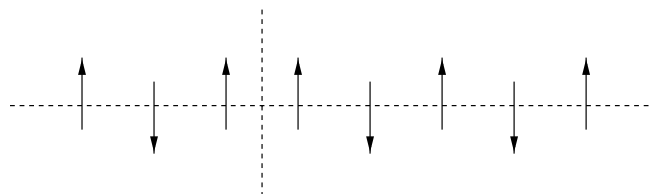
$$\langle \vec{S}_i \cdot \vec{S}_j \rangle \propto (-1)^{|i-j|} / |i - j| \quad (3.3)$$

where the logarithmic corrections have been omitted.

This result is supported by bosonization [47, 48] or conformal field theory [49]. The total spin of the ground state is zero. The anti-ferromagnetic $s = \frac{1}{2}$ -chain lies in between a RVB-system and a Néel system. It resembles the RVB-system because it has no preferred spin direction. It is close to the Néel system because it has a vanishing energy gap and shows strong, quasi-long-range, anti-ferromagnetic correlations.

3.1.2. Spinons

Observing the behaviour of higher-dimensional anti-ferromagnets that show a finite sublattice magnetization the groundstate spin flips with $\Delta S^z = \pm 1$ are the low lying excitations, one would expect the spin of an elementary excitation from the $S = 0$ ground state to be $S = 1$. But this is not the case. The spin of an elementary excitation, a so-called *spinon*, is $S = 1/2$ [50]. Graphically, these excitations can be interpreted as domain walls between

Figure 3.2.: Representation of a $S = 1/2$ -spinon as a domain wall stemming from Néel-like order.

two ground state patterns. This is shown in fig. 3.2 for a Néel-like structure and in fig. 3.3 for a RVB-like structure. In the RVB-scenario the total spin associated with the excitation is $S = 1/2$. Both representations are strongly simplified. The true ground state



Figure 3.3.: Representation of a $S = 1/2$ -spinon as a domain wall stemming from RVB-like order.

is a complicated superposition. The Néel-like state is superposed by a varying number of spin exchange processes. The RVB-like state is mixed with states of different range of the singlet pairs. In higher dimensions these domain walls can not be the low lying excitations since the energy increases like L^{d-1} with L being the linear extension of the system.

3.2. The XXZ -Heisenberg model

The Hamiltonian of the anisotropic Heisenberg model for a chain of L sites is given by

$$H = J \sum_{i=1}^L (S_i^x S_{i+1}^x + S_i^y S_{i+1}^y + \Delta S_i^z S_{i+1}^z) \quad (3.4)$$

where $S_i^a = \frac{1}{2}\sigma_i^a$, σ_i^a are the Pauli spin operators with components $a = x, y, z$ at site i . The region $0 \leq \Delta \leq 1$ is parametrized by $\Delta = \cos \gamma$. This model is related to the six-vertex model by the Trotter-Suzuki mapping described in section 2.5. In order to understand the approach to the thermodynamics of this model in [7] a few properties of the underlying six-vertex model should be explained.

3.2.1. Identification of excitations in BAE-patterns

From [5, 6] we know the complete classification of the excitations of the six-vertex model in the Bethe-Ansatz approach. For the two leading eigenvalues the Bethe ansatz numbers are real and the $\Lambda_0(x)$ is analytic and non-zero in the strip given in appendix D.1. For the low lying excitations there are $\frac{M}{2} - m$ real Bethe ansatz numbers. The other m Bethe ansatz numbers have non-vanishing imaginary parts.

Already Bethe [1] formulated the so-called string hypothesis for the isotropic ferromagnetic Heisenberg chain, that excited states are characterized by distributions of Bethe ansatz numbers (roots) in which strings of arbitrary length are grouped. A string of length $2L + 1$ is defined as a set of $2L + 1$ complex numbers $\{z_j\}$ of the form

$$z_j = x + iy, \quad x \in \mathbb{R}, \quad y = -L, -L + 1, \dots, L - 1, L, \quad L \in \mathbb{N}/2. \quad (3.5)$$

In the repulsive regime $0 < \gamma < \frac{\pi}{2}$ only two string lengths can show up

1. 2-strings: pairs of roots v_u, v_d with $|\text{Im } v_u|, |\text{Im } v_d| < \gamma$ and $\text{Im } v_u - \text{Im } v_d = \gamma$,
2. 1-strings: single moments v with $-(\pi - \gamma) < \text{Re } v < -\gamma$.

An excited state in the repulsive regime is then characterized by a certain configuration of 1- and 2-strings. Its eigenvalue function $\Lambda(v)$ has ν zeros $\Theta_1, \dots, \Theta_\nu$ on the real axis with $\nu = 2 \times$ number of 1- and 2-strings. The numbers Θ_i are called holes because they fulfill $p(\Theta_i) = -1$ like the roots and can therefore be regarded as missing roots.

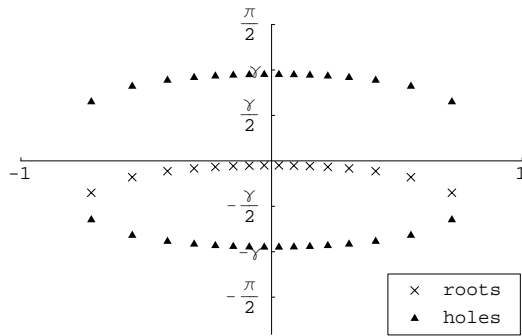


Figure 3.4.: Distribution for holes and roots for the leading eigenvalue. $\beta = 12$ and $h = 0.6$ ($\gamma = \frac{\pi}{3}$).

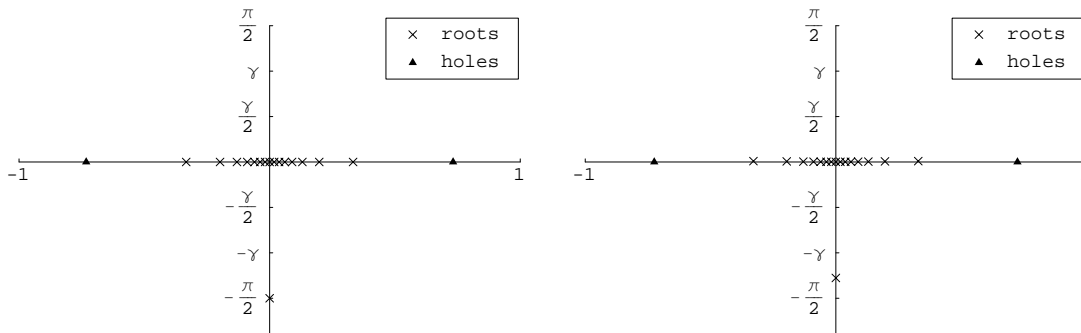


Figure 3.5.: Distribution of roots and holes for a 1-string solution for anisotropy parameter $\gamma = \pi/3$, reciprocal temperature $\beta = 3.0$, in the left figure $h = 0$ and in the right figure $h = 0.6$. Only the two new holes close to the real axis are shown. Note that for the left figure the 1-string is situated exactly at $-i\pi/2$ and the holes lie on the real axis. For positive magnetic field (right figure) the 1-string is shifted upwards.

This is what we know from analytical investigations of the six-vertex model. The model regarded here is an inhomogeneous model that is based on the six-vertex model, but it depends on the temperature and the external magnetic field. Here, the analytical calculation of the patterns would be rather cumbersome. So the patterns have been calculated numerically by solving the BAE.

For the leading eigenvalue the BAE-pattern is shown in fig. 3.4¹. Here the position of roots and holes are not on straight lines but the straight contour with imaginary part $-\frac{\gamma}{2}$ separates the roots from the holes. The numerical investigation of the BAE for a large range of temperature and magnetic field shows that this property holds in general.

¹I am grateful to Masahiro Shiroishi, member of our group, who made the figures with the BAE-patterns available to me.

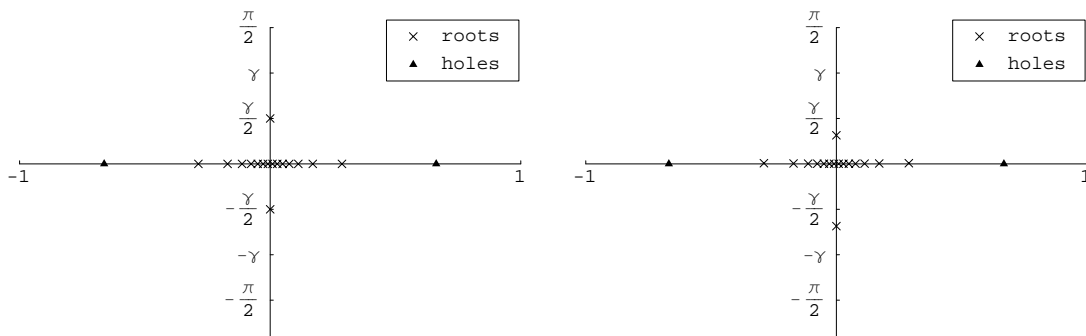


Figure 3.6.: Distribution of roots and holes for a 2-string solution for anisotropy parameter $\gamma = \pi/3$, reciprocal temperature $\beta = 3.0$, in the left figure $h = 0$ and in the right figure $h = 0.6$. Only the two new holes close to the real axis are shown. Note that for on the left the 2-string is symmetric with respect to the real axis and situated approximately at $\pm i\gamma/2$; the holes lie on the real axis. For positive magnetic field on the right the 2-string is shifted downwards.

For $h = 0$ the roots are on the real axis and the holes are on the contours $\text{Im } x = \pm i\gamma$. This is an important requirement for the derivation of the non-linear integral equations in appendix D.

Fig. 3.5 for the 1-string case shows that for fixed temperature and magnetic field $h = 0$ the 1-string is located at $x = -i\frac{\pi}{2}$. When increasing the magnetic field this string is shifted upwards on the imaginary axis.

If we consider the 2-string in fig. 3.6 for the same temperature and the same fields we see that the 2-string is shifted downwards. If we considered a fixed magnetic field and

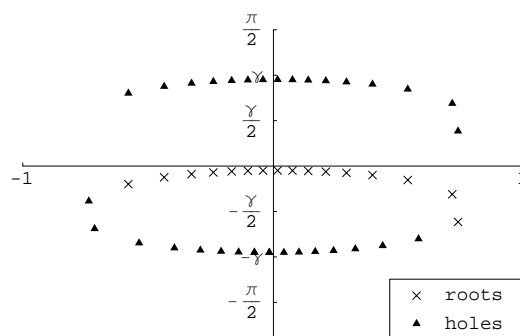


Figure 3.7.: The pattern of the 1-string case for $\beta = 12$ and $h = 0.6$.

decreasing temperature we would qualitatively get the same motion of the strings. In fig. 3.7 the 1-string pattern for a low temperature and fixed magnetic field is given. The 1-string moved to the right and left the imaginary axis. Thus, at a certain temperature (magnetic field) with fixed magnetic field (temperature) the 1-string leaves the imaginary axis. The further investigation the BAE-pattern at this critical temperature T_c (field h_c) shows that the 1- and 2-string patterns are identical. This means a degeneracy of the related eigenvalues. Below (above) T_c (h_c) the patterns lead to complex conjugate eigenvalues.

This behaviour should influence the longitudinal spin-spin correlation length of the model

because the string patterns are connected to those excitations that do not change the magnetization.

This scenario motivates the derivation in the following sections. First, the integral equations for the leading eigenvalue are derived. These equations have the important advantage over the BAE that the limit for *infinite* Trotter number can be easily taken. So the question arises, whether the motion of the strings can be described for infinite² Trotter number by means of the integral equations. To this end the integral equations have to be modified so that the next-leading eigenvalues can be calculated and therefrom the correlation length as described in section 2.2.

²In all figures of this section we have a *finite* Trotter number $M = 32$.

3.3. The non-linear integral equations (NLIE) for the XXZ -model at arbitrary temperature

Instead of dealing with coupled non-linear equations for the Bethe ansatz numbers we work with (2.74) on the basis of functional equations following [7, 27, 20].

3.3.1. The non-linear integral equations

Now we come to the mathematical formulation of the equations. Shortly, the usefulness of the following functions will become obvious

$$\begin{aligned} \mathfrak{a}(x) &= \frac{1}{p(x - i\frac{\gamma}{2})}, & \mathfrak{A}(x) &= 1 + \mathfrak{a}(x), \\ \bar{\mathfrak{a}}(x) &= p(x + i\frac{\gamma}{2}), & \bar{\mathfrak{A}}(x) &= 1 + \bar{\mathfrak{a}}(x) \end{aligned} \quad (3.6)$$

where \mathfrak{a} , $\bar{\mathfrak{a}}$ etc. denote independent functions which are related by complex conjugation actually only if $\bar{\omega} = 1/\omega$ [7] (see the definitions of ω and p in (2.72)). Quite generally $\mathfrak{a}(x)$ and $\bar{\mathfrak{a}}(x)$ are very small for real x in the limit of large values of M . The functions $\mathfrak{A}(x), \bar{\mathfrak{A}}(x)$ in turn are close to 1. In terms of these functions $\Lambda(x)$ can be written in two ways

$$\begin{aligned} \Lambda(x - i\frac{\gamma}{2}) &= \frac{s}{\omega} \Phi(x - i\gamma) \frac{q(x + i\frac{\gamma}{2})}{q(x - i\frac{\gamma}{2})} \mathfrak{A}(x), \\ \Lambda(x + i\frac{\gamma}{2}) &= s\omega \Phi(x + i\gamma) \frac{q(x - i\frac{\gamma}{2})}{q(x + i\frac{\gamma}{2})} \bar{\mathfrak{A}}(x). \end{aligned} \quad (3.7)$$

Now we recall that all eigenvalues $\Lambda(x)$ are analytic in the complex plane. For a while we focus our study on the two largest eigenvalues with only real Bethe ansatz numbers. Each of these functions $\Lambda(x)$ is non-zero in a strip $-\gamma < \text{Im } x < \gamma$ where the logarithm defines an analytic function. The Fourier transform of $\ln \Lambda(x)$ can therefore be calculated in two different ways by integrals with integration paths along $\text{Im } x = -\frac{\gamma}{2}$ and $\text{Im } x = \frac{\gamma}{2}$ using the two different representations (3.7) of Λ in terms of the functions q , \mathfrak{A} and $\bar{\mathfrak{A}}$. Of course both calculations yield the same result due to Cauchy's theorem thus imposing a non-trivial relation on the Fourier transforms of $\ln q(x)$, $\ln \mathfrak{A}(x)$ and $\ln \bar{\mathfrak{A}}(x)$. Next we observe that the transform of $\ln \mathfrak{a}(x)$ is given in terms of the transforms of $\ln q(x)$, or alternatively by $\ln \mathfrak{A}(x)$ and $\ln \bar{\mathfrak{A}}(x)$. In fact this reasoning should be applied to the derivatives of all mentioned functions because $\ln q(x)$ does not admit a Fourier transform in contrast to $[\ln q(x)]'$. The detailed derivation is given in appendix D. To the final equation for the Fourier transform of $\ln \mathfrak{a}(x)$ the inverse transform can be applied resulting in the non-linear

equations stated here for *infinite* trotter number M

$$\begin{aligned}
\ln \mathfrak{a}(x) &= -\frac{\pi\beta}{\gamma} \frac{1}{\cosh \frac{\pi}{\gamma} x} + \frac{\pi}{\pi - \gamma} \frac{\beta h}{2} \\
&+ \int_{-\infty}^{\infty} k(x-y) \ln \mathfrak{A}(y) dy - \int_{-\infty}^{\infty} k(x-y-i\gamma+i\epsilon) \ln \bar{\mathfrak{A}}(y) dy, \\
\ln \bar{\mathfrak{a}}(x) &= -\frac{\pi\beta}{\gamma} \frac{1}{\cosh \frac{\pi}{\gamma} x} - \frac{\pi}{\pi - \gamma} \frac{\beta h}{2} \\
&+ \int_{-\infty}^{\infty} k(x-y) \ln \bar{\mathfrak{A}}(y) dy - \int_{-\infty}^{\infty} k(x-y+i\gamma-i\epsilon) \ln \mathfrak{A}(y) dy
\end{aligned} \tag{3.8}$$

with

$$k(x) = \frac{1}{2\pi} \int_{-\infty}^{\infty} \frac{\sinh(\frac{\pi}{2} - \gamma)k}{2 \cosh \frac{\gamma}{2}k \sinh \frac{\pi - \gamma}{2}k} e^{ikx} dk, \tag{3.9}$$

external magnetic field h and inverse temperature β . Lastly, we want to find an equation for $\Lambda(x)$ in terms of $\mathfrak{A}(x)$ and $\bar{\mathfrak{A}}(x)$. For this purpose we may use any of the two equations (3.7). However, it is more convenient to multiply both equations with the result

$$\Lambda(x - i\frac{\gamma}{2})\Lambda(x + i\frac{\gamma}{2}) = \Phi(x - i\gamma)\Phi(x + i\gamma)\mathfrak{A}(x)\bar{\mathfrak{A}}(x) \tag{3.10}$$

where the right-hand side does not involve $q(x)$ anymore. This equation is the so-called “inversion identity” [16] for finite M . Taking the logarithm it is solved immediately by Fourier transforms

$$\ln \Lambda(x) = -\beta\epsilon_0 + \frac{1}{2\gamma} \int_{-\infty}^{\infty} \frac{\ln [\mathfrak{A}\bar{\mathfrak{A}}(x)]}{\cosh \frac{\pi}{\gamma} x} dx. \tag{3.11}$$

ϵ_0 describes the ground state energy of the chain (see [7]).³

It should be remarked that the auxiliary functions are related to the density functions of spinons and anti-spinons by $\mathfrak{a}(x) = \frac{\rho(x)}{\rho^h(x)}$ and $\bar{\mathfrak{a}}(x) = \frac{\bar{\rho}(x)}{\bar{\rho}^h(x)}$ [58].

The simplest excitation is given by a 1-string that is shifted to infinity so that only two holes remain in the pattern with the $\frac{M}{2} - 1$ roots staying on the real axis. The integral equations of this *pure 2-hole case* are derived in appendix D.1 and have the following

³Here again the expression is given for infinite Trotter number.

form

$$\begin{aligned}
\ln a(x) &= -\frac{\pi\beta}{\gamma} \frac{1}{\cosh \frac{\pi}{\gamma} x} + \pi i \\
&+ \frac{\pi}{\pi - \gamma} \frac{\beta h}{2} - K\left(x - \left(\Theta_1 + i\frac{\gamma}{2}\right)\right) - K\left(x - \left(\Theta_2 + i\frac{\gamma}{2}\right)\right) \\
&+ \int_{-\infty}^{\infty} k(x-y) \ln \mathfrak{A}(y) dy - \int_{-\infty}^{\infty} k(x-y - i\gamma + i\epsilon) \ln \bar{\mathfrak{A}}(y) dy, \\
\ln \bar{a}(x) &= -\frac{\pi\beta}{\gamma} \frac{1}{\cosh \frac{\pi}{\gamma} x} - \pi i \\
&- \frac{\pi}{\pi - \gamma} \frac{\beta h}{2} + K\left(x - \left(\Theta_1 - i\frac{\gamma}{2}\right)\right) + K\left(x - \left(\Theta_2 - i\frac{\gamma}{2}\right)\right) \\
&+ \int_{-\infty}^{\infty} k(x-y) \ln \bar{\mathfrak{A}}(y) dy - \int_{-\infty}^{\infty} k(x-y + i\gamma - i\epsilon) \ln \mathfrak{A}(y) dy.
\end{aligned} \tag{3.12}$$

$K(x)$ is proportional to the antiderivative of $k(x)$ yielding $K'(x) = 2\pi i k(x)$. These equations have to be solved under the subsidiary conditions

$$a\left(\Theta_{1,2} + i\frac{\gamma}{2}\right) = -1. \tag{3.13}$$

When the position of the 1-string remains finite there are again two holes and a 1-string y_0 leading to an additional term in the equations (see the principal remarks in appendix D)

$$\begin{aligned}
\ln a(x) &= -\frac{\pi\beta}{\gamma} \frac{1}{\cosh \frac{\pi}{\gamma} x} + \pi i + \ln \frac{\sinh \frac{\pi}{\pi-\gamma} (x - (y_0 + \frac{3}{2}\gamma i))}{\sinh \frac{\pi}{\pi-\gamma} (x - (y_0 + \frac{1}{2}\gamma i))} \\
&+ \frac{\pi}{\pi - \gamma} \frac{\beta h}{2} - K\left(x - \left(\Theta_1 + i\frac{\gamma}{2}\right)\right) - K\left(x - \left(\Theta_2 + i\frac{\gamma}{2}\right)\right) \\
&+ \int_{-\infty}^{\infty} k(x-y) \ln \mathfrak{A}(y) dy - \int_{-\infty}^{\infty} k(x-y - i\gamma + i\epsilon) \ln \bar{\mathfrak{A}}(y) dy, \\
\ln \bar{a}(x) &= -\frac{\pi\beta}{\gamma} \frac{1}{\cosh \frac{\pi}{\gamma} x} - \pi i + \ln \frac{\sinh \frac{\pi}{\pi-\gamma} (x - (y_0 - \frac{1}{2}\gamma i))}{\sinh \frac{\pi}{\pi-\gamma} (x - (y_0 + \frac{1}{2}\gamma i))} \\
&- \frac{\pi}{\pi - \gamma} \frac{\beta h}{2} + K\left(x - \left(\Theta_1 - i\frac{\gamma}{2}\right)\right) + K\left(x - \left(\Theta_2 - i\frac{\gamma}{2}\right)\right) \\
&+ \int_{-\infty}^{\infty} k(x-y) \ln \bar{\mathfrak{A}}(y) dy - \int_{-\infty}^{\infty} k(x-y + i\gamma - i\epsilon) \ln \mathfrak{A}(y) dy
\end{aligned} \tag{3.14}$$

and one more subsidiary condition

$$a(y_0 + i\frac{\gamma}{2}) = -1. \tag{3.15}$$

For 2-string excitations the equations are identical to (3.14) upon the replacement of y_0 by y_+ which denotes the upper of the roots forming the 2-string.

3.3.2. Description of the string motion

In this section we want to determine the influence of the magnetic field on the location of the 1- and 2-strings. Let us start with the integral equations for the 1- and 2-strings from (3.14).

As described in the section 3.2.1 a 1-string is located at $x = -i\frac{\pi}{2}$ for $h = 0$ and moves upwards when increasing the magnetic field. A 2-string consisting of two Bethe ansatz rapidities y_- and y_+ in the lower and upper half plane is located symmetrically to the real axis for zero magnetic field. It moves downwards upon introducing a positive magnetic field $h > 0$. We mentioned before that equation (3.14) is also valid for a 2-string if y_0 is replaced by y_- (the root y_+ does not appear explicitly).

3.3.3. Analytic continuation

Unfortunately, $y_0 + i\gamma/2$ lies outside the strip of convergence of expression (3.14). However, in appendix D.4 an integral expression for $\alpha(x)$ with x in the lower half-plane is derived

$$\begin{aligned} \ln \alpha(x) = & \frac{\pi}{\pi - \gamma} \beta h + R(x - (\theta_1 + i\frac{\gamma}{2})) + R(x - (\theta_2 + i\frac{\gamma}{2})) \\ & + \ln \left[\frac{\sinh \frac{\pi}{\pi - \gamma} (x - y_0 - i\frac{3}{2}\gamma)}{\sinh \frac{\pi}{\pi - \gamma} (x - y_0 + i\frac{1}{2}\gamma)} \right] \\ & - \int_{-\infty}^{\infty} dy [r(x - y) \ln \mathfrak{A}(y) - r(x - y - i\gamma + i\epsilon) \ln \bar{\mathfrak{A}}(y)]. \end{aligned} \quad (3.16)$$

The functions $r(x)$ and $R(x)$ are defined in appendix D.4. Note that the functions on the right-hand side have real arguments, i.e. they are those calculated from (3.14), while the argument of the left-hand side of the equation is of course in the lower half plane.

For the following line of arguments it is useful to have a picture of the strips of convergence of expressions (3.14) and (3.16) for function the α , see fig. 3.8.

The limitations of convergence are due to poles of the kernel function $k(x)$ for $x = \pm i\gamma$ and in $r(x)$ for $x = -(\pi - \gamma)i$, $-\gamma i$, see (D.26). In eq. (3.14) the imaginary part of x ($= z + i\gamma/2$) must neither be larger than γ , nor lower than 0 (because of poles of $k(x - y)$ and $k(x - y - i\gamma)$ respectively). Thus $-\gamma/2 < \text{Im } z < \gamma/2$. Similarly, for eq. (3.16) we have $-(\pi - 2\gamma) < \text{Im } x < -\gamma$ (because of poles of $r(x - y - i\gamma)$ and $r(x - y)$ respectively), hence $-(\pi - 3\gamma/2) < \text{Im } z < -3\gamma/2$.

It seems that (3.14) and (3.16) can not be used for those points lying between the “first” and “second strip”. However, the function $\alpha(x)$ is analytic and the analytic continuation of expression (3.16) from $\text{Im } x < -\gamma$ to $-\gamma < \text{Im } x < 0$ is easily done. This yields the old expression (3.16) and due to the singularity of $r(x - y)$ at $x - y = -i\gamma$ a contribution according to Cauchy of the additive term $\ln \mathfrak{A}(x + i\gamma)$ on the right-hand side

$$\ln \alpha(x) = \text{“rhs. of (3.16)”} + \ln \mathfrak{A}(x + i\gamma). \quad (3.17)$$

For this $\alpha(x + i\gamma)$ expression (3.14) is convergent. If furthermore $x = y_0 + i\gamma/2$ or $x = y_- + i\gamma/2$, the additional term even vanishes as $\alpha(y_j + i3\gamma/2) = 0!$

3.3.4. Crossover scenario

The solution of (3.14) under the subsidiary conditions (3.15) and (3.13) (by use of (3.16)) leads to qualitatively different patterns for weak and strong magnetic fields with a crossover

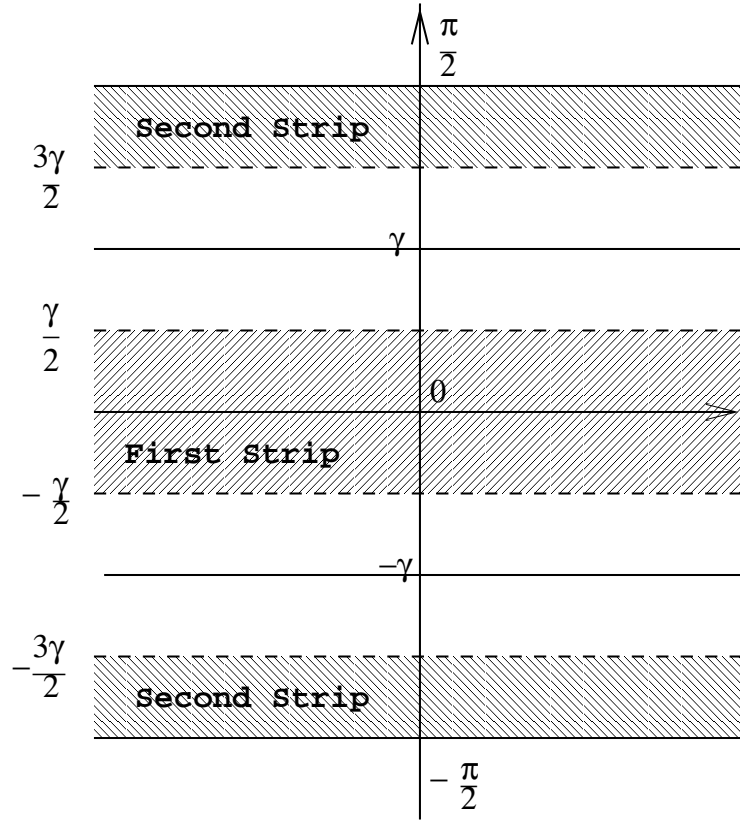


Figure 3.8.: Regions of the complex z plane where $\alpha(z+i\gamma/2)$ as appearing in the subsidiary condition 3.15 can be calculated. In the “first” and “second strip” expressions (3.14) and (3.16) are convergent, respectively.

of the corresponding eigenvalues of the quantum transfer matrix at some critical magnetic field h_c , see fig. 3.9.

$0 < h < h_c$:

The position of the roots are fixed by the constraints $\alpha(y_0+i\gamma/2) = -1$ and $\alpha(y_{\pm}+i\gamma/2) = -1$. For $h \gtrsim 0$ we see by looking at fig. 3.8 that y_0 does lie in the “second strip” and y_+ lies in the “first strip”, not so y_- . However, in (3.17) above it was shown that (3.16) can still be applied!

Next, we want to show that y_- moves into the lower half-plane for increasing $h > 0$ as claimed above. Inserting $y_- + i\gamma/2$ for x in (3.16) yields:

$$\begin{aligned} \ln(1) &= \frac{\pi}{\pi - \gamma} \beta h \\ &+ \ln \left[\frac{\sinh \frac{\pi}{\pi - \gamma} (y_- + i\frac{\gamma}{2} - \theta_1 + i\frac{\gamma}{2}) \sinh \frac{\pi}{\pi - \gamma} (y_- + i\frac{\gamma}{2} - \theta_2 + i\frac{\gamma}{2})}{\sinh \frac{\pi}{\pi - \gamma} (y_- + i\frac{\gamma}{2} - \theta_1 - i\frac{\gamma}{2}) \sinh \frac{\pi}{\pi - \gamma} (y_- + i\frac{\gamma}{2} - \theta_2 - i\frac{\gamma}{2})} \right] \end{aligned} \quad (3.18)$$

where the integral terms were ignored because they are of lower magnitude, at least for sufficiently low temperature. For $h > 0$ we find from the latter equation that the real

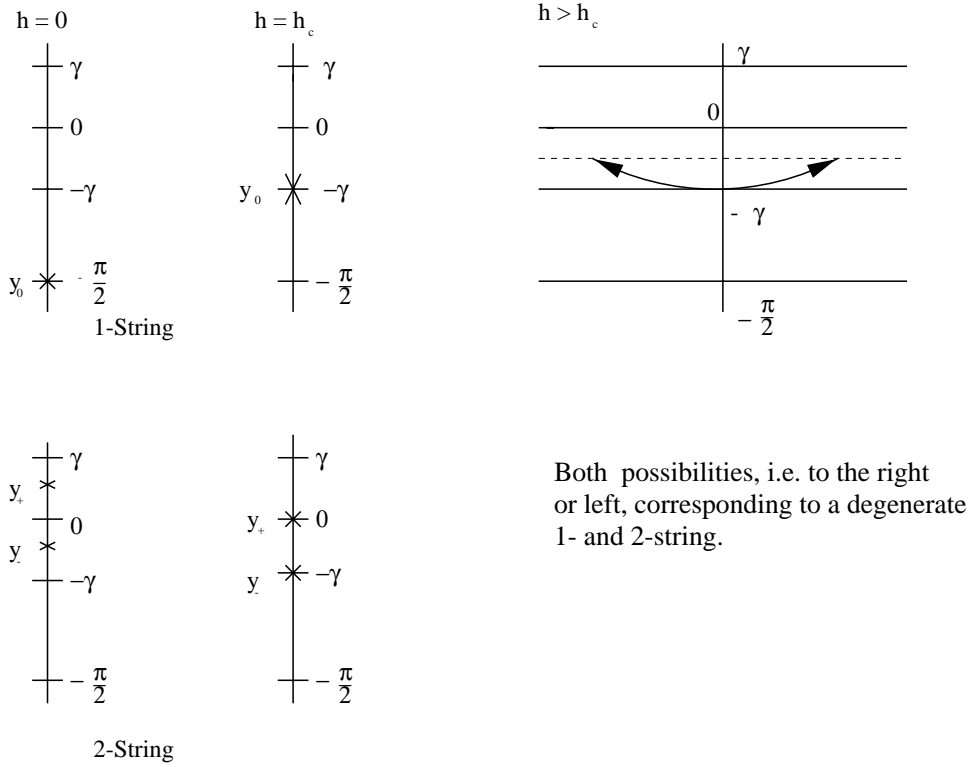


Figure 3.9.: Crossover scenario

part of the logarithm is negative, using $\text{Im } \theta_j \sim 0$ we conclude $\text{Im}(y_- + i\gamma/2) < 0$. This confirms the picture of the evolution of the root y_- shown in fig. 3.9.

Next we study the constraint for the second root of the 2-string, this will fix $y_+ - y_-$. Evaluating (3.14) for the 2-string at $y_+ + i\gamma/2$ yields

$$\begin{aligned} \ln(1) &= -\frac{\pi\beta}{\gamma} \frac{1}{\cosh \frac{\pi}{\gamma}(y_+ + i\frac{\gamma}{2})} + \frac{\pi}{\pi - \gamma} \frac{\beta h}{2} \\ &+ \ln \left[\frac{\sinh \frac{\pi}{\pi - \gamma}(y_+ - y_- - i\gamma)}{\sinh \frac{\pi}{\pi - \gamma}(y_+ - y_-)} \right] \end{aligned} \quad (3.19)$$

where at low temperatures the θ_j terms are of order $\mathcal{O}(1)$ and thus have been ignored like the integral terms. Using $\gamma/2 < \text{Im}(y_+ + i\gamma/2) \leq \gamma$ we see that the first term on the right-hand side has positive real part and is of order $\mathcal{O}(\beta)$ like the magnetic field term. In order to satisfy the equation at low temperatures $y_+ - y_- - i\gamma$ has to vanish, thus the real part of the logarithmic term is large and negative canceling the positive real parts as required. In conclusion for low temperatures, y_+ and y_- form a 2-string with the same real coordinates and imaginary parts differing by γ . In total, the crossover scenario proposed in fig. 3.9 is confirmed. For arbitrary temperatures and magnetic field we have to solve the integral equations numerically.

3.4. Crossover in the correlation length

This section is dedicated to the presentation of the results from solving the integral equations for the 1- and 2-string case numerically. In order to understand the figures that will be shown in this section the examination of the crossover scenario explained in the last section is crucial. In that section we stated that when considering a fixed temperature the augmentation of the magnetic field beyond a critical value leads to the degeneracy of the eigenvalues of the 1- and 2-string excitations in the sense that the eigenvalues of the QTM are complex conjugate which leads to identical correlation lengths (first of figures 3.10). We get the same scenario by fixing the magnetic field and decreasing the temperature so that temperature and magnetic field act in roughly opposite ways which can be inferred in part from their appearance in the combination h/T in the NLIE.

The second one of the figures 3.10 shows that the position of the 1-string and the former lower part of the 2-string are equal up to the sign of the real part. The numerical investigations show that the eigenvalues of the string solutions are in fact complex conjugate below the critical temperature and therefore they can not be distinguished any more. Above that temperature the eigenvalues are real with $\Lambda_{1s} > \Lambda_{2s}$.

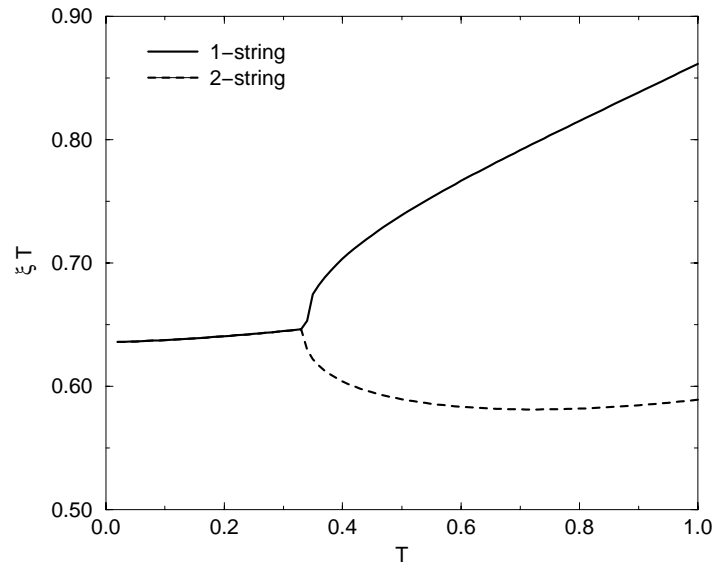
At the critical temperature the two eigenvalues have indeed the same value. So we have a level crossing of Λ_{1s} and Λ_{2s} . This crossing is the reason for the non-analytic behaviour of the correlation length visible in figure 3.10. This singularity at T_c is of square root type. Most significant is the non-analytical behaviour of the Fermi momentum k_F . At low temperature the oscillations are incommensurate and at zero temperature the Fermi momentum k_F and magnetization m are strictly related by $k_F = (1/2 - m)\pi$, a relation which ceases to hold at elevated temperatures. At sufficiently high temperatures the oscillations are commensurate with $k_F = \pi/2$.

The crossover scenario could have been expected due to the following reason:

For temperatures below T_c we expect a behaviour in accordance to conformal field theory. Then we have $2k_F$ -oscillations that are not equal to π . In the high temperature limit one expects the system to behave Ising-like. Here, exact $2k_F = \pi$ -oscillations can be found. Therefore, a non-analytic property of the oscillations at the critical temperature can be expected if the Ising-like behaviour is observed to maintain when decreasing the temperature up to the crossover temperature.

From this point of view, it should be possible to see the crossover in the correlation length analytically in the integral equations. This can be a task for future investigations.

Degeneracy manifesting in the correlation length



Degeneracy of string solutions

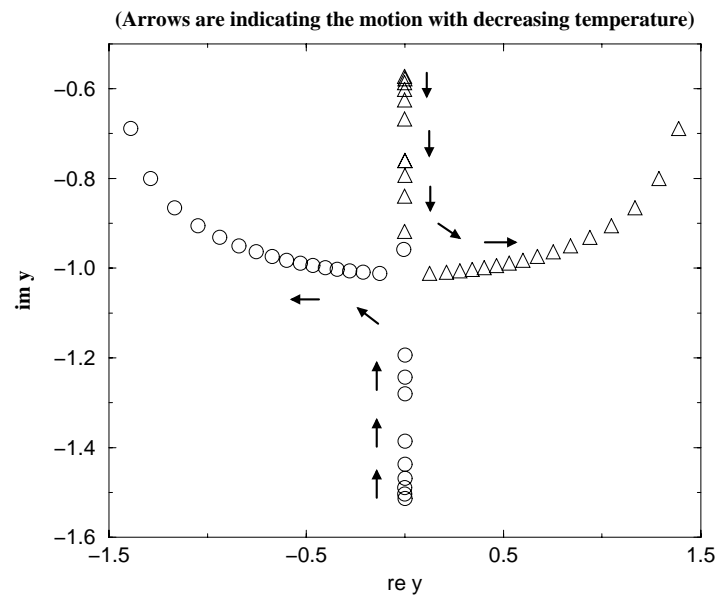
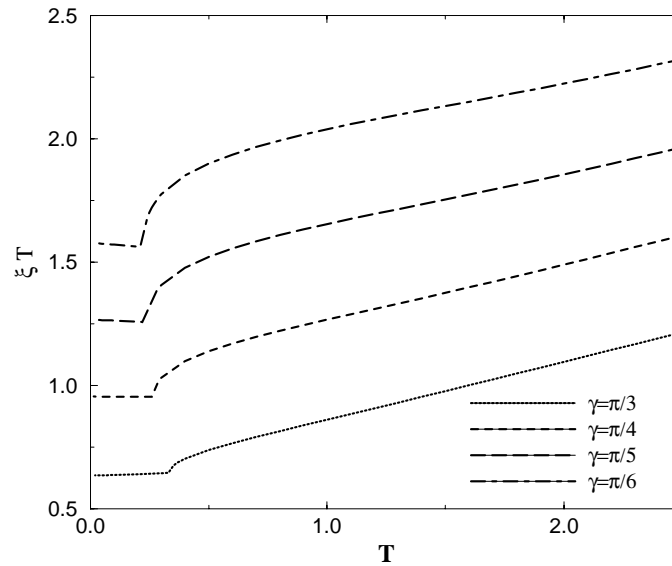


Figure 3.10.: 1. The degeneracy of the eigenvalues for the 1- and 2-string excitations leads to identical correlation lengths for temperatures lower than the crossover temperature. 2. Degeneracy of the string positions for temperatures below the crossover temperature (Magnetic field $h = 0.1$, anisotropy parameter $\gamma = \frac{\pi}{3}$).

Crossover in correlation length of the XXZ chain

(external magnetic field $h=0.1$)



Deviation from $2k_F = \pi$ oscillations

(external magnetic field $h=0.1$)

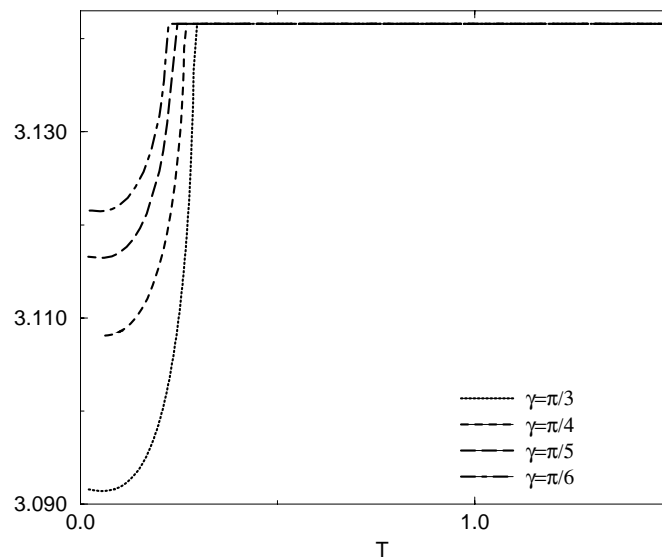


Figure 3.11.: Crossover in the correlation length driven by temperature for different values of the anisotropy parameter γ . Fixed external magnetic field $h = 0.1$.

4. The Drude weight at finite temperature

Since this second part of the work is mainly concerned with the calculation of the Drude weight for at finite temperatures for models that are exactly solvable by means of the Bethe ansatz, a detailed introduction shall be given here.

The Drude weight is derived on the basis of Takahashi's formulation of the thermodynamics of the XXX -chain [9]. In the ground state the quasi-momenta (rapidities) are all real numbers. But for arbitrary eigenstates quasi-momenta are in general complex numbers.¹ The calculation of the energy eigenvalue of the lowest energy state in the thermodynamic limit is then reduced to the determination of the distribution function of quasi-momenta. This distribution function must satisfy a linear integral equation. In case of the free energy the rapidities are complex numbers. The *string hypothesis* is stating that the rapidities group together to form strings in the rapidity plane in the limit of a large system.

This assumption seems to be too strong and there are some counter examples in some extreme cases. This is a very controversial point of the thermodynamic Bethe ansatz equations (TBA) for exactly solvable models. However, equations obtained by use of the string hypothesis seem to give the correct free energy and other thermodynamic quantities. Once accepted this hypothesis, we must consider the distribution functions for strings with lengths $1, 2, \dots$. In the general case for arbitrary anisotropy parameter $\Delta = \cos \gamma$ a set of coupled integral equations is derived which has an infinite number of unknown functions. This set is then truncated to one with a finite number of unknown functions because the asymptotic behaviour of the distribution function for a long string can be calculated.

In some special cases one gets a finite set of equations. For $\gamma = \frac{\pi}{\nu}$, ν integer, this is fulfilled. Zotos [36] has calculated the Drude weight for this case.²

So exact solvability means that we get a closed expression for, e.g. the free energy. But this expression can still contain infinitely many unknown functions, as long as there are no special cases considered. In this chapter we present a different approach based on the thermodynamics described in section (3.3). This way results in expressions for thermodynamic quantities with a *finite* number of unknown functions for *arbitrary* values of the anisotropy parameter, especially $\gamma = 0$, the isotropic point. Therefore, the quantitative results can be calculated *exactly*, only restricted by numerical errors of computing.

In the following the traditional methods and their relation to the Drude weight will be explained. Then we present the alternative derivation. But first, the Drude weight should be introduced.

4.1. Linear Response and Drude weight at $T = 0$

Now we want to explain how the Drude weight appears when examining the linear response [28, 34] of a system to an applied electrical field. Here we follow the description given in Dagotto's review [39]. We consider the hamiltonian

$$\hat{H} = \hat{H}_0 + \hat{V} = -t \sum_j \left(e^{ieA_x(j,t)} c_{j+1}^\dagger c_j + e^{-ieA_x(j,t)} c_j^\dagger c_{j+1} \right) + \mathcal{H}_{int}. \quad (4.1)$$

¹This does not hold for all integrable chains. For the delta-function Boson gas [54], for example the momenta are real for all eigenstates.

²The finiteness of the number of unknown functions is already given if $\frac{\gamma}{\pi}$ is a rational number.

\hat{H}_0 is defined as the Hamiltonian in absence of a vector field but including the fermionic interactions, while \hat{V} contains the field dependence and it vanishes when $A_x(j, t) = 0$. The model is coupled to an external classical vector potential $A_x(j, t)$ where j denotes a site of the one-dimensional lattice. The gauge-invariant way to couple particles on a lattice with a $U(1)$ -gauge field is to introduce phase factors in the kinetic-energy hopping term.

The phase factors are defined on the bond between two lattice sites. A particle hopping to the next site gathers this factor in its wave function. After once having hopped through the whole ring it has collected the phase $\Phi = \int A_x(r) dr$.

We now use $r, r+a$ for the position of two neighbouring lattice sites for later convenience (a is the lattice constant). Expanding the exponentials in powers of the electric charge e it can be easily shown that

$$\hat{V} = -e \sum_r \hat{j}_x(r) A_x(r, t) - \frac{e^2}{2} \sum_r \hat{K}_x(r) A_x(r, t)^2 + \dots \quad (4.2)$$

where the paramagnetic current-density operator is defined as $\hat{j}_x(r) = it (c_{r+a}^\dagger c_r - c_r^\dagger c_{r+a})$ and the operator $\hat{K}_x(r) = -t (c_{r+a}^\dagger c_r + c_r^\dagger c_{r+a})$ is the kinetic-energy density.

The total linear-response current is thus given by

$$\hat{J}_x(r, t) = e \hat{j}_x(r) + e^2 \hat{K}_x(r) A_x(r, t) + \dots \quad (4.3)$$

where the first term is the paramagnetic current density and the second corresponds to the diamagnetic contribution.

The next step in the calculation of the conductivity $\sigma(\omega)$ for the fermionic model is to evaluate the mean value of the total current operator $\hat{J}_x(r, t)$ in the ground state of the Hamiltonian. As a starting point, let us derive the expectation value of an arbitrary time-dependent operator $\hat{O}(t)$ in the ground state of a given system. Following well known steps described in several textbooks (see for example [31]) and working at first order in the external field in \hat{V} it is possible to show that the following approximation holds

$$\begin{aligned} \langle \psi(t) | \hat{O}(t) | \psi(t) \rangle &= \langle \phi_0 | \hat{O}(t) | \phi_0 \rangle \\ &+ i \int_{-\infty}^t dt_1 \left[e^{iE_0(t_1-t)} \langle \phi_0 | \hat{V} e^{-i\hat{H}_0(t_1-t)} \hat{O} | \phi_0 \rangle \right. \\ &\left. - e^{iE_0(t-t_1)} \langle \phi_0 | \hat{O} e^{-i\hat{H}_0(t-t_1)} \hat{V} | \phi_0 \rangle \right] + \dots \end{aligned} \quad (4.4)$$

In the derivation of (4.4) we made explicit use of the definition of an operator in interaction representation, i.e. $\hat{O}(t) = e^{i\hat{H}_0 t} \hat{O} e^{-i\hat{H}_0 t}$ and the time evolution of a state which is given by

$$|\psi(t)\rangle = \hat{T} \exp \left[-i \int_{-\infty}^t dt_1 \hat{V}(t_1) \right] |\phi_0\rangle \quad (4.5)$$

where \hat{T} is the time-ordering operator, and $|\phi_0\rangle$ is the ground state of the system in *absence* of the external field which has energy E_0 .

Let us now specialize equation (4.4) to our problem, i.e. consider $\hat{O}(t) = \hat{J}_x(r, t)$. Defining

the Fourier transform of the vector field as $A_x(r, t) = \int_{-\infty}^{\infty} d\omega A_x(r, \omega) e^{-i\omega t}$ [with a similar definition for the transformation of the current $\langle \hat{J}_x(r, \omega) \rangle$] and after straightforward algebra it can be shown that

$$\begin{aligned} \langle \hat{J}_x(r, \omega) \rangle &= e^2 \langle \hat{K}_x \rangle A_x(r, \omega) + ie^2 \sum_{r'} \int_0^{\infty} d\tau \cdot \\ &\langle \phi_0 | \left[\hat{j}_x(r) e^{-i(\hat{H}_0 - E_0 - \omega)\tau} \hat{j}_x(r') - \hat{j}_x(r') e^{-i(\hat{H}_0 - E_0 + \omega)\tau} \hat{j}_x(r) \right] | \phi_0 \rangle \cdot \\ &A_x(r', \omega) \end{aligned} \quad (4.6)$$

where (1) the paramagnetic current in the ground state without external fields is assumed to vanish $\langle \phi_0 | \hat{j}_x(r) | \phi_0 \rangle = 0$, (2) the change of variables $t - t_1 \rightarrow \tau$ was carried out and (3) the notation $\langle \hat{K}_x \rangle = \langle \phi_0 | \hat{K}_x(r) | \phi_0 \rangle$ was introduced since this mean value is site-independent in the ground state of the model defined with periodic boundary conditions. Equation (4.6) can be further simplified by working in momentum space. Defining the spatial Fourier transform as

$$A_x(r, \omega) = \frac{1}{L} \sum_q A_x(q, \omega) e^{iqr} \quad (4.7)$$

and applying the operator identity $\int_0^{\infty} dx e^{i\hat{a}x - \epsilon x} = i/(\hat{a} + i\epsilon)$ where ϵ is a constant and \hat{a} an arbitrary operator we arrive at a *general* equation for the response of the total current to an arbitrary but small vector field in the x -direction

$$\begin{aligned} \langle \hat{J}_x(q, \omega) \rangle &= e^2 \langle \hat{K}_x \rangle A_x(q, \omega) \\ &+ e^2 \left(\frac{1}{L} \left\langle \phi_0 | \hat{j}_x(-q) \frac{1}{\hat{H}_0 - E_0 + \omega + i\epsilon} \hat{j}_x(q) | \phi_0 \right\rangle \right. \\ &\left. + \frac{1}{L} \left\langle \phi_0 | \hat{j}_x(q) \frac{1}{\hat{H}_0 - E_0 - \omega - i\epsilon} \hat{j}_x(-q) | \phi_0 \right\rangle \right) A_x(q, \omega). \end{aligned} \quad (4.8)$$

ϵ is a small parameter introduced to regularize the poles that will appear at particular values of the frequency. Now, let us study the special case of the response to an electric field defined by $A_x(q = 0, \omega) = E_x(q = 0, \omega)/(i\omega + \delta)$ where δ is a small number describing the adiabatic turning-on of the field. We consider zero momentum since we are interested in a *uniform* electric field. In linear-response theory the conductivity is defined through the relation $\langle \hat{J}_x(q = 0, \omega) \rangle = \sigma_{xx}(\omega) \langle E_x(q = 0, \omega) \rangle$. By introducing a complete set of eigenfunctions of H_0 , $I = \sum_n |\phi_n\rangle \langle \phi_n|$ we get for $\sigma_{xx}(\omega)$

$$\begin{aligned} \sigma_{xx}(\omega) &= \frac{e^2}{i\omega + \delta} \left[\langle \hat{K}_x \rangle + \frac{1}{L} \sum_{n \neq 0} \left| \langle \phi_0 | \hat{j}_x(0) | \phi_n \rangle \right|^2 \cdot \right. \\ &\left. \left(\frac{1}{E_n - E_0 + \omega + i\epsilon} + \frac{1}{E_n - E_0 - \omega - i\epsilon} \right) \right], \end{aligned} \quad (4.9)$$

and for the imaginary part of the conductivity

$$\begin{aligned} \text{Im}\sigma_{xx}(\omega) = & -\frac{e^2}{\omega} \left[\langle \hat{K}_x \rangle + \frac{1}{L} \sum_{n \neq 0} \left| \langle \phi_0 | \hat{j}_x(0) | \phi_n \rangle \right|^2 \right. \\ & \left. \left(\frac{E_n - E_0 - \omega}{(E_n - E_0 - \omega)^2 + \epsilon^2} + \frac{E_n - E_0 + \omega}{(E_n + E_0 + \omega)^2 + \epsilon^2} \right) \right]. \end{aligned} \quad (4.10)$$

The real part is calculated by using the identity $1/(u + i\epsilon) = P(1/u) - i\pi\delta(u)$, valid in the limit of small ϵ where P denotes the principal part

$$\sigma_1(\omega) = \text{Re}\sigma_{xx}(\omega) = \tilde{D}\delta(\omega) + \frac{e^2\pi}{L} \sum_{n \neq 0} \frac{\left| \langle \phi_0 | \hat{j}_x | \phi_n \rangle \right|^2}{E_n - E_0} \delta(\omega - (E_n - E_0)) \quad (4.11)$$

where the so-called *Drude weight* D is given by

$$D = \frac{\tilde{D}}{2\pi e^2} = \langle K_x \rangle - \frac{1}{L} \sum_{n \neq 0} \frac{\left| \langle \phi_0 | \hat{j}_x(q=0) | \phi_n \rangle \right|^2}{E_n - E_0}. \quad (4.12)$$

The second term in equation (4.11) describes the incoherent, regular background.

Actually, it can be shown that for an insulator D converges exponentially to zero with increasing lattice size while for a metal it converges to a nonzero constant which implies *zero* resistance in the ground state. This is not surprising since in the model there is no dissipative mechanism. A model with $D \neq 0$ can correspond to a perfect metal or a superconductor showing that the vanishing of the resistivity in the ground state is only a necessary condition for achieving superconductivity, but it is not sufficient [53, 55].

4.1.1. Twisted boundary conditions and external fields

We come back to the Hamiltonian (4.1) and want to explain its relation to the Aharonov-Bohm effect [38]. From this effect we know that the wave function of the charged fermion gathers a phase $\Psi \rightarrow e^{i\phi}\Psi$ after once having hopped through the whole ring in presence of an external field causing the twist in the boundary conditions.

It is important to notice that this is related to the $U(1)$ -gauge symmetry of the model. Because of this symmetry we have the freedom to incorporate the gathered phase by hopping from one site to the next one by transforming the fermionic operators. The transformation $c_i = q_i \tilde{c}_i$ with $q_i = e^{i\varphi_i}$ does not affect the fermionic anti-commutation relations. If we then apply the hopping through the whole ring ($\prod \tilde{c}_{i+1} \tilde{c}_i$) to, e.g. one electron the wave function also gets the Aharonov-Bohm phase factor. In other words, the $U(1)$ -gauge symmetry gives us the freedom to incorporate the twist in the fermionic operators.

4.1.2. Curvature of energy levels and Drude weight

Kohn [29] formulated the problem of twisted boundary conditions in first quantization. He considered Hamiltonians of the structure

$$\mathcal{H}(k) = \sum_i [(p_i + k)^2 + V_i] + U. \quad (4.13)$$

V_i is the external potential and U is the potential energy of the interaction. $k = 1/i\omega E_x e^{i(\omega+\delta)t} = -eA_x$ is the minimal coupling of the vector field. In appendix E second order perturbation theory is performed in order to get an expression for the second derivative of the energy levels with respect to the field.³ Comparing (E.8) (with $\langle K_x \rangle = t$) for the ground state to the imaginary part of the conductivity (4.10) we get

$$\lim_{\omega \rightarrow 0} \omega \operatorname{Im} \sigma_{xx} = -\frac{1}{L} \frac{\partial^2 E_0}{\partial \phi^2}. \quad (4.14)$$

On the other hand, we see

$$\begin{aligned} D &= \frac{1}{2L} \left\{ \langle K_x \rangle L - 2 \sum_{n \neq 0} \frac{|\langle \phi_0 | \hat{j}_x(q=0) | \phi_n \rangle|^2}{E_n - E_0} \right\} = \lim_{\omega \rightarrow 0} \frac{1}{2} \omega \operatorname{Im} \sigma_{xx} \\ &= \frac{1}{2L} \frac{\partial^2 E_0}{\partial \phi^2}. \end{aligned} \quad (4.15)$$

In this way the Drude weight is related to the curvature of the ground state energy depending on the twist.

4.1.3. Drude weight at arbitrary temperature

It is clear that the linear response of the system to an applied flux is not only restricted to the ground state. The flux will cause a shift of an arbitrary energy level E_n of the unperturbed system. Thus, the same calculation can be performed in order to get a ‘‘Drude’’-weight D_n to the eigenstate $|n\rangle$. However, we need a thermodynamical formulation taking into account that now every energy level has a certain probability p_n of appearance. This is provided by using the usual canonical ensemble, that is weighting the states with the well known Boltzmann factors

$$D_n = \frac{1}{L} \left[\frac{1}{2} \langle -\hat{T} \rangle - \sum_{m \neq n} p_n \frac{|\langle n | \hat{j} | m \rangle|^2}{E_m - E_n} \right] \quad (4.16)$$

leading to

$$D = \frac{1}{L} \sum_n e^{-\beta \epsilon_n} \frac{1}{2} \frac{\partial^2 \epsilon_n(\phi)}{\partial \phi^2} \Big|_{\phi \rightarrow 0} \quad (4.17)$$

with $\langle \hat{T} \rangle$, the thermal expectation value and $p_n = e^{-\beta E_n}$, the Boltzmann weight.

The problem has been reduced to the calculation of the curvature of energy levels. So far, we have just spoken about conductivity in the sense of moving charge carriers. But as we are concerned with the XXZ -model we have to think about the relation of spin and charge transport. We note that the XXZ -model is equivalent via the Jordan-Wigner transformation [52] to the spinless fermion model

$$\mathcal{H} = J \sum_i \left[-\frac{1}{2} (c_{i+1}^\dagger c_i + c_i^\dagger c_{i+1}) + \Delta \left(c_i^\dagger c_i - \frac{1}{2} \right) \left(c_{i+1}^\dagger c_{i+1} - \frac{1}{2} \right) \right]. \quad (4.18)$$

In this mapping the fermion density-density correlation function is nothing but the $S_z - S_z$ -correlator. Thus, the description of fermion transport directly translates into spin language.

³Here: $k = -eA_x$.

4.2. The Drude weight with magnons

In this section we shall review the calculation of the Drude weight for the critical XXZ -model in [36]. In this work the method that has been used for the Hubbard model [35] and other hopping models [33] was adapted to the Heisenberg model.

At first, we want to give a short summary of the coordinate Bethe ansatz [1, 56]. One starts with the Hamiltonian for the XXZ -chain

$$H = J \sum_{i=1}^N (S_i^x S_{i+1}^x + S_i^y S_{i+1}^y + \Delta S_i^z S_{i+1}^z) - h \sum_{j=1}^N S_j^z \quad (4.19)$$

with $\Delta = \cos \gamma$ and $0 \leq \Delta \leq 1$. We note that $S^z = \sum S_i^z$ is a conserved quantity and we are looking for eigenstates at $S^z = N/2 - M$ suggesting that we consider a background of N spins pointing up denoted as $|0\rangle$. Applying S_n^- at site n will flip the concerned spin. Thus, the eigenfunction for a given magnetization M is the following superposition

$$\Psi = \sum f(n_1, n_2, \dots, n_M) S_{n_1}^- S_{n_2}^- \cdots S_{n_M}^- |0\rangle. \quad (4.20)$$

Next we assume the wave function is written as follows

$$f(n_1, n_2, \dots, n_M) = \sum_P A(P) \exp \left(i \sum_{j=1}^M k_{P_j} n_j + \frac{1}{2} \sum_{j<l} \phi_{P_j, P_l} \right) \quad (4.21)$$

where the summation is over the permutations of $\{1, 2, \dots, M\}$. k_1, k_2, \dots, k_M are called quasi-momenta. These momenta k_α and the phase shifts $\phi_{\alpha\beta}$ which characterize the wave functions are expressed in terms of rapidities x_α

$$\begin{aligned} \cot \left(\frac{k_\alpha}{2} \right) &= \cot \left(\frac{\gamma}{2} \right) \tanh \left(\frac{\gamma x_\alpha}{2} \right), \\ \cot \left(\frac{\phi_{\alpha\beta}}{2} \right) &= \cot \left(\frac{\gamma}{2} \right) \tanh \left(\frac{\gamma(x_\alpha - x_\beta)}{2} \right). \end{aligned} \quad (4.22)$$

Imposing periodic boundary conditions on the Bethe ansatz wave function the following relations are obtained

$$\left\{ \frac{\sinh \frac{1}{2} \gamma (x_\alpha + i)}{\sinh \frac{1}{2} \gamma (x_\alpha - i)} \right\}^N = -e^{i\phi N} \prod_{\beta=1}^M \left\{ \frac{\sinh \frac{1}{2} \gamma (x_\alpha - x_\beta + 2i)}{\sinh \frac{1}{2} \gamma (x_\alpha - x_\beta - 2i)} \right\}. \quad (4.23)$$

As stated in [9] the solutions of equation (4.23) are grouped into strings of order n_j , ($j = 1, \dots, \nu$) and parity⁴ $v_j = \pm 1$. This is the string hypothesis.

For $\theta = \pi/\nu$ the allowed strings are either of order $n_j = j$, ($j = 1, \dots, \nu - 1$) and parity $v_j = +$ and are of the form

$$x_{\alpha,+}^{n,k} = x_\alpha^n + (n + 1 - 2k)i + \mathcal{O}(e^{-\delta N}), \quad k = 1, 2, \dots, n \quad (4.24)$$

or of length $n_\nu = 1$ and parity $v_\nu = -$ and are of the form

$$x_{\alpha,-} = x_\alpha + i\nu + \mathcal{O}(e^{-\delta N}), \quad \delta > 0. \quad (4.25)$$

⁴There are two types of strings: one type has its centre on the real axis (parity +) and the other type has its centre on a straight line parallel to the real axis (parity -)[26].

In principle, equation (4.23) determines the position of every rapidity. Taking advantage of the string conjecture we multiply all equations (4.23) belonging to members of the same string. For this problem we have the following BAE in logarithmic representation

$$N\theta_j(x_\alpha^j) = 2\pi I_\alpha^j + \sum_{k=1}^{\infty} \sum_{\beta=1}^{M_k} \Theta_{jk}(x_\alpha^j - x_\beta^k) + n_j \phi N, \quad \alpha = 1, 2, \dots, M_j \quad (4.26)$$

where I_α^j are integers or half-integers and M_k is the number of strings of type k . The other functions are given as

$$\theta_j(x) = f(x; n_j, v_j), \quad (4.27)$$

$$\begin{aligned} \Theta_{jk}(x) &= f(x; |n_j - n_k|, v_j v_k) + f(x; n_j + n_k, v_j v_k) \\ &\quad + 2 \sum_{i=1}^{\min(n_j, n_k) - 1} f(x; |n_j - n_k| + 2i, v_j v_k), \end{aligned} \quad (4.28)$$

$$f(x; n, v) = 2v \tan^{-1}[(\cot(n\pi/2\nu))^v \tanh(\pi x/2\nu)]. \quad (4.29)$$

In the thermodynamic limit we get integral equations for the densities of excitations ρ_j and hole densities ρ_j^h [26]

$$\lambda_j(\rho_j(x) + \rho_j^h(x)) = a_j(x) - \sum_k T_{jk} * \rho_k(x) \quad (4.30)$$

where $*$ denotes the convolution $a * b(x) = \int_{-\infty}^{\infty} a(x-y)b(y) dy$ and

$$a_j(x) = \frac{1}{2\pi} \frac{d}{dx} \theta_j(x), \quad T_{jk}(x) = \frac{1}{2\pi} \frac{d}{dx} \Theta_{jk}(x). \quad (4.31)$$

The sum over k is constrained to the allowed strings given in our case by the equations (4.24) and (4.25) and $\lambda_j = 1$, $j = 1, \dots, \nu - 1$, $\lambda_\nu = -1$.

Minimizing the free energy we obtain the standard Bethe ansatz equations for the equilibrium densities $\eta_j = \rho_j^h / \rho_j$ at temperature $T = 1/\beta$

$$\ln \eta_j = -2\nu \sin(\pi/\nu) J a_j \beta + \sum_{k=1}^{\nu-1} \lambda_k T_{jk} * \ln(1 + \eta_k^{-1}). \quad (4.32)$$

These relations define the temperature dependent effective dispersions $\epsilon_j = (1/\beta) \ln(\rho_j^h / \rho_j)$. In the string representation the energy is given by

$$E = N \sum_{j=1}^{\infty} \int_{-\infty}^{\infty} \left(-2\nu \sin\left(\frac{\pi}{\nu}\right) J a_j(x) \right) \rho_j(x) dx. \quad (4.33)$$

These are the results of the standard thermodynamic Bethe ansatz by Takahashi [9] in the following referred to as standard TBA. On this basis Zotos [36] calculated an expression for the Drude weight by determination of the finite size correction to these TBA-equations. The final expression for the Drude-weight is

$$D = \frac{1}{2} \sum_j \int_{-\infty}^{\infty} \left[(\rho_j + \rho_j^h) \frac{\partial g_j^{(1)}}{\partial \phi} \right]^2 \frac{d}{dx} \left(\frac{-1}{1 + e^{\beta \epsilon_j}} \right) \left(\frac{1}{\rho_j + \rho_j^h} \frac{d\epsilon_j}{dx} \right) dx \quad (4.34)$$

with $x_N^j = x_\infty^j + \frac{g_j^{(1)}}{N} + \frac{g_j^{(2)}}{N^2}$ being the finite size correction of the spectral parameters. The coefficients $g_j^{(i)}$ depend on the twist ϕ .

We do not need to explain the methods that have been used to obtain this result due to the following reason:

In the next section we show the equivalence of the non-linear integral equations (3.8) to certain integral equations derived by standard TBA, but *without* using the string hypothesis.

Therefore, it is possible to proceed in the same manner in order to derive an expression for the Drude weight and the same techniques are applied. But it is not necessary to deal with (up to) infinitely many integral equations for arbitrary anisotropy parameter.

4.3. The connection between standard TBA and the quantum transfer matrix approach

We now want to connect the two different approaches we have been presenting in section 3.3 and 4.2. As described before the standard TBA consists in principle of introducing magnon densities or, as excitations are concerned, string densities for which integral equations can be derived. The integral equations based on the QTM-approach are using skillfully chosen auxiliary functions containing the whole thermodynamic information. However, a disadvantage of this approach lies in the involved nature of the mathematical constructions which are not physically intuitive (see appendix D). These complications present a serious shortcoming with respect to generalizations to other integrable, notably itinerant fermion models. Here a review of observations made in [40] is given that make contact between standard TBA with magnons and the integral equations (3.8).

We start with the Bethe ansatz equations in (4.23) with a scaled spectral parameter $\frac{1}{2}\gamma x \rightarrow x$ leading to momentum k and energy ϵ

$$k(x) = i \log \frac{\sinh(x - i\gamma/2)}{\sinh(x + i\gamma/2)}, \quad \epsilon(x) = J \frac{\sin \gamma}{2} k'(x) - h \quad (4.35)$$

where real values are obtained for $\text{Im } x = 0$ and $-\pi/2$ defining magnon bands of type “+” and “-”. Any two magnons with spectral parameters x and y scatter with phase shift $\theta(x - y)$ where

$$\theta(z) = -i \log \frac{\sinh(z - i\gamma)}{\sinh(z + i\gamma)}. \quad (4.36)$$

Next, we apply standard TBA as in section 4.2, but just to these magnons and ignore the

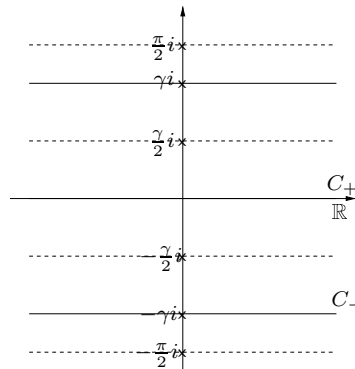


Figure 4.1.: Integration contours for the integral equations.

bound states (strings). However, the magnons of the $-$ band are considered for spectral parameter x with $\text{Im } x = -\gamma$, hence avoiding the branch cut in the scattering phase.

The density functions for the particles ϱ_j and the holes ϱ_j^h for the bands $j = +, -$ give rise to the definition of the ratio function $\eta_j = \varrho_j^h / \varrho_j$. The analysis shows that η_+ and η_- are analytic continuations of each other. Quantitatively, we have $\eta_-(x + i\gamma) = \eta_+(x) =: \eta(x)$ subject to the non-linear integral equation

$$\log \eta(x) = \beta \epsilon(x) + \int_C \kappa(x - y) \log \left(1 + \frac{1}{\eta(y)} \right) dy \quad (4.37)$$

where $\kappa(x) = \frac{1}{2\pi}\theta'(x)$ and C is a contour consisting of the paths C_+ and C_- with $\text{Im } y = 0$ and $-\gamma$ encircled in clockwise manner. Substituting $\log(1 + \frac{1}{\eta}) = \log(1 + \eta) - \log \eta$ we find

$$\begin{aligned} \log \eta(x) = -\beta\bar{\epsilon}(x) &+ \int_{C_+} \bar{\kappa}(x-y) \log(1 + \eta(y)) dy \\ &- \int_{C_-} \bar{\kappa}(x-y) \log\left(1 + \frac{1}{\eta(y)}\right) dy \end{aligned} \quad (4.38)$$

with

$$\bar{\kappa}(x) := \frac{1}{2\pi} \int \frac{\sinh(\frac{\pi}{2} - \gamma)k}{2 \cosh \frac{\gamma}{2}k \sinh \frac{\pi-\gamma}{2}k} e^{ikx} dx \quad (4.39)$$

and

$$\bar{\epsilon}(x) = J \frac{\sin \gamma}{2} \frac{\pi}{\gamma} \frac{1}{\cosh \frac{\pi}{\gamma}x} + \frac{\pi}{2(\pi - \gamma)} h. \quad (4.40)$$

The explicit calculation is given in appendix C. Equations (4.38) are equivalent to those obtained in (3.8). The free energy is given as

$$f = -\frac{T}{2\pi} \int_{-\infty}^{\infty} e_0(x) \ln [(1 + \eta(x))(1 + \eta^{-1}(x - i\gamma))] dx \quad (4.41)$$

in analogy to (3.11). We note that $\eta_- = \frac{1}{\eta}$. In the above construction we assumed that magnons (on paths C_{\pm}) are elementary excitations and contain all information about the thermodynamics. Bound states were implicitly taken into account by use of the exact scattering phase probed in the analyticity strip. The *a posteriori* success of that reasoning is important due to two reasons. First, the construction is as simple as the standard TBA, however avoiding the problems of dealing with density functions for (up to) infinite many bound states. This may be of great advantage in the study of more complicated systems. Second, we have a simple particle approach to the Heisenberg chain which will allow to deal with problems occurring when calculating the Drude weight with the alternative method as described in section 4.2. In particular, we can use standard TBA without strings and at the same time we can avoid the technical problems arising when dealing with the NLIE in the spinon approach in section 3.3. The formulation of the Drude weight problem in this special magnon picture will be done in the remainder of this work.

We can now apply the standard TBA-methods on the contours C_+ and C_- knowing that a simple particle-hole transformation on *one* contour ensures the equivalence to the integral equations (3.8). In this way we avoid technical problems that appeared in [22] when calculating in the direct spinon approach.

4.4. Alternative derivation of the Drude weight

Suppose we have a system with just two elementary excitations (quasi-particles) which shall be denoted by “magnon” and “anti-magnon”, respectively⁵. The energy and momentum are parametrized by a spectral parameter $\lambda : \epsilon(\lambda), p(\lambda)$. The scattering phases of particles with momenta λ, μ are denoted by matrix elements $\Theta_{\alpha\beta}(\lambda - \mu)$ with $\alpha, \beta = 1, 2$ where 1 denotes a “magnon” and 2 an “anti-magnon”. For such a system we write down the BAE for a chain of length L with twist angle ϕ

$$Lp(\lambda_{1j}) + \sum_{l \neq j} \Theta_{11}(\lambda_{1j} - \lambda_{1l}) + \sum_l \Theta_{12}(\lambda_{1j} - \lambda_{2l}) = 2\pi I_{1j} + \phi, \quad (4.42)$$

$$Lp(\lambda_{2j}) + \sum_l \Theta_{21}(\lambda_{2j} - \lambda_{1l}) + \sum_{l \neq j} \Theta_{22}(\lambda_{2j} - \lambda_{2l}) = 2\pi I_{2j} - \phi. \quad (4.43)$$

Introduce now a counting-function $Z \propto \frac{I}{L}$ in the following sense

$$Z_\alpha(\lambda_\alpha) = \frac{1}{2\pi} p(\lambda_\alpha) + \frac{1}{2\pi L} \sum_\beta \sum_l \Theta_{\alpha\beta}(\lambda_\alpha - \lambda_{\beta l}) - \frac{\phi_\alpha}{2\pi L}. \quad (4.44)$$

We get the density functions $\rho_\alpha(\lambda_\alpha) + \rho_\alpha^h(\lambda_\alpha)$ by differentiating this expression with respect to λ_α because

$$\#particles + \#holes = (\rho_\alpha + \rho_\alpha^h) \Delta\lambda_\alpha = \left(Z_\alpha(\lambda_\alpha + \Delta\lambda_\alpha) - Z_\alpha(\lambda_\alpha) \right) / 2\pi \quad (4.45)$$

holds. We then have

$$\rho_\alpha(\lambda_\alpha) + \rho_\alpha^h(\lambda_\alpha) = \frac{1}{2\pi} p'(\lambda_\alpha) + \frac{1}{2\pi L} \sum_\beta \sum_l \Theta'_{\alpha\beta}(\lambda_\alpha - \lambda_{\beta l}). \quad (4.46)$$

In the thermodynamic limit this can be written as

$$\rho_\alpha(\lambda) + \rho_\alpha^h(\lambda) = \frac{1}{2\pi} p'(\lambda) + \frac{1}{2\pi} \sum_\beta \Theta'_{\alpha\beta} * \rho_\beta \quad (4.47)$$

where $p'(\lambda) = \epsilon^{(0)}(\lambda)$.⁶ We need now an expression for $\rho_\alpha^h/\rho_\alpha$ which gives rise to the definition of the dressed energy $\epsilon_\alpha = -T \ln(\rho_\alpha^h/\rho_\alpha)$. We shall get this by a variation of the free energy with respect to the distribution functions and do this in some detail. To this end we need the free energy per site. The entropy is given as

$$s = \frac{S}{L} = \sum_\alpha \int_{-\infty}^{\infty} ([\rho_\alpha + \rho_\alpha^h] \ln(\rho_\alpha + \rho_\alpha^h) - \rho_\alpha \ln \rho_\alpha - \rho_\alpha^h \ln \rho_\alpha^h) d\lambda, \quad (4.48)$$

for the energy per site we have

$$e = \frac{E}{L} = \sum_\alpha \int_{-\infty}^{\infty} \epsilon_\alpha \rho_\alpha d\lambda, \quad (4.49)$$

$$\epsilon_{1/2} = \epsilon \pm \frac{h}{2}. \quad (4.50)$$

⁵Note that now the names of the quasi-particles are meant in the sense of section 4.3 and the particles are on the contours of figure 4.1.

⁶ $p'(\lambda)$ is positive (negative) on C_+ (C_-) of figure 4.1.

This leads us to an expression for the free energy per site

$$\begin{aligned} f &= e - Ts \\ &= \sum_{\alpha} \left(\int_{-\infty}^{\infty} \epsilon_{\alpha} \rho_{\alpha} d\lambda - T \int_{-\infty}^{\infty} \left([\rho_{\alpha} + \rho_{\alpha}^h] \ln(\rho_{\alpha} + \rho_{\alpha}^h) - \rho_{\alpha} \ln \rho_{\alpha} - \rho_{\alpha}^h \ln \rho_{\alpha}^h \right) d\lambda \right). \end{aligned} \quad (4.51)$$

The variation with respect to the distribution-functions gives us

$$0 = \sum_{\alpha} \left(\frac{\delta f}{\delta \rho_1} + \frac{\delta f}{\delta \rho_1^h} \right) \quad (4.52)$$

under the restriction

$$\delta \rho_{\alpha} + \delta \rho_{\alpha}^h = \frac{1}{2\pi} \sum_{\beta} \Theta'_{\alpha\beta} * \delta \rho_{\beta}. \quad (4.53)$$

Therefrom we gain

$$\delta \rho_{\alpha}^h = \frac{1}{2\pi} \sum_{\beta} \Theta'_{\alpha\beta} * \delta \rho_{\beta} - \delta \rho_{\alpha} \quad (4.54)$$

and further

$$\begin{aligned} 0 &= \sum_{\alpha} \left[\int_{-\infty}^{\infty} \left(\epsilon_{\alpha} - T \ln \left(1 + \frac{\rho_{\alpha}}{\rho_{\alpha}^h} \right) \right) \delta \rho_{\alpha} d\lambda \right. \\ &\quad \left. - \frac{T}{2\pi} \int \ln \left(1 + \frac{\rho_{\alpha}^h}{\rho_{\alpha}} \right) \left[\sum_{\beta} \Theta'_{\alpha\beta} * \delta \rho_{\beta} - 2\pi \delta \rho_{\alpha} \right] d\lambda \right]. \end{aligned} \quad (4.55)$$

Using $\Theta'(-\lambda) = \Theta'^T(\lambda)$ and rewriting the second part we find

$$\begin{aligned} &\int_{-\infty}^{\infty} \ln \left(1 + \frac{\rho_{\alpha}^h}{\rho_{\alpha}} \right) \left[\sum_{\beta} \Theta'_{\alpha\beta} * \delta \rho_{\beta} - 2\pi \delta \rho_{\alpha} \right] d\lambda \\ &= \sum_{\beta} \left(\int_{-\infty}^{\infty} \ln \left(1 + \frac{\rho_{\alpha}^h}{\rho_{\alpha}} \right) * \Theta_{\alpha\beta}^{T'} \delta \rho_{\beta} \right) - 2\pi \int_{-\infty}^{\infty} \ln \left(1 + \frac{\rho_{\alpha}^h}{\rho_{\alpha}} \right) \delta \rho_{\alpha}. \end{aligned} \quad (4.56)$$

Bringing all this together we get an integral equation for the dressed energy ϵ_{α} or in our notation for $\ln a_{\alpha}$ with $a_{\alpha} = \frac{\rho_{\alpha}^h}{\rho_{\alpha}}$ ($A_{\alpha} = 1 + a_{\alpha}$). This equation reads as follows

$$\underbrace{\ln a_{\alpha}(\lambda)}_{-\beta \epsilon_{\alpha}} = -\beta \epsilon_{\alpha}^{(0)}(\lambda) + \frac{1}{2\pi} \sum_{\beta} \Theta'_{\alpha\beta} * \ln A_{\beta}. \quad (4.57)$$

As we need the derivative of the dressed energy later on we shall give the corresponding equation right here

$$\epsilon'_{\alpha}(\lambda) = \epsilon_{\alpha}^{(0)'} - \frac{T}{2\pi} \sum_{\beta} \Theta''_{\alpha\beta} * \ln A_{\beta}. \quad (4.58)$$

For the Drude weight we have to calculate finite size effects. Therefore, we make the following ansatz for the parameter λ [32]

$$\lambda_{\alpha j} = \lambda_{\alpha j}^{\infty} + \frac{g_{\alpha j}^{(1)}}{L} + \frac{g_{\alpha j}^{(2)}}{L^2} \quad (4.59)$$

with the coefficients $g_{\alpha j}^{(k)}$ depending on ϕ_{α} . By use of this ansatz we expand the counting function up to order of $1/L^2$ and get

$$\begin{aligned} Z_{\alpha}(\lambda) &= \frac{1}{2\pi} p(\lambda) + \frac{1}{2\pi L} \sum_{\beta} \sum_l \Theta_{\alpha\beta}(\lambda_{\alpha} - \lambda_{\beta l}^{\infty}), \\ &- \frac{1}{2\pi L} \sum_{\beta} \sum_l \Theta'_{\alpha\beta}(\lambda_{\alpha} - \lambda_{\beta l}^{\infty}) \frac{g_{\beta l}^{(1)}}{L} - \frac{\phi_{\alpha}}{2\pi L}, \\ &+ \frac{1}{2\pi L} \sum_{\beta} \sum_l \Theta''_{\alpha\beta}(\lambda_{\alpha} - \lambda_{\beta l}^{\infty}) \left(\frac{g_{\beta l}^{(1)}}{2L} \right)^2, \\ &- \frac{1}{2\pi L} \sum_{\beta} \sum_l \Theta'_{\alpha\beta}(\lambda_{\alpha} - \lambda_{\beta l}^{\infty}) \frac{g_{\beta l}^{(2)}}{L^2}. \end{aligned} \quad (4.60)$$

Assume now that in the thermodynamic limit the coefficients behave like

$$g_{\alpha l}^{(i)} \rightarrow g_{\alpha}^{(i)}(\lambda_{\alpha l}^{\infty}). \quad (4.61)$$

Then we can write the counting function in the form

$$Z_{\alpha}(\lambda) = Z_{\alpha}^{\infty}(\lambda) + \frac{Z_{\alpha}^{(1)}}{L}(\lambda) + \frac{Z_{\alpha}^{(2)}}{L^2}(\lambda), \quad (4.62)$$

$$Z_{\alpha}^{(\infty)}(\lambda) = \frac{1}{2\pi} p(\lambda) + \frac{1}{2\pi} \sum_{\beta} \Theta_{\alpha\beta} * \rho_{\beta}(\lambda), \quad (4.63)$$

$$Z_{\alpha}^{(1)}(\lambda) = -\frac{1}{2\pi} \sum_{\beta} \Theta'_{\alpha\beta} * (g_{\beta}^{(1)} \rho_{\beta}) - \frac{\phi_{\alpha}}{2\pi}, \quad (4.64)$$

$$Z_{\alpha}^{(2)}(\lambda) = \frac{1}{2\pi} \sum_{\beta} \left(\frac{1}{2} \Theta''_{\alpha\beta} \left(g_{\beta}^{(1)2} \rho_{\beta} \right) - \Theta'_{\alpha\beta} * (g_{\beta}^{(2)} \rho_{\beta}) \right). \quad (4.65)$$

In the next step we use the ansatz for λ a second time in the sense that

$$Z_{\alpha}(\lambda_{\alpha j}) = Z_{\alpha} \left(\lambda_{\alpha j}^{\infty} + \frac{g_{\alpha j}^{(1)}}{L} + \frac{g_{\alpha j}^{(2)}}{L^2} \right). \quad (4.66)$$

We shall expand this again up to the order of $1/L^2$ and finally get the following

$$\begin{aligned}
Z_\alpha(\lambda_{\alpha j}) &= Z_\alpha(\lambda_{\alpha j}^\infty) + \frac{1}{L} Z'_\alpha(\lambda_{\alpha j}^\infty) g_{\alpha j}^{(1)} \\
&+ \frac{1}{L^2} \left[\frac{1}{2} Z''_\alpha(\lambda_{\alpha j}^\infty) g_{\alpha j}^{(1)^2} + Z'_\alpha(\lambda_{\alpha j}^\infty) g_{\alpha j}^{(2)} \right] \\
&= Z_\alpha(\lambda_{\alpha j}^\infty) + \frac{1}{L} \left[Z_\alpha^{(1)}(\lambda_{\alpha j}^\infty) + Z_\alpha^{\infty'}(\lambda_{\alpha j}^\infty) g_{\alpha j}^{(1)} \right] \\
&+ \frac{1}{L^2} \left[Z_\alpha^{(2)}(\lambda_{\alpha j}^\infty) + Z_\alpha^{(1)'}(\lambda_{\alpha j}^\infty) g_{\alpha j}^{(1)} + \frac{1}{2} Z_\alpha^{\infty''}(\lambda_{\alpha j}^\infty) g_{\alpha j}^{(1)^2} \right. \\
&\left. + Z_\alpha^{\infty'}(\lambda_{\alpha j}^\infty) g_{\alpha j}^{(2)} \right] = \frac{2\pi I_\alpha}{L}.
\end{aligned} \tag{4.67}$$

This equation has to be satisfied in each order of L and we get the conditions for our auxiliary functions from

$$\begin{aligned}
Z_\alpha^{(1)}(\lambda_{\alpha j}^\infty) + Z_\alpha^{\infty'}(\lambda_{\alpha j}^\infty) g_{\alpha j}^{(1)} &= 0 \\
Z_\alpha^{(2)}(\lambda_{\alpha j}^\infty) + Z_\alpha^{(1)'}(\lambda_{\alpha j}^\infty) g_{\alpha j}^{(1)} + \frac{1}{2} Z_\alpha^{\infty''}(\lambda_{\alpha j}^\infty) g_{\alpha j}^{(1)^2} + Z_\alpha^{\infty'}(\lambda_{\alpha j}^\infty) g_{\alpha j}^{(2)} &= 0.
\end{aligned} \tag{4.68}$$

In more detail this reads as follows

$$\begin{aligned}
\varphi_\alpha(g_\alpha^{(1)} \rho_\alpha) &= \frac{\phi_\alpha}{2\pi} + \frac{1}{2\pi} \sum_\beta \Theta'_{\alpha\beta} * (g_\beta^{(1)} \rho_\beta), \\
\varphi_\alpha(g_\alpha^{(2)} \rho_\alpha) &= l'_\alpha + \frac{1}{2\pi} \sum_\beta \Theta'_{\alpha\beta} * (g_\beta^{(2)} \rho_\beta), \\
l_\alpha &= \frac{1}{2} (\rho_\alpha + \rho_\alpha^h) g_\alpha^{(1)^2} - \frac{1}{4\pi} \sum_\beta \Theta'_{\alpha\beta} * (g_\beta^{(1)^2} \rho_\beta)
\end{aligned} \tag{4.69}$$

where $\varphi_\alpha = 1 + e^{\beta\epsilon_\alpha} = (\rho_\alpha + \rho_\alpha^h)/\rho_\alpha$. If we focus again on the Drude weight we are more interested in the derivatives with respect to ϕ_α which shall be denoted by dots

$$\begin{aligned}
\varphi_\alpha(\dot{g}_\alpha^{(1)} \rho_\alpha) &= \pm \frac{1}{2\pi} + \frac{1}{2\pi} \sum_\beta \Theta'_{\alpha\beta} * (\dot{g}_\beta^{(1)} \rho_\beta), \\
\varphi_\alpha(\ddot{g}_\alpha^{(2)} \rho_\alpha) &= f'_\alpha + \frac{1}{2\pi} \sum_\beta \Theta'_{\alpha\beta} * (\ddot{g}_\beta^{(2)} \rho_\beta), \\
f_\alpha = \ddot{l}_\alpha &= (\rho_\alpha + \rho_\alpha^h) \dot{g}_\alpha^{(1)^2} - \frac{1}{2\pi} \sum_\beta \Theta'_{\alpha\beta} * (\dot{g}_\beta^{(1)^2} \rho_\beta).
\end{aligned} \tag{4.70}$$

These are the relevant integral equations for the auxiliary functions. For the Drude weight D we have to sum up the curvatures of the energy levels with respect to ϕ_α . Therefore, we have to expand the energy function up to second order. As the first order correction term is linear in ϕ_α we just write down the second order term which shall be denoted by

$$E_2 = \sum_\alpha \int_{-\infty}^{\infty} \left(\frac{1}{2} \epsilon_\alpha^{(0)''} g_\alpha^{(1)^2} \rho_\alpha + \epsilon_\alpha^{(0)'} g_\alpha^{(2)} \rho_\alpha \right) d\lambda \tag{4.71}$$

and the second derivative of this is

$$2D = \ddot{E}_2 = \sum_{\alpha} \int_{-\infty}^{\infty} \left(\epsilon_{\alpha}^{(0)''} \dot{g}_{\alpha}^{(1)^2} \rho_{\alpha} + \epsilon_{\alpha}^{(0)'} \ddot{g}_{\alpha}^{(2)} \rho_{\alpha} \right) d\lambda. \quad (4.72)$$

In principle this is the derived result. But this expression is not suitable for numerical studies as even in the free-fermion case the individual integral expressions are diverging, however the complete sum of integrals is finite. In order to derive a more convenient result for numerical calculations we begin with the following identities

$$\begin{aligned} a_{\alpha} &= \sum_{\beta} T_{\alpha\beta} * A_{\beta}, \\ b_{\alpha} &= \sum_{\beta} T_{\alpha\beta} * B_{\beta}, \\ \Rightarrow \sum_{\alpha} \int B_{\alpha} a_{\alpha} d\lambda &= \sum_{\alpha} \int A_{\alpha} b_{\alpha} d\lambda. \end{aligned} \quad (4.73)$$

In the following we leave out \sum_{α} for the sake of brevity and rewrite (4.70) and (4.57) as follows

$$\begin{aligned} \varphi_{\alpha} \ddot{g}_{\alpha}^{(2)} \rho_{\alpha} - f'_{\alpha} &= \frac{1}{2\pi} \sum_{\beta} \Theta'_{\alpha\beta} * (\ddot{g}_{\beta}^{(2)} \rho_{\beta}), \\ \epsilon_{\alpha}^{(0)'} - \epsilon'_{\alpha} &= \frac{1}{2\pi} \sum_{\beta} \Theta'_{\alpha\beta} * \left(\frac{1}{\beta} \ln A_{\beta} \right)', \\ \varphi_{\alpha} = 1 + e^{\beta\epsilon_{\alpha}} \quad , \quad A_{\alpha} = 1 + e^{-\beta\epsilon_{\alpha}}. \end{aligned} \quad (4.74)$$

We are now able to write down the following identity

$$\begin{aligned} &\int_{-\infty}^{\infty} \frac{1}{\beta} \left(\varphi_{\alpha} \ddot{g}_{\alpha}^{(2)} \rho_{\alpha} (\ln A_{\alpha})' - f'_{\alpha} (\ln A_{\alpha})' \right) d\lambda \\ &= \int_{-\infty}^{\infty} \left((\epsilon_{\alpha}^{(0)'} - \epsilon'_{\alpha}) \ddot{g}_{\alpha}^{(2)} \rho_{\alpha} \right) d\lambda. \end{aligned} \quad (4.75)$$

Using that $(\ln A_{\alpha})' = -\frac{\beta\epsilon'_{\alpha}}{\varphi_{\alpha}}$ this reads

$$\begin{aligned} &\int_{-\infty}^{\infty} \epsilon_{\alpha}^{(0)'} \ddot{g}_{\alpha}^{(2)} \rho_{\alpha} d\lambda = - \int_{-\infty}^{\infty} \frac{1}{\beta} f'_{\alpha} (\ln A_{\alpha})' d\lambda \\ &= - \int_{-\infty}^{\infty} (\varphi_{\alpha} \dot{g}_{\alpha}^{(1)^2} \rho_{\alpha})' \left(\frac{1}{\beta} \ln A_{\alpha} \right)' d\lambda + \int_{-\infty}^{\infty} \sum_{\beta} \left(\frac{1}{\beta} \ln A_{\alpha} \right)' \Theta'_{\alpha\beta} d\lambda \end{aligned} \quad (4.76)$$

where

$$\sum_{\beta} \left(\frac{1}{\beta} \ln A_{\alpha} \right)' \Theta'_{\alpha\beta} = \epsilon_{\alpha}^{(0)'} - \epsilon'_{\alpha}. \quad (4.77)$$

Inserting (4.77) and using integration by parts⁷

$$\int_{-\infty}^{\infty} \epsilon_{\alpha}^{(0)'} \ddot{g}_{\alpha}^{(2)} \rho_{\alpha} d\lambda = \int_{-\infty}^{\infty} (\varphi_{\alpha} \dot{g}_{\alpha}^{(1)2} \rho_{\alpha}) \left(\frac{1}{\beta} \ln A_{\alpha} \right)' d\lambda + \int_{-\infty}^{\infty} (-\epsilon_{\alpha}^{(0)''} + \epsilon_{\alpha}^{\prime\prime}) (\dot{g}_{\alpha}^{(1)2} \rho_{\alpha}) d\lambda. \quad (4.78)$$

This results in a new expression for the Drude weight. But first we write down

$$\left(\frac{1}{\beta} \ln A_{\alpha} \right)' = \left(-\frac{\epsilon_{\alpha}'}{\varphi_{\alpha}} \right)' = -\frac{\epsilon_{\alpha}''}{\varphi_{\alpha}} + \frac{\beta \epsilon_{\alpha}^{\prime 2}}{\varphi_{\alpha} A_{\alpha}}. \quad (4.79)$$

It can be easily seen that again terms cancel and we get the following expression for the Drude weight

$$\begin{aligned} D &= \frac{1}{2} \sum_{\alpha} \left(\int_{-\infty}^{\infty} \epsilon_{\alpha}^{(0)'} \ddot{g}_{\alpha}^{(2)} \rho_{\alpha} d\lambda + \int_{-\infty}^{\infty} \epsilon_{\alpha}^{(0)''} (\dot{g}_{\alpha}^{(1)2} \rho_{\alpha}) d\lambda \right) \\ &= \frac{1}{2} \sum_{\alpha} \beta \int_{-\infty}^{\infty} \frac{\dot{g}_{\alpha}^{(1)2} \rho_{\alpha} \epsilon_{\alpha}^{\prime 2}}{A_{\alpha}} d\lambda. \end{aligned} \quad (4.80)$$

This is the expression we deal with. This can be formulated in terms of “thermodynamic” derivatives in the following way.

We start with equation (4.57)

$$\ln a_{\alpha}(\lambda) = -\beta \epsilon_{\alpha}^0(\lambda) \pm \beta h + \frac{1}{2\pi} \sum_{\beta} \theta'_{\alpha\beta} * \ln A_{\beta}. \quad (4.81)$$

Differentiating with respect to β and setting $h = 0$ gives an expression that has the same structure as equation (4.47), noting that $(1 + \frac{\rho_{\alpha}^h}{\rho_{\alpha}}) * \rho_{\alpha} = A_{\alpha}/a_{\alpha}$. By comparison we can conclude

$$-\frac{1}{2\pi} \frac{\partial}{\partial \beta} \ln A_{\alpha} = \rho_{\alpha}. \quad (4.82)$$

When differentiating with respect to h we can compare with equation (4.70) and get

$$\dot{g}_{\alpha}^{(1)} \rho_{\alpha} = \pm \frac{1}{2\pi} \frac{\partial}{\partial \beta h} \ln A_{\alpha}. \quad (4.83)$$

The Drude weight (4.80) now looks like

$$D = -\frac{\sin \gamma}{4\pi\beta} \sum_{\alpha=1-\infty}^2 \int_{-\infty}^{\infty} \frac{\left(\frac{\partial}{\partial \beta h} \ln A_{\alpha} \right)^2 \varphi_{\alpha}^2 (\ln A)^2}{\partial_{\beta} A_{\alpha}} dx. \quad (4.84)$$

It remains a remark about the consistency of our derivation. We know from section 4.3 that the equations (3.8) are equivalent to the equations (4.37) when carrying out a particle-hole transformation only on the integration contour $\text{Im } x = -\gamma$. We want to do this in the result for the second integrand of Drude weight expression (4.84) by replacing

⁷There are no boundary terms because the functions on the different integration contours are analytic continuations of each other as explained in section 4.3.

$$\tilde{a}(x) = 1/a_2(x).$$

We have

$$\frac{\left(\frac{\partial}{\partial\beta h} \ln A_2\right)^2 \left(\frac{A_2}{a_2}\right)^2 \ln A_2'^2}{\partial_\beta A_2} = -\frac{\left(\frac{\partial}{\partial\beta h} \ln \tilde{A}_2\right)^2 \left(\frac{\tilde{A}_2}{\tilde{a}_2}\right)^2 \ln \tilde{A}_2'^2}{\partial_\beta \tilde{A}_2}. \quad (4.85)$$

The minus sign cancels when minding that the kernels of the two different TBA-equations (4.38) and (4.81) have opposite signs what can be expressed in opposite integration contours. So the expression for the Drude weight is form-invariant under the particle-hole transformation ensuring the equivalence to the NLIE (3.8) obtained by the quantum transfer matrix approach.

In the end we see that we could have also done the whole derivation in the spinon picture.

4.4.1. The Drude weight for $T = 0$

In order to derive the value of the Drude weight for $h = 0$ and $T = 0$ we start with

$$D = -\frac{\sin \gamma}{4\pi\beta} \sum_{\alpha=1}^2 \int_{-\infty}^{\infty} \frac{\left(\frac{\partial}{\partial\beta h} \ln A_{\alpha}\right)^2 \varphi_{\alpha}^2(\ln A)^{\prime 2}}{\partial_{\beta} A_{\alpha}} dx. \quad (4.86)$$

Next, this expression is to be calculated in the low temperature limit. The involved auxiliary functions show a certain scaling behaviour in the regime of low temperatures. As a matter of fact only the asymptotic behaviour of the involved functions determines thermodynamic quantities as the free energy or the susceptibility (see [10]). For this purpose one has to calculate in the scaling limit $x \rightarrow x \pm \frac{\gamma}{\pi} \ln \beta$. We have

$$\begin{aligned} \ln a_{\alpha}(x) &\approx -\beta \sin \gamma \frac{\pi}{\gamma} \frac{1}{\cosh \frac{\pi}{\gamma} x} \rightarrow -2\beta \sin \gamma \frac{\pi}{\gamma} e^{-\frac{\pi}{\gamma}|x|}, \\ \frac{\partial}{\partial x} \left(-\frac{\pi}{\gamma} \frac{\sin \gamma}{\cosh \frac{\pi}{\gamma} x} \right) &\rightarrow \mp \frac{\pi}{\gamma} \left(-2 \sin \gamma \frac{\pi}{\gamma} e^{-\frac{\pi}{\gamma}|x|} \right), \\ \frac{\partial}{\partial \beta} \left(-\frac{\pi}{\gamma} \frac{\sin \gamma}{\cosh \frac{\pi}{\gamma} x} \right) &\rightarrow \frac{\pi}{\gamma} \frac{1}{\beta} \left(-2 \sin \gamma \frac{\pi}{\gamma} e^{-\frac{\pi}{\gamma}|x|} \right). \end{aligned} \quad (4.87)$$

This can be used to replace

$$\frac{\frac{\partial}{\partial x} \ln A_{\alpha}}{\frac{\partial}{\partial \beta} \ln A_{\alpha}} = \mp \frac{\pi}{\gamma} \beta. \quad (4.88)$$

Now the same identity as in (4.73) is employed for the derivative of the integral equations (4.81) with respect to the spectral parameter x denoted as \prime and the second derivative of these equations with respect to the product βh , denoted as $\prime\prime$. The result is

$$\begin{aligned} &\int \left(\frac{\ddot{a}_{\alpha}}{a} - \frac{\dot{a}_{\alpha}^2}{a_{\alpha}^2} \right) \frac{a'_{\alpha}}{1+a_{\alpha}} dx = \\ &\int \left(\frac{\ddot{a}_{\alpha}}{1+a_{\alpha}} - \frac{\dot{a}_{\alpha}^2}{(1+a_{\alpha})^2} \right) \left(\frac{a'_{\alpha}}{a_{\alpha}} - \beta \epsilon'_0 \right) dx \\ &\Rightarrow - \int \frac{\dot{a}_{\alpha}^2 a'_{\alpha}}{a_{\alpha}^2 (1+a_{\alpha})^2} dx = \int \left(\frac{\ddot{a}_{\alpha}}{1+a_{\alpha}} - \frac{\dot{a}_{\alpha}^2}{(1+a_{\alpha})^2} \right) \beta \epsilon'_0 dx \end{aligned} \quad (4.89)$$

where the a_{α} -expression on the right hand side is $-\left[\ln(1+a_{\alpha})\right]'' = (\ln A_{\alpha})''$. With $\epsilon'_0 = \frac{\pi}{\gamma} \epsilon_0$ in the scaling limit and $\frac{\partial}{\partial \beta h} = \frac{1}{\beta} \frac{\partial}{\partial h}$ we get for the Drude weight (4.84)

$$D = \frac{\sin \gamma}{2\gamma} \left(\frac{\pi}{\gamma} \right)^2 \frac{\partial^2}{\partial h^2} \left(-\frac{1}{\beta} \frac{1}{2\gamma} \int 2e^{-\frac{\pi}{\gamma}|x|} \ln A_1 A_2(x) dx \right). \quad (4.90)$$

From (3.11) we see that the expression in brackets is the free energy f . Hence, the second derivative with respect to h gives the magnetic susceptibility χ . The zero temperature susceptibility $\chi_0 = \frac{1}{2\frac{\pi}{\gamma}(\pi-\gamma)}$ [7] can be inserted, giving the final result for the zero temperature Drude weight

$$D = \frac{\pi \sin \gamma}{4\gamma(\pi - \gamma)}. \quad (4.91)$$

This is exactly the result derived in [30]. The numerical investigation of (4.84) confirms this result and vice versa.

4.5. Results

In this section the numerical results of the calculation of the Drude weight are presented. From fig. 4.2 we see that for anisotropy parameter values close to the free fermion case ($\gamma = \frac{\pi}{2}$) it seems that $D(T)$ is monotonically decreasing with temperature. However, for values of γ closer to the isotropic point ($\gamma = 0$) there is a maximum showing up. Coming close to the isotropic point the slope at T close to zero is getting steeper. The occurrence

Drude weight at finite temperature for different anisotropy parameters γ

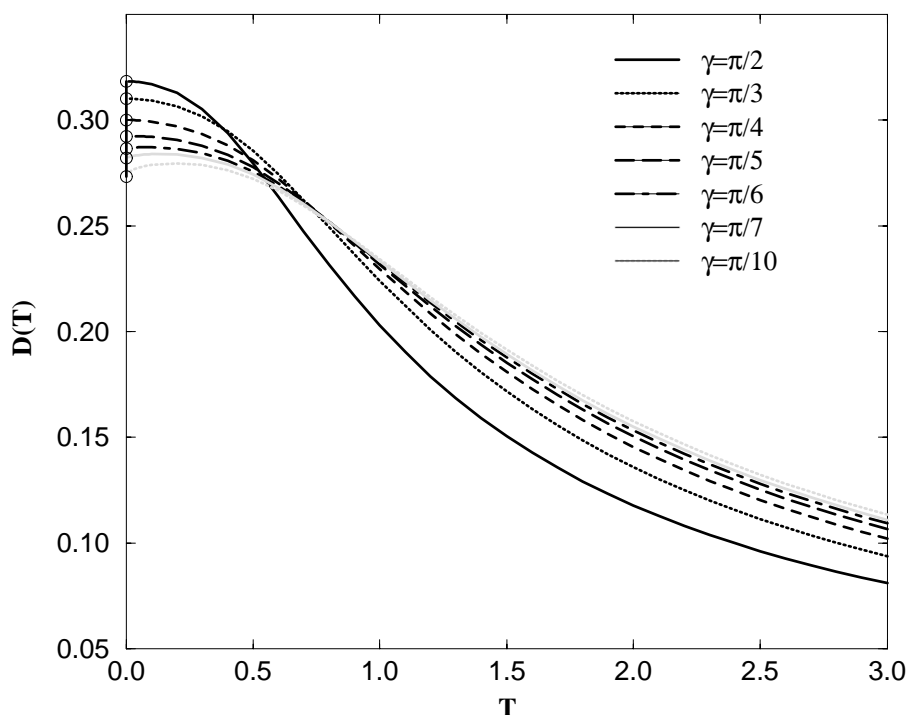


Figure 4.2.: The Drude weight in the temperature range $T = 0.01 - 3.0$ for different anisotropy parameters γ . The circles are indicating the analytically calculated value of the Drude weight at $T = 0$: $D(\gamma) = \frac{\pi \sin \gamma}{4\gamma(\pi - \gamma)}$.

of this maximum is plausible due to the following reason: It can be shown [39] that for an insulator the Drude weight drops exponentially to zero for $T \rightarrow 0$. As a short definition, an insulator is a gapped system. For anisotropy parameter $\Delta > 1$ the model regarded here has a gap. Thus, we can conclude that the Drude weight shows a maximum for some finite temperature. From this point of view it is reasonable that close to the isotropic point $\Delta = 1$ a maximum can appear.

From the analytic calculation in section 4.4.1 it can be seen that the Drude weight at very low temperature is closely related to the magnetic susceptibility. It is known [19] and analytically calculated [10] that the magnetic susceptibility shows logarithmic corrections for very low temperatures giving rise to an infinite slope at $T = 0$ in the magnetic sus-

ceptibility. Fig. 4.3 shows the Drude weight at $\gamma = 0$. This figure seems to confirm the appearance of logarithmic corrections for the Drude weight at the isotropic point of the XXZ -Heisenberg model. The limit $\gamma \rightarrow 0$ can be taken easily in the NLIE by a simple rescaling of temperature and spectral parameter and the Drude weight for the isotropic Heisenberg model can be calculated exactly in the limits of numerical accuracy. The main results in [36] were that the Drude weight is monotonically decreasing for all anisotropy parameters $\gamma \neq 0$ and that the Drude weight vanishes at the isotropic point for all $T > 0$. These results can not be confirmed. In the approach described here we get the maximal regular extension of the ground state results for $T > 0$ and we have a maximum showing up in the Drude weight.

Lastly, we want to comment on the high temperature behaviour. For high temperatures

Logarithmic corrections in the Drude weight for $\gamma=0$

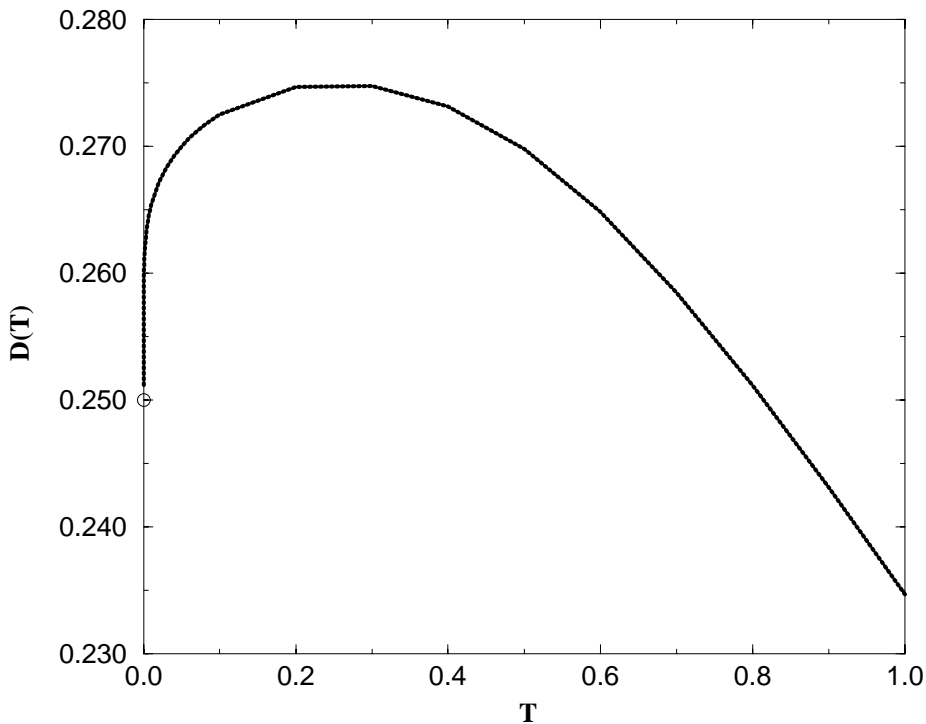


Figure 4.3.: The Drude weight at the isotropic point $\gamma = 0$. A very steep slope close to $T = 0$ can be observed. This slope is infinite at precisely $T = 0$.

the Drude weight decreases as $1/T$ as can be seen in fig. 4.4 in accordance with [36].

High temperature behaviour of $D(T)$

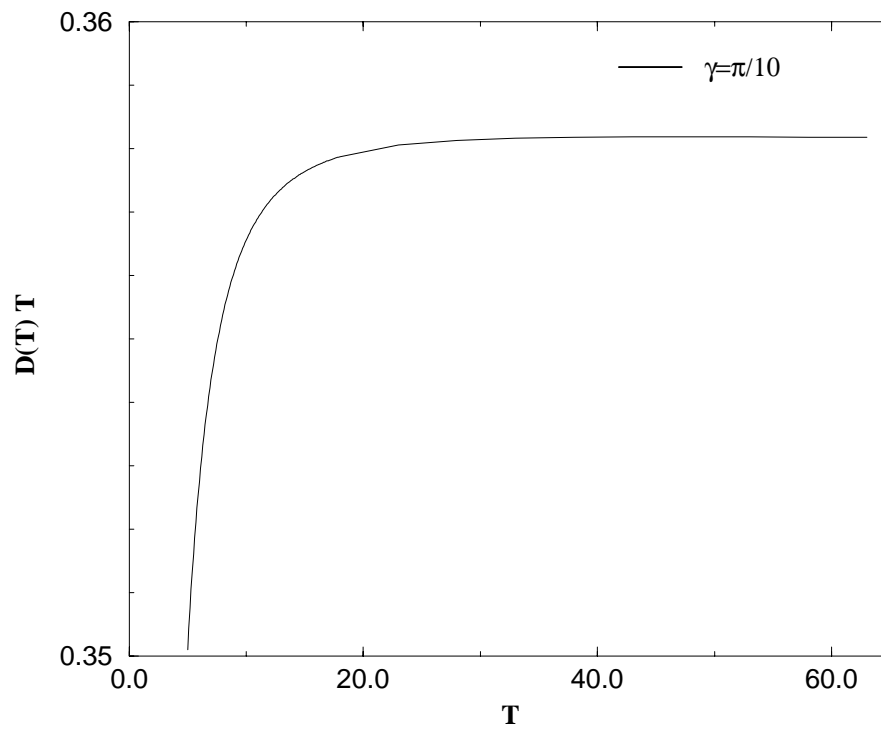


Figure 4.4.: The Drude weight at high temperature showing a $1/T$ -decrease ($\gamma = \frac{\pi}{10}$).

5. Summary and outlook

In this work two different temperature-dependent quantities of the anisotropic Heisenberg chain have been investigated.

First, the longitudinal spin-spin correlation length of the model at *finite* temperature was calculated.

This quantity is of interest because the system can be expected to behave very different in the regimes of low and high temperature.

In the following we regard the system with a finite and fixed magnetic field. The low temperature properties are described satisfactorily by conformal field theory. This theory predicts $2k_F$ -oscillations of the correlation function with $2k_F \neq \pi$ in the low temperature limit.

In the high temperature regime the system should show classical aspects similar to the classical Ising model. Therefore, π -oscillations should be observed. Thus a break down of the quantum mechanical description at a certain crossover temperature is to be expected.

For the calculation we started with a formulation of the thermodynamic Bethe ansatz equations in terms of auxiliary functions that are determined as solutions of non-linear integral equations (NLIE) [7]. In the direct formulation of the NLIE the largest eigenvalue of the quantum transfer matrix and thus the free energy can be calculated. In order to calculate correlation lengths one needs in addition one of the next-leading eigenvalues. On the level of Bethe ansatz numbers excited states are characterized by patterns that differ in their structure from the pattern for the leading eigenvalue. The relevant patterns for the longitudinal correlation length are the 1- and 2-string patterns that show approximately the usual string structure. Now integral equations for these patterns have to be derived which is carried out by deforming the integral contours of the equations for the leading eigenvalue. However, from the analysis of, for example the 1-string pattern, it can be seen that the moving 1-string leaves the analyticity strip of these equations when decreasing temperature (magnetic field fixed). Hence, a reformulation of the NLIE in this region is required. In this way equations for the whole temperature range or all string positions are obtained and the correlation length for *arbitrary* temperature can be calculated numerically by solving the NLIE iteratively. As a result a degeneracy of the two next-leading eigenvalues at a critical temperature T_c is observed. Below that temperature the eigenvalues are complex conjugate. This degeneracy of the 1-and 2-string solution leads to a crossover in the correlation length which is also tangible in the non-analytic behaviour of the $2k_F$ -oscillations. Below T_c these oscillations are incommensurate. Thus, the physical expectations are confirmed.

Second, the Drude weight of the anisotropic Heisenberg chain was calculated.

This project was motivated by the results obtained in [36] that were completely based on

the standard TBA [40].

The main results were a monotonous decrease of the Drude weight with temperature and the vanishing of this weight for $T > 0$ at the isotropic point. However, the TBA-approach shows some technical difficulties that could be overcome by a calculation that combines the quantum transfer matrix approach and the TBA-technique.

The approach used here is based on the formulation of the thermodynamics by Takahashi [9]. In principle the curvature of the energy levels with respect to the twist incorporated in the boundary conditions is investigated. From a finite size analysis we get integral equations and a closed expression for the Drude weight. In this approach all excited states are characterized by strings which makes the calculations quite cumbersome and leads in general to infinitely many integral equations that can only be treated by a truncation procedure which is hard to control. To overcome such problems one is interested in a formulation by means of the NLIE because in this case there is only a *finite* set of integral equations. In the course of the investigation it turned out that the most elegant derivation can be done when taking advantage of the equivalence of the NLIE and equations obtained by the technique of the standard TBA. Then, the derivation of the Drude weight by the traditional ansatz can be adopted. By this strategy the *exact* Drude weight for *finite* temperature is obtained. In contrast to the conventional calculations the derivation holds for arbitrary anisotropy parameter. Thus, even the Drude weight at the isotropic point for arbitrary temperature is exactly calculable which remains an unsolved problem in the other approach. Therefore, logarithmic corrections in the Drude weight of this model are observed the first time.

The results in [36] can not be confirmed. In the approach described here we get the maximal regular extension of the $T = 0$ -results for $T > 0$, especially for the isotropic case and we have a maximum showing up in the Drude weight.

In future projects other models like the supersymmetric tJ -model [37] that can also be treated by NLIE, can be examined with respect to crossover phenomena in the correlation lengths. What concerns the Drude weight, the technique of this work can be used to calculate the same quantity for the supersymmetric tJ -model and the Hubbard model [51]. From a more mathematical point of view it is likely that the logarithmic corrections can be calculated analytically in the same way as for the magnetic susceptibility in [10].

A. Jacobian elliptic functions and related quantities

Elliptic functions are complex, meromorphic and doubly periodic functions. We define quarter-periods K, K' , modulus k and conjugate modulus k'

$$\begin{aligned}
K &= \frac{1}{2\pi} \prod_{n=1}^{\infty} \left(\frac{1+q^{2n-1}}{1-q^{2n-1}} \frac{1-q^{2n}}{1+q^{2n}} \right)^2 \\
K' &= \frac{1}{\pi} K \ln\left(\frac{1}{q}\right) \\
k &= 4q^{\frac{1}{2}} \prod_{n=1}^{\infty} \left(\frac{1+q^{2n}}{1+q^{2n-1}} \right)^4 \\
k' &= \prod_{n=1}^{\infty} \left(\frac{1-q^{2n-1}}{1+q^{2n-1}} \right)^4
\end{aligned} \tag{A.1}$$

where $k^2 + k'^2 = 1$, and the nome $q = \exp(-\pi K'/K)$, $0 < q < 1$. The Jacobian elliptic functions sn , cn , dn and the related snh , cnh , dnh functions are

$$\begin{aligned}
\text{sn}(u) &= k^{-\frac{1}{2}} \frac{H(u)}{\Theta(u)}, \quad \text{snh}(u) = -i \text{sn}(iu) \\
\text{cn}(u) &= \frac{k'^{\frac{1}{2}}}{k} \frac{H_1(u)}{\Theta(u)}, \quad \text{cnh}(u) = \text{cn}(iu) \\
\text{dn}(u) &= k^{\frac{1}{2}} \frac{\Theta_1(u)}{\Theta_1(u)}, \quad \text{dnh}(u) = \text{dn}(iu)
\end{aligned} \tag{A.2}$$

where $H(u), \Theta(u)$ are given as

$$\begin{aligned}
H(u) &= 2q^{\frac{1}{4}} \sin\left(\frac{\pi u}{2K}\right) \prod_{n=1}^{\infty} \left(1 - 2q^{2n} \cos\left(\frac{\pi u}{K}\right) + q^{4n} \right) (1 - q^{2n}) \\
\Theta(u) &= \prod_{n=1}^{\infty} \left(1 - 2q^{2n-1} \cos\left(\frac{\pi u}{K}\right) + q^{4n-2} \right) (1 - q^{2n}) \\
H_1(u) &= H(u + K) \\
\Theta_1(u) &= \Theta(u + K)
\end{aligned} \tag{A.3}$$

which satisfy the identities

$$\begin{aligned}
H(u + iK') &= iq^{-\frac{1}{4}} \exp\left(-\frac{i\pi u}{2K}\right) \Theta(u) \\
\Theta(u + iK') &= iq^{-\frac{1}{4}} \exp\left(-\frac{i\pi u}{2K}\right) H(u) \\
\text{sn}(u + iK') &= \frac{1}{k \text{sn}(u)}.
\end{aligned} \tag{A.4}$$

The last function we have to look at is the combination

$$h(u) = -i\Theta(0)H(iu)\Theta(iu) \quad (\text{A.5})$$

which satisfies

$$\begin{aligned} h(u + i2K) &= -h(u) \\ h(u + K') &= -q^{-\frac{1}{2}} \exp\left(\frac{\pi u}{K}\right) h(u). \end{aligned} \quad (\text{A.6})$$

At last a necessary addition formula for elliptic functions is given by

$$\operatorname{sn}(u - v) = \frac{\operatorname{sn}(u) \operatorname{cn}(v) \operatorname{dn}(v) - \operatorname{cn}(u) \operatorname{dn}(u) \operatorname{sn}(v)}{1 - k^2 \operatorname{sn}^2(v)}. \quad (\text{A.7})$$

B. Parameterization of the eight- and six-vertex model

We follow the derivation in [8] and start with the solvability condition for the 8-vertex-model in terms of the Boltzmann weights (see 2.23)

$$\begin{aligned} \Delta &:= \frac{w_j^2 - w_k^2}{w_l^2 - w_n^2} \text{ invariant under the exchange } w \rightarrow w' \\ &(i, j, k, n \text{ are cyclic permutations of } \{1, 2, 3, 4\}), \text{ or} \\ \Delta &:= \frac{a^2 + b^2 - c^2 - d^2}{2(ab + cd)} \text{ invariant under the exchange } a \rightarrow a' \dots \\ \Gamma &:= \frac{ab - cd}{ab + cd}. \end{aligned} \tag{B.1}$$

First, we eliminate d between the two equations for Δ and γ . This gives

$$2\Delta(1 + \gamma)ab = a^2 + b^2 - c^2 - a^2b^2\gamma^2c^{-2} \tag{B.2}$$

where

$$\gamma := \frac{1 - \Gamma}{1 + \Gamma} = \frac{cd}{ab}. \tag{B.3}$$

Equation (B.2) is a symmetric biquadratic relation between $\frac{a}{c}$ and $\frac{b}{c}$. If $\frac{b}{c}$ is given it is a quadratic equation for $\frac{a}{c}$ with discriminant

$$\Delta(1 + \gamma)^2 \left(\frac{b}{c}\right)^2 - \left[\left(\frac{b}{c}\right)^2 - 1\right] \left[1 - \gamma^2 \left(\frac{b}{c}\right)^2\right]. \tag{B.4}$$

This is a quadratic form in $\left(\frac{b}{c}\right)^2$ and can be written as

$$\left(1 - y^2 \left(\frac{b}{c}\right)^2\right) \left(1 - k^2 y^2 \left(\frac{b}{c}\right)^2\right) \tag{B.5}$$

where k and y only depend on Δ and γ being given by

$$\begin{aligned} k^2 y^2 &= \gamma^2 \\ (1 + k^2) y^2 &= 1 + \gamma^2 - \Delta^2 (1 + \gamma)^2. \end{aligned} \tag{B.6}$$

We want to parametrize $\frac{b}{c}$ as a function of some variable u (say) so that the square root of (B.5) is meromorphic. A convenient choice is

$$\frac{b}{c} = y^{-1} \operatorname{sn} iu \tag{B.7}$$

where $\operatorname{sn} u$ is the Jacobian elliptic dn function of argument u and modulus k (see appendix A) and the factor i in the argument is introduced for later convenience. The square root of (B.5) is then $\operatorname{cn} iu$ and $\operatorname{dn} iu$ so the solution of (B.2) is

$$\frac{a}{c} = \frac{y [\Delta(1 + \gamma) \operatorname{sn} iu + y \operatorname{cn} iu \operatorname{dn} iu]}{y^2 - \gamma^2 (\operatorname{sn} iu)^2}. \quad (\text{B.8})$$

This is a meromorphic function of u . It can be simplified defining λ by

$$k \operatorname{sn} i\lambda = -\frac{\gamma}{y}. \quad (\text{B.9})$$

Then (B.1) and (B.6) give

$$\begin{aligned} y &= \operatorname{sn} i\lambda, \quad \gamma = k(\operatorname{sn} i\lambda)^2, \\ \Gamma &= \frac{(1 + k(\operatorname{sn} i\lambda)^2)}{(1 - k(\operatorname{sn} i\lambda)^2)} \\ \Delta &= -\frac{\operatorname{cn} i\lambda \operatorname{dn} i\lambda}{(1 - k(\operatorname{sn} i\lambda)^2)}. \end{aligned} \quad (\text{B.10})$$

Using (A.7) for the addition of elliptic functions (B.8) gives

$$\frac{a}{c} = \frac{\operatorname{sn} i(\lambda - u)}{\operatorname{sn} i\lambda}, \quad (\text{B.11})$$

so from (B.3) and (B.10)

$$\frac{d}{c} = k \operatorname{sn} iu \operatorname{sn} i(\lambda - u). \quad (\text{B.12})$$

The function $\operatorname{sn} u$ is a generalization of the trigonometric sine function. For $k = 0$ it reduces to $\sin u$. Introduce snh by

$$\operatorname{snh} u = -i \operatorname{sn} iu = i \operatorname{sn}(-iu). \quad (\text{B.13})$$

It is a meromorphic function of u , u is real. Now we can give a summarized expression for the weights

$$a : b : c : d = \operatorname{snh}(\lambda - u) : \operatorname{snh} u : \operatorname{snh} \lambda : k \operatorname{snh} \lambda \operatorname{snh}(\lambda - u). \quad (\text{B.14})$$

With snh substituted by the Theta-functions H and Θ

$$\operatorname{snh} u = -ik^{-\frac{1}{2}} \frac{H(ui)}{\Theta(ui)}, \quad (\text{B.15})$$

we finally get the parameterization of the four different weights of the eight-vertex model ($u = \frac{1}{2}(\lambda + v)$)

$$\begin{aligned} a &= -i\rho\Theta(i\lambda)H\left[\frac{1}{2}i(\lambda - v)\right]\Theta\left[\frac{1}{2}i(\lambda + v)\right] \\ b &= -i\rho\Theta(i\lambda)\Theta\left[\frac{1}{2}i(\lambda - v)\right]H\left[\frac{1}{2}i(\lambda + v)\right] \\ c &= -i\rho H(i\lambda)\Theta\left[\frac{1}{2}i(\lambda - v)\right]\Theta\left[\frac{1}{2}i(\lambda + v)\right] \\ d &= i\rho H(i\lambda)H\left[\frac{1}{2}i(\lambda - v)\right]H\left[\frac{1}{2}i(\lambda + v)\right]. \end{aligned} \quad (\text{B.16})$$

Now let us consider the special case of the six-vertex model as a special case of the eight-vertex-model. From above we have

$$\frac{d}{c} = k \operatorname{sn} iu \operatorname{sn} i(\lambda - u). \quad (\text{B.17})$$

As we want to achieve $d = 0$ we should take the limit $k \rightarrow 0$. Taking this limit in (B.11) one gets

$$\frac{a}{c} = \frac{\sinh(\lambda - u)}{\sinh \lambda} \quad (\text{B.18})$$

and for $\frac{b}{c}$

$$\frac{b}{c} = \frac{\sinh u}{\sinh \lambda} \quad (\text{B.19})$$

which gives

$$\begin{aligned} a &= \varrho \sinh(\lambda - u) \\ b &= \varrho \sinh(u) \\ c &= \varrho \sinh(\lambda) \\ \Delta &= -\cosh(\lambda). \end{aligned} \quad (\text{B.20})$$

In (B.7) we had the freedom to introduce a factor i . If we do not do so we get

$$\begin{aligned} a &= \varrho \sin(\lambda - u) \\ b &= \varrho \sin(u) \\ c &= \varrho \sin(\lambda) \\ \Delta &= -\cos(\lambda). \end{aligned} \quad (\text{B.21})$$

Different parameterizations lead to different regions in the phase diagram, as explained in section 2.4.

C. The connection between spinon and magnon approach

Here the explicit calculation in order to connect the integral equations (3.8) to the equations (4.37) gained by the “magnon” approach is given. After the substitution on the contour C_+ (4.38) reads

$$\begin{aligned} \ln \eta(x) &= \beta \epsilon(x) + \int_{C_+} \kappa(x-y) \ln(1+\eta(y)) dy \\ &- \int_{C_+} \kappa(x-y) \ln \eta(y) dy - \int_{C_-} \kappa(x-y) \ln \left(1 + \frac{1}{\eta(y)}\right) dy. \end{aligned} \quad (\text{C.1})$$

Using the notation for the Fourier transform of the logarithmic derivative (D.2) and setting \hat{t} for the Fourier transform of $\epsilon'(x)$ and $\hat{\kappa}$ for the one of κ , we get

$$\begin{aligned} \mathfrak{F}_k [\ln \eta]' &= \beta \hat{t} + \hat{\kappa} \mathfrak{F}_k [\ln(1+\eta)]' \\ &- e^{\gamma k} \hat{\kappa} \mathfrak{F}_k^{C_-} \left[\ln \left(1 + \frac{1}{\eta}\right) \right]' - \hat{\kappa} \mathfrak{F}_k [\ln \eta]'. \end{aligned} \quad (\text{C.2})$$

This can be resolved for $\mathfrak{F}_k [\ln \eta]'$

$$\mathfrak{F}_k [\ln \eta]' = \beta \frac{\hat{t}}{1+\hat{\kappa}} + \frac{\hat{\kappa}}{1+\hat{\kappa}} \mathfrak{F}_k [\ln(1+\eta)]' - e^{\gamma k} \frac{\hat{\kappa}}{1+\hat{\kappa}} \mathfrak{F}_k \left[\ln \left(1 + \frac{1}{\eta}\right) \right]'. \quad (\text{C.3})$$

The Fourier transforms are

$$\begin{aligned} \hat{t} &= ik \frac{\sinh \frac{\pi-\gamma}{2} k}{\sinh \frac{\pi}{2} k} \\ \hat{\kappa} &= \frac{\sinh(\frac{\pi}{2} - \gamma)k}{\sinh \frac{\pi}{2} k}. \end{aligned} \quad (\text{C.4})$$

The equations have to be integrated once and the constants are determined by the requirement that the regarded functions have constant asymptotics. From the comparison to equation (3.9) we see $\frac{\hat{\kappa}}{1+\hat{\kappa}} = \hat{k}$. In that manner one obtains the equations that are equivalent to (3.8), respecting that $J = 2$ was chosen above. We get the factor $\sin \gamma$ of (4.35) if we transform $\beta \rightarrow \sin \gamma \beta$ in (3.8). This means that two of the coupling constants in (2.50) are equal to 1.

D. Derivation of the non-linear integral equations for the XXZ -Heisenberg model

In order to derive appropriate integral equations it is necessary to give some comments on the properties of the involved functions. One of the essential ingredients of the here presented method is the identification of certain analyticity regions of the functions $\Phi(x)$, $q(x)$ $\Lambda_0(x)$, i.e. strips in the complex plane where these functions are *analytic and non-zero* (ANZ). The analytic properties of the eigenvalue functions of the six-vertex model were intensively studied in [5, 6]. For details we refer to these publications. For the leading eigenvalue with $n = M/2$ the analyticity domains are given by

$$\begin{aligned} \Phi(x) & \quad \text{ANZ in } 0 < \text{Im}(x) < \pi \\ q(x) & \quad \text{ANZ in } -\pi < \text{Im}(x) < 0 \\ \Lambda_0(x) & \quad \text{ANZ in } -\gamma < \text{Im}(x) < \gamma. \end{aligned} \tag{D.1}$$

$\Lambda_0(x)$ denotes the largest eigenvalue. All Bethe ansatz numbers are real for $h = 0$. It should be emphasized that the scenario changes when low lying excitations are examined. Then complex Bethe ansatz numbers turn up and the ANZ-property of the eigenvalue does not hold anymore. In the following only the case $h = 0$ is considered. For arbitrary magnetic field it is important that roots and holes are separated from each other and that they are positioned in a bounded region. Then the whole derivation proceeds in an analogous way.

The main idea is to apply Cauchy's theorem to the Fourier transforms of the logarithmic derivative of $\Lambda(x)$.

We define the Fourier transform along an integration path \mathcal{C} where the real part¹ varies from $-\infty$ to ∞

$$\mathfrak{F}_k^{\mathcal{C}} [\ln f]' = \int_{\mathcal{C}} [\ln f(x)]' e^{-ikx} dx. \tag{D.2}$$

Whenever two of these Fourier transforms have integration paths that lie in the analyticity region of the transformed function and the transforms do not enclose singularities of this function the two Fourier transforms are equal due to Cauchy's theorem.

¹ $\mathfrak{F}_k [\ln f]'$ denotes the transform along the real axis.

D.1. Integral equations for the leading eigenvalue Λ_0

We start with the equations (3.7) for the eigenvalue $\Lambda(x)$. The Fourier transform of the first equation gives

$$\begin{aligned} & \int_{-\infty}^{\infty} [\ln \Lambda(x - i\gamma/2)]' e^{-ikx} dx = e^{\frac{\gamma}{2}k} \mathfrak{F}_k [\ln \Lambda]' \\ & = e^{(\gamma-\pi)k} \mathfrak{F}_k [\ln \Phi]' + \mathfrak{F}_k [\ln \mathfrak{A}]' + (e^{(\pi-\frac{\gamma}{2})k} - e^{\frac{\gamma}{2}k}) \mathfrak{F}_k [\ln q]'. \end{aligned} \quad (\text{D.3})$$

The second expression leads to

$$\begin{aligned} & \int_{-\infty}^{\infty} [\ln \Lambda(x + i\gamma/2)]' e^{-ikx} dx = e^{-\frac{\gamma}{2}k} \mathfrak{F}_k [\ln \Lambda]' \\ & = e^{-\gamma k} \mathfrak{F}_k [\ln \Phi]' + \mathfrak{F}_k [\ln \bar{\mathfrak{A}}]' + (e^{\frac{\gamma}{2}k} - e^{(\pi-\frac{\gamma}{2})k}) \mathfrak{F}_k [\ln q]'. \end{aligned} \quad (\text{D.4})$$

We get the Fourier transform of $[\ln \Lambda]'$ on the real axis because the paths can be shifted to that axis. Hence there are two different expressions for $\mathfrak{F}_k [\ln \Lambda]'$ that can be equated and are resulting in a term for $\mathfrak{F}_k [\ln q]'$

$$\begin{aligned} & h(k) \mathfrak{F}_k [\ln q]' = \\ & (e^{-\frac{\gamma}{2}k} - e^{\frac{\gamma}{2}k - \pi k}) \mathfrak{F}_k [\ln \Phi]' + e^{\frac{\gamma}{2}k} \mathfrak{F}_k [\ln \bar{\mathfrak{A}}]' - e^{-\frac{\gamma}{2}k} \mathfrak{F}_k [\ln \mathfrak{A}]' \end{aligned} \quad (\text{D.5})$$

with $h(k) := 4e^{\frac{\pi}{2}} \cosh \frac{\gamma}{2}k \sinh \frac{\pi-\gamma}{2}k$. Now let us recall the definition of $\mathfrak{a}(x)$ by $p(x)$ given in (3.6)

$$\mathfrak{a}(x) = \frac{1}{p(x - i\frac{\gamma}{2})} = \frac{1}{\omega^2} \frac{\Phi(x)q(x - i\frac{3}{2}\gamma)}{\Phi(x - i\gamma + i\pi)q(x + i\frac{\gamma}{2} - i\pi)}. \quad (\text{D.6})$$

$\ln \mathfrak{a}(x)$ can be Fourier transformed in the usual manner and $\mathfrak{F}_k [\ln q]'$ from (D.5) can be inserted leading to

$$\begin{aligned} \mathfrak{F}_k [\ln \mathfrak{a}]' & = (1 - e^{(\gamma-\pi)k})(1 - g(k)) \mathfrak{F}_k [\ln \Phi]' + g(k) \mathfrak{F}_k [\ln \mathfrak{A}]' \\ & - g(k) e^{\gamma k} \mathfrak{F}_k [\ln \bar{\mathfrak{A}}]'. \end{aligned} \quad (\text{D.7})$$

$g(k)$ is defined as

$$g(k) := \frac{\sinh(\frac{\pi}{2} - \gamma)k}{2 \cosh \frac{\gamma}{2}k \sinh \frac{\pi-\gamma}{2}k}. \quad (\text{D.8})$$

The terms involving \mathfrak{A} and $\bar{\mathfrak{A}}$ are convolution terms when transformed back. Whereas the $\mathfrak{F}_k [\ln \Phi]'$ -expression can be treated explicitly. We have got

$$\Phi := \Phi_1 \cdot \Phi_2, \quad \Phi_{1/2} := \left(\sinh \frac{1}{2}(x \pm x_M) \right)^{\frac{M}{2}}, \quad x_M = i\frac{\gamma}{2} - i\frac{\beta}{M}. \quad (\text{D.9})$$

Taking the logarithm the product converts into a sum.

With $\mathfrak{F}_k [\ln \sinh]' = -i \frac{1}{1 - \exp(-\pi k)}$ the Fourier transform of, e.g the logarithmic derivative of Φ_1 can be calculated minding the shift in the definition. The result is to be multiplied with the prefactor of the $\mathfrak{F}_k [\ln \Phi]'$ -term leading to

$$\hat{\psi}_1(k) = -i \frac{M}{2} \frac{e^{\frac{\beta}{M}}}{\cosh \frac{\gamma}{2} k}. \quad (\text{D.10})$$

This can be transformed back

$$\psi_1(x) = -\frac{M \pi}{2 \gamma} \frac{1}{\sinh \left(\frac{\pi}{\gamma} \left(x + i \frac{\beta}{M} - i \frac{\gamma}{2} \right) \right)}. \quad (\text{D.11})$$

As we want to derive integral equations for $\ln \mathfrak{a}(x)$, ψ has to be integrated ($\Psi_1'(x) = \psi_1(x)$)

$$\Psi_1(x) = \frac{M}{2} \ln \tanh \left(\frac{\pi}{2\gamma} \left(x + i \frac{\beta}{M} - i \frac{\gamma}{2} \right) \right). \quad (\text{D.12})$$

The complete set of equations reads

$$\begin{aligned} \ln \mathfrak{a}(x) &= +\frac{\pi}{\pi - \gamma} \frac{\beta h}{2} \\ &\frac{M}{2} \ln \left(\tanh \left(\frac{\pi}{2\gamma} \left(x + i \frac{\beta}{M} - i \frac{\gamma}{2} \right) \right) \tanh \left(\frac{\pi}{2\gamma} \left(x - i \frac{\beta}{M} + i \frac{\gamma}{2} \right) \right) \right), \\ &+ \int_{-\infty}^{\infty} k(x-y) \ln \mathfrak{A}(y) dy - \int_{-\infty}^{\infty} k(x-y-i\gamma+i\epsilon) \ln \bar{\mathfrak{A}}(y) dy, \\ \ln \bar{\mathfrak{a}}(x) &= -\frac{\pi}{\pi - \gamma} \frac{\beta h}{2} \\ &\frac{M}{2} \ln \left(\tanh \left(\frac{\pi}{2\gamma} \left(x + i \frac{\beta}{M} - i \frac{\gamma}{2} \right) \right) \tanh \left(\frac{\pi}{2\gamma} \left(x - i \frac{\beta}{M} + i \frac{\gamma}{2} \right) \right) \right) \\ &+ \int_{-\infty}^{\infty} k(x-y) \ln \bar{\mathfrak{A}}(y) dy - \int_{-\infty}^{\infty} k(x-y+i\gamma-i\epsilon) \ln \mathfrak{A}(y) dy. \end{aligned} \quad (\text{D.13})$$

These are the integral equations for *finite* Trotter number M . It remains a remark about the constants appearing in the equations. From the definition of $\mathfrak{a}(x)$ and $\bar{\mathfrak{a}}(x)$ in terms of $p(x)$, $\mathfrak{a}(x)$ consists of sinh-functions. The limit $x \rightarrow \infty$ can be taken easily. Therefrom $\ln \mathfrak{A}(\infty)$ and $\ln \bar{\mathfrak{A}}(\infty)$ is known and the free constants can be determined.

The limit of *infinite* Trotter number has to be executed only in the inhomogeneity term

$$\Psi(x) = \lim_{M \rightarrow \infty} \ln \left(\tanh \left(\frac{\pi}{2\gamma} \left(x + i \frac{\beta}{M} - i \frac{\gamma}{2} \right) \right) \tanh \left(\frac{\pi}{2\gamma} \left(x - i \frac{\beta}{M} \right) \right) \right) = -\frac{\pi \beta}{\gamma} \frac{1}{\cosh \frac{\pi}{\gamma} x}. \quad (\text{D.14})$$

In that manner one gets the equations (3.8). These equations show arguments ϵ in the convolutions that create convergence. The derivation above is done at the borders of the convergence strip. However, the numerical calculation shows that the difference of the convolutions without the implementation of the ϵ -arguments is finite.

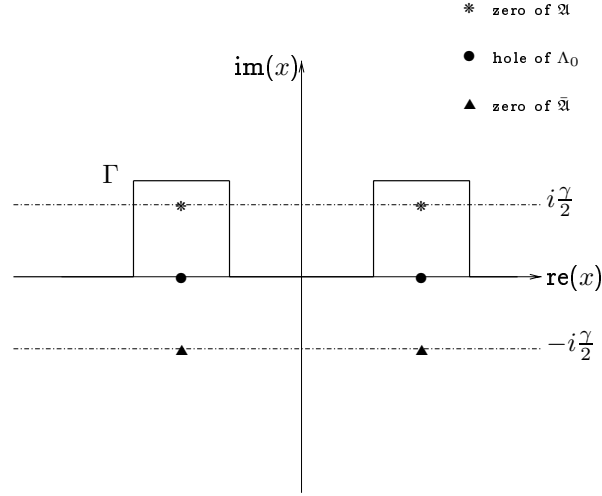


Figure D.1.: Integration contour for the pure two hole case

D.2. Excitations I: pure two hole case

The main difference to the leading eigenvalue is now that two holes in the former ANZ -domain of Λ_0 occur. Now for example the integration path for $\mathfrak{A}(x)$ has to be deformed in order to get a domain avoiding the two holes shown in fig. D.1. In the domain limited by $\mathbb{R} + i\frac{\gamma}{2}$ and $\Gamma - i\frac{\gamma}{2}$ are no singularities. Thus, the two Fourier transforms of $[\ln \Lambda]'$ calculated on the paths have the same result. Now we follow the same way as in equation (D.3). The Fourier transform of the first equation of (3.7) is taken on the contour $\mathfrak{L} : x \in \Gamma$

$$\begin{aligned} \int_{\Gamma} [\ln \Lambda(x - i\gamma/2)]' e^{-ikx} dx &= e^{\frac{\gamma}{2}k} \mathfrak{F}_k [\ln \Lambda]' \\ &= e^{(\gamma-\pi)k} \mathfrak{F}_k [\ln \Phi]' + \mathfrak{F}_k^{\Gamma} [\ln \mathfrak{A}]' + (e^{(\pi-\frac{\gamma}{2})k} - e^{\frac{\gamma}{2}k}) \mathfrak{F}_k [\ln q]'. \end{aligned} \quad (\text{D.15})$$

The second expression is taken on the contour $\mathfrak{L} : x \in \Gamma$, too:

$$\begin{aligned} \int_{\Gamma} [\ln \Lambda(x + i\gamma/2)]' e^{-ikx} dx &= e^{-\frac{\gamma}{2}k} \mathfrak{F}_k [\ln \Lambda]' \\ &= e^{-\gamma k} \mathfrak{F}_k [\ln \Phi]' + \mathfrak{F}_k [\ln \bar{\mathfrak{A}}]' + (e^{\frac{\gamma}{2}k} - e^{(\pi-\frac{\gamma}{2})k}) \mathfrak{F}_k [\ln q]'. \end{aligned} \quad (\text{D.16})$$

Whenever possible the contours of the transforms have been shifted to the real axis. Again the different expressions for $\mathfrak{F}_k [\ln \Lambda]'$ can be equated and are resulting in a term for $\mathfrak{F}_k [\ln q]'$

$$\begin{aligned} h(k) \mathfrak{F}_k [\ln q]' &= (e^{-\frac{\gamma}{2}k} - e^{(\frac{\gamma}{2}-\pi)k}) \mathfrak{F}_k [\ln \Phi]' \\ &\quad + e^{\frac{\gamma}{2}k} \mathfrak{F}_k [\ln \bar{\mathfrak{A}}]' - e^{-\frac{\gamma}{2}k} \mathfrak{F}_k^{\Gamma} [\ln \mathfrak{A}]'. \end{aligned} \quad (\text{D.17})$$

As in the case of the leading eigenvalue $\mathfrak{F}_k [\ln q]'$ is inserted in the transform of the definition of $\ln a$ giving

$$\begin{aligned} \mathfrak{F}_k [\ln a]' &= (1 - e^{(\gamma-\pi)k})(1 - g(k))\mathfrak{F}_k [\ln \Phi]' + g(k)\mathfrak{F}_k^\Gamma [\ln \mathfrak{A}]' \\ &\quad - g(k)e^{\gamma k}\mathfrak{F}_k [\ln \bar{\mathfrak{A}}]'. \end{aligned} \tag{D.18}$$

The difference to the case of the leading eigenvalue consists of the integration contour Λ for the $\ln \mathfrak{A}$ -depending convolution. This contour encircles the zeros $\Theta_{1,2} + i\frac{\gamma}{2}$ of \mathfrak{A} giving simple poles for its logarithmic derivative of \mathfrak{A} . The poles can be removed by the residual theorem causing two additional terms in the integral equations. We have

$$\begin{aligned} \ln a(x) &= \frac{\pi}{\pi - \gamma} \frac{\beta h}{2} \\ &\quad - K \left(x - \left(\Theta_1 + i\frac{\gamma}{2} \right) \right) - K \left(x - \left(\Theta_2 + i\frac{\gamma}{2} \right) \right) + \pi i + \\ &\quad \frac{M}{2} \ln \left(\tanh \left(\frac{\pi}{2\gamma} \left(x + i\frac{\beta}{M} - i\frac{\gamma}{2} \right) \right) \tanh \left(\frac{\pi}{2\gamma} \left(x - i\frac{\beta}{M} + i\frac{\gamma}{2} \right) \right) \right) \\ &\quad + \int_{-\infty}^{\infty} k(x-y) \ln \mathfrak{A}(y) dy - \int_{-\infty}^{\infty} k(x-y-i\gamma+i\epsilon) \ln \bar{\mathfrak{A}}(y) dy, \\ \ln \bar{a}(x) &= -\frac{\pi}{\pi - \gamma} \frac{\beta h}{2} \\ &\quad + K \left(x - \left(\Theta_1 - i\frac{\gamma}{2} \right) \right) + K \left(x - \left(\Theta_2 - i\frac{\gamma}{2} \right) \right) - \pi i + \\ &\quad \frac{M}{2} \ln \left(\tanh \left(\frac{\pi}{2\gamma} \left(x + i\frac{\beta}{M} - i\frac{\gamma}{2} \right) \right) \tanh \left(\frac{\pi}{2\gamma} \left(x - i\frac{\beta}{M} + i\frac{\gamma}{2} \right) \right) \right) \\ &\quad + \int_{-\infty}^{\infty} k(x-y) \ln \bar{\mathfrak{A}}(y) dy - \int_{-\infty}^{\infty} k(x-y+i\gamma-i\epsilon) \ln \mathfrak{A}(y) dy. \end{aligned} \tag{D.19}$$

The constants in the equations have changed because the q -function has only $M/2 - 1$ factors and the function $K(x)$ has non-vanishing anti-symmetric asymptotics.

D.3. Excitations II: 1-string case

Now we want to consider the case of a 1-string, that is a root with non-vanishing imaginary part. First we note that every 1- or 2-string causes the appearance of two real holes that can be treated as in the the pure 2-hole case. In addition a complex root y_0 occurs with $\gamma < \text{im } y_0 < \pi - \gamma$. As a consequence, the zero y_0 appears in the former ANZ-strip of the q -function.

$a(x)$ is defined as

$$a(x) = \omega^2 \frac{\Phi(x)q(x - i\frac{3}{2}\gamma)}{\Phi(x - i\gamma)q(x + i\frac{\gamma}{2} - i\pi)}. \tag{D.20}$$

Thus, a is vanishing at $y_0 + i(\frac{3}{2}\gamma - \pi)$ and diverging at $y_0 - \frac{1}{2}\gamma$ and so does \mathfrak{A} . The scenario of poles and zeros concerning the involved functions is given in fig. D.2. This

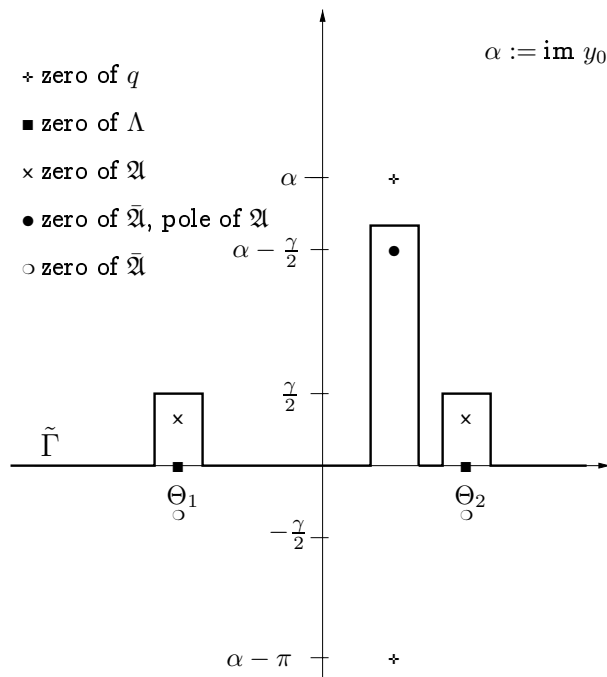


Figure D.2.: integration contour for the 1-string case

pattern of zeros and poles of the auxiliary functions forces us to perform the Fourier transforms along deformed integration paths in order to meet the requirements for the above-mentioned application of Cauchy's theorem. Therefore, the path $\tilde{\Gamma}$ is introduced that basically follows the real axis from $-\infty$ to ∞ , but is deformed in such a way as to encircle the points $\theta_i + i\frac{\gamma}{2}$ and $y_0 - i\frac{\gamma}{2}$ clockwise. The paths $\tilde{\Gamma} - i\frac{3}{2}\gamma$ and $\tilde{\Gamma} + i(\frac{\gamma}{2} - \pi)$ do not enclose any singularities of $q(x)$, so that in the Fourier transform of $[\ln a]'$ we are allowed to deform them to straight lines and move them close to the real axis from below

$$\mathfrak{F}_k [\ln a]' = (1 - e^{(\gamma-\pi)k}) \mathfrak{F}_k' [\ln \Phi]' + (e^{\frac{3}{2}\gamma k} - e^{(\pi-\frac{\gamma}{2})k}) \mathfrak{F}_k^- [\ln q]'. \quad (\text{D.21})$$

Instead of giving the whole derivation of the non-linear integral equation again for this case, it is more convenient to explain a few basic principles. When comparing fig. D.1 with fig. D.2 one comes to the conclusion that every additional term in the equations results from the encircling of the occurring singularities. Let us put this in the rule:

- Choose the paths in such a way that all singularities of $[\ln \Lambda]'$ are avoided and that all roots are enclosed.

Assuming that this holds, the whole derivation can be done as in the case of the leading eigenvalue and one finally gets the equations

$$\begin{aligned}
 \ln \mathfrak{a}(x) &= \frac{\pi}{\pi - \gamma} \frac{\beta h}{2} + \pi i + \\
 &\frac{M}{2} \ln \left(\tanh\left(\frac{\pi}{2\gamma}\left(x + i\frac{\beta}{M} - i\frac{\gamma}{2}\right)\right) \tanh\left(\frac{\pi}{2\gamma}\left(x - i\frac{\beta}{M} + i\frac{\gamma}{2}\right)\right) \right) \\
 &+ \int_{\tilde{\Gamma}} k(x-y) \ln \mathfrak{A}(y) dy - \int_{\tilde{\Gamma}} k(x-y-i\gamma+i\epsilon) \ln \bar{\mathfrak{A}}(y) dy \\
 \ln \bar{\mathfrak{a}}(x) &= -\frac{\pi}{\pi - \gamma} \frac{\beta h}{2} - \pi i + \\
 &\frac{M}{2} \ln \left(\tanh\left(\frac{\pi}{2\gamma}\left(x + i\frac{\beta}{M} - i\frac{\gamma}{2}\right)\right) \tanh\left(\frac{\pi}{2\gamma}\left(x - i\frac{\beta}{M} + i\frac{\gamma}{2}\right)\right) \right) \\
 &+ \int_{\tilde{\Gamma}} k(x-y) \ln \bar{\mathfrak{A}}(y) dy - \int_{\tilde{\Gamma}} k(x-y+i\gamma-i\epsilon) \ln \mathfrak{A}(y) dy.
 \end{aligned} \tag{D.22}$$

Therefore, the creation of the additional terms happens in the calculation of the convolutions along the paths. In other words: now the treatment of the regarded excitation can be done *subsequently*. Technically this is done by differentiating the equations and using the residue theorem. In that way one gets equation (3.14) for the 1-string case.

D.4. Derivation of the integral expressions for the second strip

“Ground state”

Employing the same method as in the previous calculations i.e. taking the Fourier transform of the logarithmic derivative of the auxiliary functions $\ln \mathfrak{A}$, $\ln \bar{\mathfrak{A}}$ etc. in the first strip we derive an explicit expression for $\ln q$. Finally, for $\text{Im } x$ in the vicinity of $-\pi/2$ we obtain the expression

$$\begin{aligned} \ln \mathfrak{a}(x) &:= \frac{\pi}{\pi - \gamma} \beta h \\ &\quad - \int_{-\infty}^{\infty} dy [r(x - y) \ln \mathfrak{A}(y) - r(x - y - i\gamma) \ln \bar{\mathfrak{A}}(y)] \end{aligned} \quad (\text{D.23})$$

where no non-trivial driving term appears. The expression for $\bar{\mathfrak{a}}(x)$ is directly obtained by use of $\bar{\mathfrak{a}}(x) = 1/\mathfrak{a}(x - i\gamma)$. For the maximum region of convergence see fig. 3.8 in the main text. The kernel $r(x)$ is given by

$$\begin{aligned} r(x) &:= \frac{1}{2\pi} \int_{-\infty}^{\infty} dk \frac{\sinh \frac{\gamma}{2} k}{\sinh(\frac{\pi - \gamma}{2} k)} e^{ik(x + i\frac{\pi}{2})} \\ &= \frac{i}{2(\pi - \gamma)} \left(\coth\left(\frac{\pi}{\pi - \gamma} x\right) - \coth\left(\frac{\pi}{\pi - \gamma} (x + i\gamma)\right) \right). \end{aligned} \quad (\text{D.24})$$

“Excited states”

We can use the above algebraic expressions for the excited states if we deform the contour of integration in (D.23) such that we avoid the singularities imposed by the 1-string or 2-string patterns. Straightening the contour out we obtain contributions due to Cauchy as supplied before

$$\begin{aligned} \ln \mathfrak{a}(x) &:= \frac{\pi}{\pi - \gamma} \beta h + R(x - (\theta_1 + i\gamma/2)) + R(x - (\theta_2 + i\gamma/2)) \\ &\quad + \ln \frac{\sinh \left[\frac{\pi}{\pi - \gamma} (x - y_0 - i\frac{3\gamma}{2}) \right]}{\sinh \left[\frac{\pi}{\pi - \gamma} (x - y_0 + i\frac{\gamma}{2}) \right]} \\ &\quad - \int_{-\infty}^{\infty} dy [r(x - y) \ln \mathfrak{A}(y) - r(x - y - i\gamma) \ln \bar{\mathfrak{A}}(y)] \end{aligned} \quad (\text{D.25})$$

with

$$R(x) := \ln \left[\frac{\sinh \frac{\pi}{\pi - \gamma} (x + i\gamma)}{\sinh \frac{\pi}{\pi - \gamma} x} \right], \quad (\text{D.26})$$

note that $R'(x) = 2\pi i r(x)$. The parameters $\theta_{1,2}$ denote the positions of the holes as usual. The same expression holds in the case of a 2-string if the lower root y_- of the 2-string is used instead of y_0 .

E. Perturbation theory for the ring Hamiltonian

Consider the Hamiltonian (4.13) with a small shift q inserted ($|q| \ll |k|$)

$$H(k+q) = \sum_i \left[\frac{1}{2} (p_i + k + q)^2 + V_i \right] + U. \quad (\text{E.1})$$

This can be expanded up to the second order

$$H(k+q) = \underbrace{H(k)}_{H_0} + \underbrace{\sum_i (p_i + k) \cdot q + \frac{q^2}{2}}_V. \quad (\text{E.2})$$

Stationary perturbation theory with the eigenfunctions Φ_{nk} of H_0 is employed

$$E_n(k) = E_n^0(k) + \langle \Phi_{nk} | V | \Phi_{nk} \rangle + \sum_{n' \neq n} \frac{|\langle \Phi_{nk} | V | \Phi_{n'k} \rangle|^2}{E_n^0 - E_{n'}^0} + \dots \quad (\text{E.3})$$

The ordinary Taylor-expansion of the energy levels gives

$$E_n = E_n^0 + \frac{\partial E_n}{\partial k} \cdot q + \frac{1}{2} \frac{\partial^2 E_n}{\partial k^2} \cdot q^2 + \dots \quad (\text{E.4})$$

In the following we use a Bloch-like structure of the eigenfunctions because of the \vec{k} -dependence in the Hamiltonian

$$\Phi_{n\vec{k}}(\vec{r}) = e^{ikx_1} u_{nk}(x_1, \dots, x_N), \quad (\text{E.5})$$

$$\int \Phi_{n\vec{k}}^* X \Phi_{n'\vec{k}} \prod_{i=1}^N dx_i = \langle n\vec{k} | X | n'\vec{k} \rangle \quad (\text{E.6})$$

with $|nk\rangle = u_{nk}(x_1, \dots, x_N)$. Now the perturbation V of eq. (E.2) is inserted in the perturbation theory expression (E.3) and this will be organized with respect to orders in q

$$E_n = E_n^0 + \frac{1}{m} \left\langle n \left| \sum_j p_j \right| n \right\rangle \cdot q + \left\{ \frac{L}{2m} + \frac{1}{2m} \sum_{n' \neq n} \frac{\left| \left\langle n \left| \sum_j p_j \right| n' \right\rangle \right|^2}{E_n^0 - E_{n'}^0} \right\} \cdot q^2 + \dots \quad (\text{E.7})$$

Comparison with (E.4) gives for the second derivative of E_n

$$\frac{\partial^2 E_n(k)}{\partial k^2} = \frac{L}{2m} - \frac{1}{m^2} \sum_{n \neq n'} \frac{\left| \langle n' | \sum_j p_j | n \rangle \right|^2}{E_n(k) - E_{n'}(k)}, \quad (\text{E.8})$$

or expressed by the current density operator \hat{j}_x and the hopping amplitude t

$$\frac{\partial^2 E_n(k)}{\partial k^2} = tL - \sum_{n \neq n'} \frac{\left| \langle n' | \hat{j}_x | n \rangle \right|^2}{E_n(k) - E_{n'}(k)}. \quad (\text{E.9})$$

We derived a special version of the *effective mass theorem*.

Bibliography

- [1] H. Bethe, Z. Physik **71**, 205 (1931)
- [2] W. Heisenberg, Z. Physik **49**, 619 (1928)
- [3] E. Ising, Z. Phys. **31**, 253 (1925)
- [4] L. Onsager, Phys. Rev. **65**, 117 (1944)
- [5] A. Klümper, J. Zittartz, Z. Phys. **B 71**, 495 (1988)
- [6] A. Klümper, J. Zittartz, Z. Phys. **B 75**, 371 (1989)
- [7] A. Klümper, Z. Phys. **B 91**, 507 (1993)
- [8] R.J. Baxter, *Exactly Solved Models in Statistical Mechanics*, Academic Press, London, (1982)
- [9] M. Takahashi, Prog. Theor. Phys. **46**, 401 (1971)
- [10] A. Klümper, cond-mat/9803225 (1998)
- [11] M. Suzuki, Phys. Rev. **B 31**, 2957 (1985)
- [12] M. Suzuki, M. Inoue, Progr. Theor. Phys. **78**, 787 (1987)
- [13] C.L. Schultz, Phys. Rev. Letters **46**, 629 (1981)
- [14] C.L. Schultz, Physica **122A**, 71 (1983)
- [15] P.W. Anderson, Science **235**, 1196 (1987)
- [16] V.E. Korepin, N.M. Bogoliubov, A.G. Izergin, *Quantum Inverse Scattering Method and Correlation Functions*, Cambridge University Press, (1993)
- [17] P.A. Bares, Thesis, ETH Zürich (1991)
- [18] B. Sutherland, Phys. Rev. **B 12**, 3795 (1975)
- [19] S. Eggert, I. Affleck, M. Takahashi, cond-mat/9404062 (1994)
- [20] A. Klümper, M. Batchelor, P. Pearce, J. Phys. **A 24**, 3111 (1991)
- [21] A. Klümper, *Ausgewählte Probleme und Lösungsmethoden der Statistischen Physik*, lectures (1994)
- [22] J. Benz, Diploma Thesis Köln (2000)

-
- [23] L.A. Takhtajan *Introduction to Algebraic Bethe Ansatz*, Lecture Notes in Physics 242, 175-219, Springer-Verlag, Berlin, Heidelberg (1985)
- [24] A.G. Izergin, V.E. Korepin, Lett. Math. Phys. **6**, 283 (1982)
- [25] P.P. Kulish, N.Yu. Reshetikhin, E.K. Sklyanin, Lett. Math. Phys. **6**, 283 (1982)
- [26] M. Takahashi, *Thermodynamics of One-Dimensional Solvable Models*, Cambridge University Press, Cambridge (1999)
- [27] A. Klümper, Eur. Phys. J. B **5**, 677-685 (1998)
- [28] R. Kubo, J. Phys. Soc. Jpn. **12**, 570 (1957)
- [29] W. Kohn, Phys. Rev. **133**, 171 (1964)
- [30] B.S. Shastry, B. Sutherland, Phys. Rev. Lett. **73**, 332 (1994)
- [31] D. Pines, P. Nozière, *Theory of Quantum Liquids*, Benjamin, New York 1966
- [32] A. Berkovits, N.G. Murthy, J. Phys. A **21**, 3703 (1988)
- [33] H. Castella, X. Zotos, P. Prelovšek, Phys. Rev. Lett. **74**, 972 (1995)
- [34] P.F. Maldague, Phys. Rev. **B16**, 2437 (1977)
- [35] S. Fujimoto, N. Kawakami, J. Phys. A **21**, 465 (1998)
- [36] X. Zotos, cond-mat/9811013 (1999)
- [37] G. Jüttner, A. Klümper, J. Suzuki, cond-mat/9611058, (1996)
- [38] Y. Aharanov, D. Bohm, Phys. Rev. **115**, 485 (1959)
- [39] E. Dagotto, Rev. Mod. Phys. **66**, 763-840 (1994)
- [40] A. Klümper, D.C. Johnston, cond-mat/0002140 (2000)
- [41] G. Uhrig, Habilitation Thesis, Köln, (1999)
- [42] N. Tsuda, K. Nasu, A. Yanase and K. Siterator, *Electronic Conduction in Oxides*, Vol. 94 of the *Springer Series in Solid-State Sciences*, Springer, Berlin (1991)
- [43] F. Gebhard, *The Metal-Insulator Transition*, Vol. 137 of the Series *Ergebnisse der exakten Naturwissenschaften*, Springer, Berlin (1937)
- [44] A. B. Harris and R. V. Lange, Phys. Rev. **157**, 295 (1967)
- [45] A. Auerbach, *Interacting Electrons and Quantum Magnetism*, *Graduate Texts in Contemporary Physics*, Springer, New York, (1994)
- [46] S. Liang, B. Doucot, P.W. Anderson, Phys. Rev. Lett. **61**, 365 (1988)
- [47] F.D.M. Haldane, Phys. Rev. Lett. **47**, 1840 (1981)
- [48] F.D.M. Haldane, J. Phys. **C14**, 2585 (1981)

-
- [49] A.M. Tsvetik, *Quantum Field Theory in Condensed Matter Physics*, Cambridge University Press (1995)
 - [50] L.D. Faddeev, L.A. Takhtajan, *Phys. Lett. A* **85**, 375 (1981)
 - [51] G. Jüttner, A. Klümper, J. Suzuki, cond-mat/9705036 (1997)
 - [52] P. Jordan, E. Wigner, *Z. Phys.* **47**, 631 (1928)
 - [53] D.J. Scalapino, S.R. White, S. Zhang, *Phys. Rev. B* **47**, 7995 (1993)
 - [54] C.N. Yang, C.P. Yang, *J. Math. Phys.* **10**, 1115 (1969)
 - [55] B.S. Shastry, B. Sutherland, *Phys. Rev. Lett.* **65**, 243 (1990)
 - [56] M. Gaudin, *La fonction d'onde de Bethe*, Ser. Scientifique, Masson, Paris (1983)
 - [57] H.F. Trotter, *Proc. Am. Math. Soc.* **10**, 545 (1959)
 - [58] A. Klümper, private communication

Kurzzusammenfassung

Im ersten Teil der vorliegenden Arbeit wird das asymptotische Verhalten der longitudinalen Spin-Spin Korrelationsfunktion der integrablen anisotropen Heisenberg-Kette untersucht. Zu diesem Zwecke wird die Quanten-Transfer-Matrix-Technik (QTM aus [7]) benutzt, mit deren Hilfe man ein nicht-lineares Integralgleichungssystem herleiten kann, durch das der größte Eigenwert der QTM bestimmt ist und damit die Thermodynamik des Systems. Modifikationen der Integrationswege machen es möglich, innerhalb des Formalismus dieser Integralgleichungen auch nächstgrößte Eigenwerte zu berechnen. Somit ist ein Verfahren zur Berechnung von Korrelationslängen erschlossen. Für nichtverschwindendes Feld $h > 0$ und hinreichend hohe Temperatur ist der zweitgrößte Eigenwert eindeutig und durch eine 1-String-Lösung der QTM gegeben. Er ist reell und negativ und führt daher zu exponentiell abfallenden Korrelationen mit antiferromagnetischer Oszillation. Bei hinreichend tiefer Temperatur ergibt sich ein anderes Verhalten: Es gibt jetzt zwei entartete zweitgrößte Eigenwerte, die komplex konjugiert sind und zur selben Korrelationslänge mit inkommensurablen Oszillationen führen.

Das oben beschriebene Szenario ist das Ergebnis der numerischen und analytischen Analyse der QTM. Man beobachtet eine wohldefinierte Crossover-Temperatur bei der die 1- und 2-String-Lösung der QTM entarten.

Im zweiten Teil wird das Drude-Gewicht der anisotropen Heisenberg-Kette analytisch berechnet. Dabei wird ein interessanter Zusammenhang [40] zwischen der QTM-Technik und dem thermodynamischen Bethe-Ansatz (TBA) ausgenutzt. Man erhält *exakte* Ergebnisse bei *endlicher* Temperatur. Desweiteren werden interessante Phänomene, wie logarithmische Korrekturen im Drude-Gewicht bei niedrigen Temperaturen beobachtet.

Zusammenfassung

In der vorliegenden Arbeit werden zwei temperaturabhängige Größen der anisotropen Heisenberg-Kette untersucht.

Zum ersten wird die longitudinale Spin-Spin-Korrelationslänge des Modells bei *endlicher* Temperatur berechnet.

Diese Größe ist von Interesse, da man ein unterschiedliches Verhalten des Systems im Limes tiefer und hoher Temperatur erwartet.

Im folgenden wird das System mit einem festen und endlichen Magnetfeld betrachtet. Für tiefe Temperaturen liefern die Aussagen der konformen Feldtheorie zufriedenstellende Voraussagen. Demnach erwartet man $2k_F$ -Oszillation der Korrelationsfunktion mit $2k_F \neq \pi$. Im Hochtemperatur-Limes sollte sich das System quasiklassisch verhalten. Daher würde man π -Oszillationen in der Korrelationsfunktion vorhersagen.

Man erwartet daher eine kritische Temperatur, bei der die quantenmechanische Beschreibung zusammenbricht und auch ein nicht-analytisches Verhalten der betroffenen Größen wäre folgerichtig.

Ausgangspunkt für die Berechnung war die Formulierung der thermodynamischen Bethe-Ansatz Gleichungen durch Hilfsfunktionen, die durch nicht-lineare Integralgleichungen (NLIE)[7] bestimmt sind. In der direkten Formulierung dienen die NLIE zur Berechnung des größten Eigenwertes der Quanten-Transfermatrix, also zur Bestimmung der freien Energie. Um Korrelationslängen innerhalb dieses Formalismus zu berechnen, ist es notwendig, auch die nächstgrößten Eigenwerte zu kennen. Auf dem Niveau der Bethe-Ansatz-Zahlen (Wurzeln) sind angeregte Zustände durch Muster von Wurzeln gekennzeichnet, die sich strukturell vom Muster für den größten Eigenwert unterscheiden. Für die longitudinale Korrelationslänge sind 1- und 2-String-Muster relevant, die zumindest annäherungsweise die String-Struktur aufzeigen, die man aus traditionellen Bethe-Ansatz-Rechnungen kennt. Man muß nun Integralgleichungen für diese Muster ableiten. Dies geschieht effektiv durch Deformation der Integrationswege in den Ausgangsintegralgleichungen. Die Analyse der Wurzelmuster, zum Beispiel für den 1-String-Fall, macht jedoch klar, daß die Deformation der Integrationswege allein nicht ausreicht, das Szenario zu beschreiben, da der 1-String den Analytizitätsbereich der NLIE verläßt, wenn man bei festem magnetischen Feld die Temperatur senkt. Daher ist eine analytische Neuformulierung der Gleichungen außerhalb dieses Bereiches notwendig. Auf diese Art erlangt man Gleichungen für den gesamten Temperaturbereich, bzw. für jede Stringposition, die numerisch durch Iteration der Integralgleichungen gelöst werden können. Man kann so die Korrelationslänge für *beliebige* Temperaturen exakt berechnen. Es wird eine Entartung der Eigenwerte für den 1- und 2-String Fall bei einer kritischen Temperatur T_c beobachtet. Unterhalb von T_c sind die Eigenwerte komplex konjugiert. Diese Entartung manifestiert sich besonders deutlich im nicht-analytischen Verhalten der $2k_F$ -Oszillationen. Unterhalb von T_c sind diese Oszillationen inkommensurabel.

Der zweite Teil der Arbeit beschäftigt sich mit der Berechnung des Drude-Gewichts der anisotropen Heisenberg-Kette. Diese Aufgabe ist durch die in [36] erzielten Ergebnisse motiviert, die sich komplett auf Methoden der Standard-TBA [40] stützen.

Als Hauptergebnisse sind dort der monotone Abfall des Drude-Gewichts mit der Temperatur bei beliebigen Anisotropie-Parametern und das Verschwinden des Drude-Gewichts für alle endlichen Temperaturen am isotropen Punkt zu nennen. Der Standard-TBA-Zugang bereitet allerdings einige technische Probleme, die hier durch eine Kombination von Quanten-Transfermatrix-Zugang und TBA-Techniken ausgeräumt werden konnten.

Die Berechnung des Drude-Gewichts stützt sich auf die übliche Formulierung der Thermodynamik von Takahashi [9]. Im Prinzip berechnet man die Krümmung der Energieniveaus bezogen auf den in die Randbedingungen eingehenden Twist. Über eine Finite-Size-Analyse erhält man Integralgleichungen und einen geschlossenen Ausdruck für das Drude-Gewicht. In diesem Zugang sind alle angeregten Zustände des Systems durch String-Lösungen charakterisiert. Es können im allgemeinen unendlich viele Integralgleichungen auftreten. Die Behandlung des Problems auf diese Art kann daher sehr mühsam sein, d.h. man kommt oft nur durch schwer kontrollierbare Näherungen zu konkreten Ergebnissen. Um solche Probleme zu vermeiden, wurde eine Formulierung des Problems durch die NLIE angestrebt, weil man dann nur einen *endlichen* Satz von Integralgleichungen behandeln muss. Im Laufe der Arbeiten stellte sich heraus, daß das Ausnutzen der Äquivalenz [40] von NLIE und Gleichungen, die auf der Basis des üblichen Verfahrens hergeleitet sind, den einfachsten Zugang bietet und man weite Teile der üblichen Rechnungen für das Drude-Gewicht übernehmen kann. So kann man das Drude-Gewicht *exakt* für *endliche* Temperaturen berechnen. Im Gegensatz zum bekannten Verfahren ist auch das Drude-Gewicht am isotropen Punkt des Modells *exakt* bestimmbar. Daher sind auch zum ersten Mal logarithmische Korrekturen im Drude-Gewicht dieses Modells beobachtet worden.

Die Resultate aus [36] konnten nicht bestätigt werden: In der vorliegenden Arbeit erhalten wir die maximale, reguläre Ausdehnung der $T = 0$ -Ergebnisse auf $T > 0$, insbesondere für den isotropen Fall, und man beobachtet ein Maximum im Drude-Gewicht.

Zukünftige Aufgaben könnten darin liegen, andere Modelle, wie das supersymmetrische tJ -Modell, die durch *NLIE* behandelbar sind, in Hinblick auf Crossover-Phänomene in den Korrelationslängen zu untersuchen. Auch das Drude-Gewicht des tJ - und Hubbard-Modells kann mit dem vorliegenden Verfahren im Prinzip bestimmt werden. Interessant ist auch die Frage nach der analytischen Berechnung der logarithmischen Korrekturen im Drude-Gewicht. Dies müßte analog zur analytischen Berechnung der Korrekturen in der magnetischen Suszeptibilität möglich sein [10].

Erklärung

Ich versichere, daß ich die von mir vorgelegte Dissertation selbständig angefertigt, die benutzten Quellen und Hilfsmittel vollständig angegeben und die Stellen der Arbeit – einschließlich Tabellen, Karten und Abbildungen –, die anderen Werken im Wortlaut oder dem Sinn nach entnommen sind, in jedem Einzelfall als Entlehnung kenntlich gemacht habe; daß diese Dissertation noch keiner anderen Fakultät oder Universität zur Prüfung vorgelegen hat; daß sie – abgesehen von unten angegebenen Teilpublikationen – noch nicht veröffentlicht worden ist sowie, daß ich eine solche Veröffentlichung vor Abschluß des Promotionsverfahrens nicht vornehmen werde. Die Bestimmungen dieser Promotionsordnung sind mir bekannt. Die von mir vorgelegte Dissertation ist von Herrn Professor Dr. A. Klümper betreut worden.

Köln, den 10. Oktober 2000

Teilpublikationen:

A. Klümper, R. Martinez, C. Scheeren, M. Shiroishi
eingereicht bei Journal of Statistical Physics

Danksagung

Ich danke Herrn Prof. Dr. A. Klümper für die Anregung zu dieser Arbeit, seine hervorragende Betreuung und seine stete Diskussionsbereitschaft.

Herrn Prof. Dr. J. Zittartz danke ich für die Ermöglichung der guten Arbeitsbedingungen an seinem Lehrstuhl und seine Unterstützung.

Für das Korrekturlesen dieser Arbeit und der sonstigen mir zuteil gewordenen Hilfe danke ich Herrn Priv.-Doz. Dr. A. Schadschneider, den Herren Dipl. Phys. A. Bühler, A. Kirchner, K. Klauck und A. Sindermann, sowie Herrn F. Brücher.

Lebenslauf

Persönliche Daten

Name: Christian Scheeren
 Geburtsdatum: 16.2.1969
 Geburtsort: Dortmund
 wohnhaft in: Mommsenstr. 2
 50935 Köln

Eltern: Werner Scheeren und
 Ingrid Scheeren, geb. Künstler

Familienstand: ledig
 Staatsangehörigkeit: deutsch

Schulbildung

1975 – 1977 Grundschule Dortmund-Aplerbeck
 1977 – 1979 Grundschule Unna-Königsborn
 1979 – 1988 Geschwister-Scholl-Gymnasium
 in Unna
 Mai 1988 Abitur

Juli 1988 – Juni 1989 Wehrdienst

Hochschulstudium

Okt. 1989 Immatrikulation an der Universität
 Dortmund, Studiengang Physik (Diplom)

September 1991 Vordiplom

Okt. 1991 - Sep. 1992 Studium an der Université Joseph Fourier
 in Grenoble/Frankreich

Okt. 1992 Aufnahme des Hauptstudiums an der
 Universität zu Köln

März 1998 Abschluß der Diplomarbeit bei
 Priv. Doz. Dr. A. Klümper

ab April 1998 Anfertigung der vorliegenden Dis-
 sertation unter Anleitung von
 Priv. Doz. Dr. A. Klümper

Arbeitsverhältnisse am Institut für Theoretische Physik, Universität zu Köln

Juni. 1997 - März. 1998 Wissenschaftliche Hilfskraft
 seit April 1998 Wissenschaftlicher Mitarbeiter